

Feasibility of externally bonded CFRP for cathodic protection

Philippe De Schoesitter

Promotoren: prof. dr. ir. Stijn Matthys, prof. dr. ir. Geert De Schutter

Masterproef ingediend tot het behalen van de academische graad van
Master in de ingenieurswetenschappen: bouwkunde

Vakgroep Bouwkundige Constructies
Voorzitter: prof. dr. ir. Luc Taerwe
Faculteit Ingenieurswetenschappen en Architectuur
Academiejaar 2010-2011



Feasibility of externally bonded CFRP for cathodic protection

Philippe De Schoesitter

Promotoren: prof. dr. ir. Stijn Matthys, prof. dr. ir. Geert De Schutter

Masterproef ingediend tot het behalen van de academische graad van
Master in de ingenieurswetenschappen: bouwkunde

Vakgroep Bouwkundige Constructies
Voorzitter: prof. dr. ir. Luc Taerwe
Faculteit Ingenieurswetenschappen en Architectuur
Academiejaar 2010-2011



Feasibility of externally bonded CFRP for cathodic protection

Philippe De Schoesitter

Promotoren: prof. dr. ir. Stijn Matthys, prof. dr. ir. Geert De Schutter

Begeleiding: ir. Dorleta Ertzibengoa Gaztelumendi

Masterproef ingediend tot het behalen van de academische graad van Master in de ingenieurswetenschappen: bouwkunde

Vakgroep Bouwkundige Constructies

Voorzitter: prof. dr. ir. Luc Taerwe

Faculteit Ingenieurswetenschappen en Architectuur

Academiejaar 2010-2011

Abstract

The technical feasibility of the usage of carbon fibres of carbon fibre reinforced polymer for externally bonded reinforcement of reinforced concrete structures (CFRP EBR) for active cathodic protection (CP) of the reinforcement steel is discussed and investigated in this dissertation. Concrete samples were wrapped with carbon fibres applied in two different fibre directions, and using several epoxy adhesives. The steel was used as the cathode and the CFRP wrap as anode for the induced current CP (ICCP). The epoxy adhesives were filled with conductive particles to make them conductive (Ni, Ag, graphite and carbon black powder). To initiate and accelerate the corrosion process, chlorides were added to the mortar mixture, and the samples were partially immersed in a NaCl bath during the ICCP program. Through linear polarization, the effectiveness of the ICCP was monitored. It was found that cathodically protected specimens had substantially lower corrosion rates. Radial fibre direction showed the most consistent results. The higher the conductivity of the epoxy, the lower the absolute corrosion rates were, and the lower the corrosion rate evolution was. Some conclusions regarding further research are drawn as well.

Keywords: active cathodic protection, CFRP, corrosion, reinforced concrete

The author gives permission to make this master dissertation available for consultation and to copy parts of this master dissertation for personal use.

In the case of any other use, the limitations of the copyright have to be respected, in particular with regard to the obligation to state expressly the source when quoting results from this master dissertation.

Feasibility of Externally Bonded CFRP for Cathodic Protection

Philippe De Schoesitter

Supervisors: Stijn MATTHYS, Geert DE SCHUTTER

Abstract: Carbon fibre reinforced polymers (CFRP) have exquisite strength and sustainability properties, which make them appropriate for reinforcement applications of concrete structures. In externally bonded reinforcement (EBR) of reinforced concrete (RC) structures, the CFRP reinforcement covers a substantial part of the structural surface. Together with the high electrical conductivity of the carbon fibres, this offers the possibility to apply a current to the CFRP fabric, for cathodic protection of the steel. The technical feasibility of the combination of CFRP EBR with CP of RC structures is both in literature and experimentally investigated and discussed in this dissertation. Cylindrical reinforced concrete specimens were wrapped with CFRP material, and protected by a cathodic current between steel and CFRP wrap. The specimens were subjected to aggressive corrosion environments. The corrosion rate was measured in different ways both during and at the end of the test program. Conclusions regarding the feasibility and further research have been drawn.

Keywords: active cathodic protection, CFRP, corrosion, reinforced concrete

I. Introduction

CFRP materials, applied as external reinforcement material on RC structures, form a protective barrier against chloride and moist penetration. This passive protection has been studied in some experimental researches [1-5]. Besides the impenetrability of the wraps, it was found in these studies that the confinement of the concrete due to CFRP wrapping has a positive influence on corrosion initiation and rate. Geometrical aspects, such as concrete cover and RC element geometry have an influence as well. For instance wrapped concrete columns show better confinement conditions than reinforced beams, and a higher concrete cover improves the confinement as well.

CFRP EBR has therefore become a popular concrete repair technique on heavily corroded RC structures for service life prolongation. The idea of using the CFRP EBR as an anode for cathodic protection has been experimentally investigated in [6]. In this experiment, heavily corroded test specimens were cathodically protected. A positive effect on total amount of corrosion products was found through mass loss and pull-out measurements. Less attention is paid to the actual corrosion rates during the CP program, and conductivity of the FRP sheets.

Epoxy resins used for FRP EBR applications are usually electrical insulators. To obtain better conductivity, polymers can be filled with conductive particles. Metal powders are commonly used for electrical applications. However, an anode material for CP should be resistant against aggressive (acid) environments. Therefore, the addition of carbon black

(CB) particles was favoured in this work, next to metal powders. The behaviour of conductive CB added to polymers is a much researched subject [7-13]. The most mentioned theory to describe this phenomenon is the percolation theory. Of greater interest in this work, is the control of viscosity properties of the filled epoxy for EBR application. To overcome this issue, the mix ratios of the epoxy resin were altered, in order to find the optimal conductivity/rheology properties for anode application.

II. Polymer conductivity

For the experimental research in this dissertation PRINTEX XE2 carbon black powder provided by the *Evonik* company was added to two different epoxy resins. Furthermore, four commercial conductive epoxies for electrical applications were provided by *Henkel*. Some relevant properties are listed in Table 1.

Adhesive	Company	Filler	Resistivity [$\Omega \cdot \text{cm}$]
Eccobond 50298	Emerson & Cuming	Ni	0,5
Eccobond 64C	Emerson & Cuming	Ni	0,02
Eccobond 60L	Emerson & Cuming	graphite	50
Eccobond 57 C	Hysol	Ag	6×10^{-4}
ECC PC 5800 Carbo	ECC	CB	119,04
Epo-Tek 353ND	EpoTek	CB	78,72

Table 1: Conductive epoxies

Spec. name	Wrap	Fibre dir.	CP	Immer-sion	Tafel sl. meas.
Ref-1,2,3	no		no	yes	no
Ref-FRP	yes	axial	no	yes	no
CP-ax	yes	axial	yes	yes	no
CP-rad	yes	radial	yes	yes	no
CP	yes	no fibres	yes	yes	no
Tafel-ref	no		no	no	yes
Tafel-50298	yes	axial	no	no	yes

Table 2: Specimen matrix

CB filled epoxies

PC 5800 CARBO epoxy resin of ECC company was filled with 9,88wt% of the CB powder. The mix ratio to obtain an acceptable viscosity (and decent curing) was altered from 1:2 to 1,32:1.

A second antistatic epoxy Epo-Tek 353ND from EpoTek company was filled with 12,97wt% of CB powder, changing the mix ratio from 10:1 to 1,64:1.

These filled epoxies are called "ECC" and "Epo" respectively.

Commercial conductive epoxies

Four epoxies with different fillers and properties were used. For specific information see Table 1.

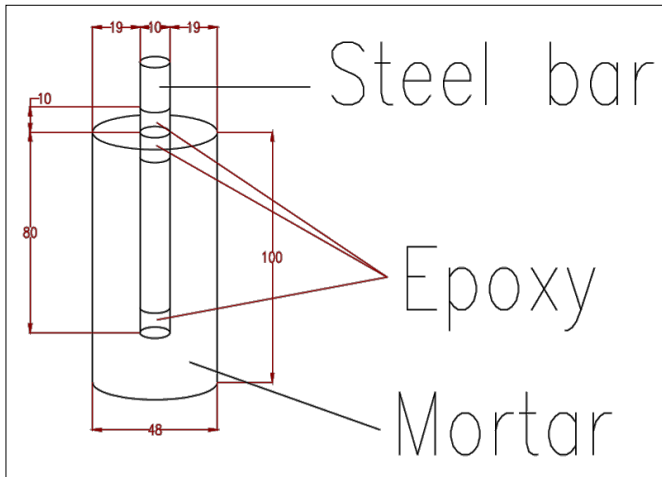


Figure 1: Lollipop specimen geometry

III. Specimen preparation

Concrete samples

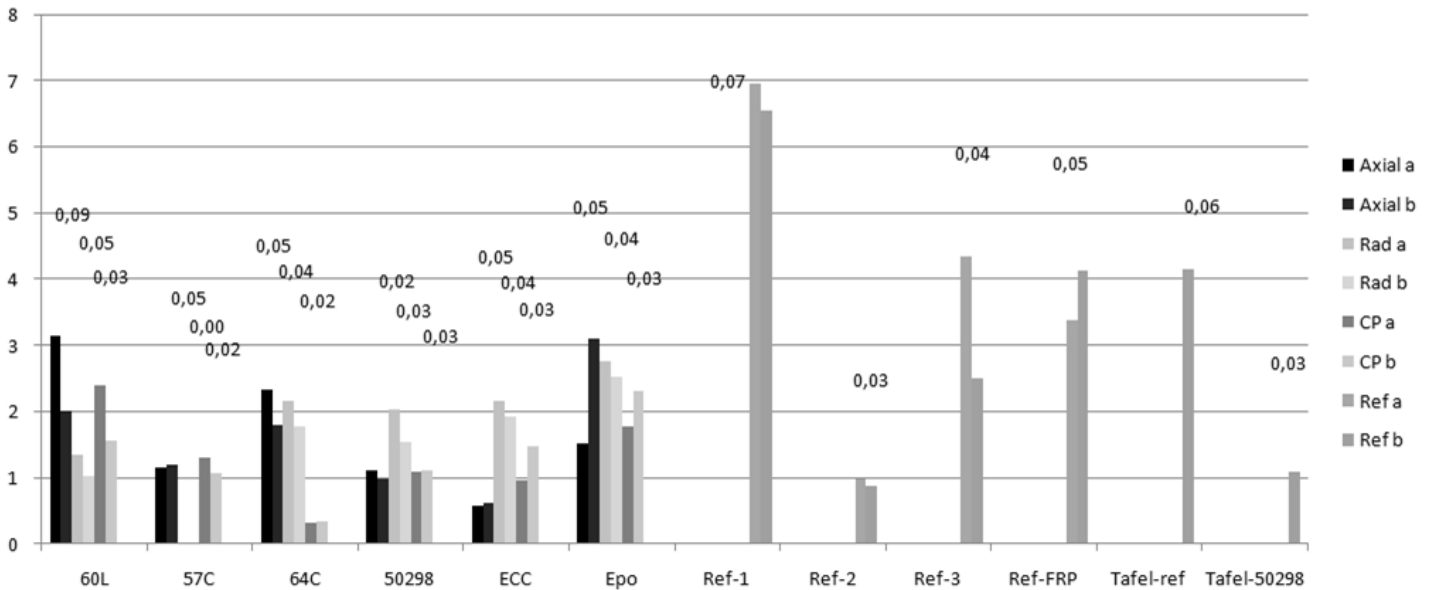


Figure 2: Results. Columns show I_{corr} from LP measurement of axial, radial, fibreless ("CP") and reference specimens, for both LP sessions ("a" and "b"). The labels indicate the mass loss percentage of axial, radial and fibreless specimens from top to bottom.

Small chloride contaminated mortar cylinders of diameter 48mm and height 100mm were prepared. A smooth steel bar was embedded in the concrete axially, over a length of 80mm. Through epoxy coating, the length of the bar that was exposed to corrosion was exactly 60mm. The mortar composition Cem:Sand:Water:NaCl was 1:3:0,65;0,07. The compression strength of the mortar at 28 days was 34,9N/mm². Figure 1 depicts the general geometry of a specimen.

CFRP wraps

The wraps consisted of wet lay-up application of PC CARBOCOMP PLUS CFRP textile of ECC company. For each type of conductive epoxy, three specimen wraps were prepared. **Ax**: axial fibre direction, **rad**: radial fibre direction, just **CP**: fibreless, just an epoxy coating. Every specimen was provided of a similar primary anode to connect to the DC power supply, and to spread the current over the anode surface. This primary anode consisted of a string of carbon fibres of height 10mm, applied radially onto the "rad" or "ax" fibres of the underlying wrap, or simply onto the epoxy of the fibreless CP specimens.

Four reference specimens were fabricated. Three of them remained unwrapped. The fourth was wrapped in a classic CFRP wrap with insulating epoxy (PC 5800 CARBO), and axial fibre direction.

Two more samples were used for Tafel slope measurements.

The specimen matrix is listed in Table 2.

IV. CP/immersion program

A protective current between steel bar (cathode) and CFRP wrap (anode) was applied to all of the "CP" specimens. The CP program was divided into two phases of 14 days. The protection current was 58,35mA/m² during the

first period and $26,53\text{mA}/\text{m}^2$ during the second period.

During this program the samples were cyclically immersed in a NaCl water solution (1,0wt%) for 1 hour every 24 hours.

The reference specimens (Ref-1,2,3 and Ref-FRP) were also immersed.

All of the specimens were treated identically during the CP/immersion program and measurements.

V. Measurements

Two linear polarization (LP) measurements were executed, to obtain instant corrosion rates: after 14 days and after 28 days. After the 28 days of test program the steel bars were removed out of the concrete to determine the steel mass loss to corrosion products, according to ASTM G1-90. The results are listed in Figure 2.

VI. Discussion

Most of the open circuit potentials (OCPs) show an upward (less negative) shift, as a result of the decrease of the protection current I_{prot} . The fibreless specimens, however, show a downward evolution, indicating a safer steel condition despite of the I_{prot} drop.

The polarization resistances are substantially higher for the protected CP specimens, compared to the unprotected references, resulting in much lower corrosion rates (40 to 70% lower on average). The Tafel extrapolation method showed high correlation with the LP measurements. The calculated B values of the Stern-Geary equation were close to 26mV, indicating an active depassivated steel condition. The corrosion current densities are calculated with $B=26\text{mV}$.

The most consistent results were found for the radially wrapped fibre configuration: all of these specimens showed a positive evolution in corrosion rate. This may be due to better confinement conditions through wrapping.

The most conducting epoxies (57C and 64C) show overall low corrosion rates, and little evolution between both measurements. The presence of the fibres is believed to have little influence on anode current spread for these epoxies.

VII. Conclusions

It can be concluded that CPrev was not achieved, as a consequence of the high initial chloride concentration in the mortar cylinders. However, ICCP was found to be effective. Some conclusions regarding future research can be drawn:

- The influence of fillers on epoxy strength characteristics should be investigated and optimized
- CB is probably not the best solution for surface conductivity. Other sustainable alternatives (e.g. carbon nanotubes) should be explored
- Possibilities to add conductive fillers during fabrication process of prefab CFRP laminates can be explored too.

- Further research for CPrev should be done without chloride addition to the mortar, with a longer CP program. This would also give the opportunity to do more LP measurements, and to have a clearer view on I_{corr} evolution.

VII. References

- [1] I. WOOTTON, L. K. SPAINHOUR, N. YAZDANI, *Corrosion of Steel Reinforcement in Carbon Fiber-Reinforced Polymer Wrapped Concrete Cylinders*, Journ. Of Composites for Constr., p.339-347, (2003)
- [2] T. EL MAADDAWY, K SOUDKI, *Carbon-Fiber-Reinforced Polymer Repair to Extend Service Life of Corroded Reinforced Concrete Beams*, Journ. Of Composites for Constr., p.187-194 (2005)
- [3] S. MASOUD, K. SOUDKI, *Evaluation of corrosion in FRP repaired RC beams*, Cement & Concrete Composites, 28, p.3969-977, (2006)
- [4] T. EL MAADDAWY, A. CHAHROUR, K. SOUDKI, *Effect of Fiber-Reinforced-Polymer Wraps on Corrosion Activity and Concrete Cracking in Chloride-Contaminated Concrete Cylinders*, Journ. Of Composites for Constr., p.139-147, (2006)
- [5] S. GADVE, A. MUKHERJEE, S.N. MALHOTRA, *Corrosion of steel reinforcements embedded in FRP wrapped concrete*, Constr. and Building Mat., 23, p.153-161, (2009)
- [6] S. GADVE, A. MUKHERJEE, S.N. MALHOTRA, *Active protection of FRP wrapped reinforced concrete structures against corrosion*, Taylor & Francis Group, London (2009)
- [7] B. WESSLING, *Dispersion as the key to processing conductive polymers*, Handbook of conducting polymers, Edited by Skotheim Elsenbaumer and Reynolds, second edition, 1998, isbn 0-8247-0050-3
- [8] M. KUPKE, H.-P. WENTZEL, K. SCHULTE, *Electrically conductive glass fibre reinforced epoxy resin*, MAT Res Innovat, 2, p.164-169, (1998)
- [9] H.S. KATZ, J.V. MILEWSKI, *Handbook of fillers for plastics*, Van Nostrand Reinhold, ISBN 0-442-26024-5 (1987)
- [10] R. SCHUELER, J. PETERMANN, K. SCHULTE, H.-P. WENTZEL, *Agglomeration and electrical Percolation Behavior of Carbon Black Dispersed in Epoxy Resin*, Wiley & Sons, (1997)
- [11] P. WANG, T. DING, *Conductivity and piezoresistivity of Conductive Carbon Black Filled Polymer Composite*, Journ. Of Applied Polymer Science, 116, p.2035-2039, (2010)
- [12] *The fundamentals of Carbon Black*, Cabot Corporation Billerica, electronic version, URL: <http://www.cabot-corp.com/Downloads/DL200808140916AM8680/> (consulted May 2011)
- [13] P.J. MORELAND et al., *Cathodic protection system and a coating composition therefor*, United States Patent, n° 5,364,511, November 15 1994.

Haalbaarheidstudie van Uitwendig Gebonden CFRP voor Kathodische Bescherming

Philippe De Schoesitter

Promotoren: Stijn MATTHYS, Geert DE SCHUTTER

Abstract: Carbonvezel versterkte polymeren (Carbon fibre reinforced polymers, CFRP) hebben uitstekende sterkte en duurzaamheidseigenschappen, waardoor ze o.m. kunnen dienen als wapening voor betonconstructies. Bij uitwendig aangebrachte vezelwapening (Externally bonded reinforcement, EBR) op gewapende betonconstructies (GB), wordt vaak een aanzienlijk deel van het betonoppervlak door de CFRP bedekt. Samen met de goede elektrische geleidbaarheid van de carbonvezels, biedt dit de mogelijkheid om een stroom door de uitwendige wapening te leiden voor kathodische bescherming (KB) van het wapeningsstaal. In dit werk werd de technische haalbaarheid van een dergelijk gecombineerd systeem experimenteel uitgeprobeerd en bediscussieerd. Cilindrische gewapende mortelproefstukken werden in CFRP gewikkeld en beschermd door een kathodische stroom tussen CFRP en staal. Intussen werden ze aan een agressief corrosiemilieu blootgesteld. De corrosiesnelheid werd gedurende de proefperiode met elektrochemische metingen bepaald. Nadien werden destructieve metingen uitgevoerd. Op basis van dit experiment en de literatuur, werden een aantal conclusies omtrent de haalbaarheid van het systeem en toekomstig onderzoek getrokken.

Sleutelwoorden: actieve kathodische bescherming, CFRP, corrosie, gewapend beton

corrosieproducten gevonden. Er werd wel minder aandacht besteed aan feitelijke corrosiesnelheid gedurende de proef en de invloed van de geleidbaarheid van de CFRP wrap.

Epoxyharsen, die gewoonlijk gebruikt worden voor CFRP EBR, bieden grote elektrische weerstand. Om deze weerstand te verkleinen, is het mogelijk om geleidende deeltjes – zoals metaalpoeders – eraan toe te voegen. Aangezien de anode voor KB bestand moet zijn tegen agressieve, zure corrosiemilieus, en metaalpoeders zelf gevoelig zijn aan corrosie, is dit wellicht niet de beste oplossing. Daarom werd in dit experiment ook gewerkt met ‘Carbon Black’ (CB) poeder: zeer geleidende deeltjes op basis van carbon. Het gedrag van CB vermengd in polymeren is al uitvoerig bestudeerd, o.m. in [7-13], en wordt gekenmerkt door een kritieke concentratie toegevoegde CB, die gepaard gaat met het plots fenomenaal stijgen van de geleidbaarheid. De theorie die het meeste is aangewend om dit gedrag te verklaren is de percolatietheorie. Een ander belangrijk fenomeen is de viscositeit van de epoxy bij het toevoegen van de CB. Dit euvel kan worden ingeperkt door de mengverhouding van de epoxy te veranderen, om een optimale viscositeit en geleidbaarheid te vinden.

I. Inleiding

CFRP materialen, aangebracht als uitwendige wapening, vormen een beschermende impermeabele laag op het beton. Deze passieve bescherming, tegen o.m. water en chloridepenetratie, is al veelvuldig bestudeerd in o.a. [1-5], waarin een positieve invloed op corrosiesnelheid van het wapeningsstaal wordt beschreven. Naast de ondoorlatendheid van de CFRP, speelt ook de betonsamendrukking door de CFRP een belangrijke rol. Ook geometrische aspecten hebben een invloed, zoals grotere betondekking, en betere samendrukking bij kolomvormige elementen, versus balken.

CFRP EBR is daarom een populaire betonherstellingstechniek geworden, bij zware betonaantasting door corrosie of andere vormen van betonrot. Het idee om CFRP EBR ook te benutten als anode voor kathodische bescherming, is reeds experimenteel uitgeprobeerd in [6]. In dit experiment werden zwaar gecorrodeerde betonmonsters behandeld met CFRP, en vervolgens in agressief milieu kathodisch beschermd. Er werd een positieve invloed op de totale hoeveelheid

II. Geleidende epoxy's

PRINTEX XE2 carbon black, geleverd door *Evonik*, werd toegevoegd aan twee verschillende epoxyharsen. Verder werden vier reeds gevulde epoxyharsen uit de handel aangewend (geleverd door *Henkel*). Enkele eigenschappen worden samengevat in Tabel 1.

Epoxyhars	Producent	Filler	Bulkweerst. [Ω .cm]
Eccobond 50298	Emerson & Cuming	Ni	0,5
Eccobond 64C	Emerson & Cuming	Ni	0,02
Eccobond 60L	Emerson & Cuming	grafiet	50
Eccobond 57 C	Hysol	Ag	6×10^{-4}
ECC PC 5800 Carbo	ECC	CB	119,04
Epo-Tek 353ND	EpoTek	CB	78,72

Tabel 1: Geleidende epoxy's

CB gevulde epoxies

PC 5800 CARBO epoxy hars van ECC werd gevuld met 9,88m% CB poeder. De mengverhouding werd veranderd van 2:1 naar 1,32:1.

Aan een tweede ‘antistatische’ epoxy, Epo-Tek 353ND van EpoTek, werd 12,97m% CB poeder toegevoegd,

Monst. naam	FRP	Vezel-richting	KB	Bad	Tafel exp.
Ref-1,2,3	nee		nee	ja	nee
Ref-FRP	ja	axiaal	nee	ja	nee
CP-ax	ja	axiaal	ja	ja	nee
CP-rad	ja	radiaal	ja	ja	nee
CP	ja	geen	ja	ja	nee
Tafel-ref	nee		nee	nee	ja
Tafel-50298	ja	axiaal	nee	nee	ja

Tabel 2: Proefstukkenmatrix

waarbij de mengverhouding veranderd werd van 10:1 to 1,64:1.

Deze gevulde epoxies worden respectievelijk ‘ECC’ en ‘Epo’ genoemd.

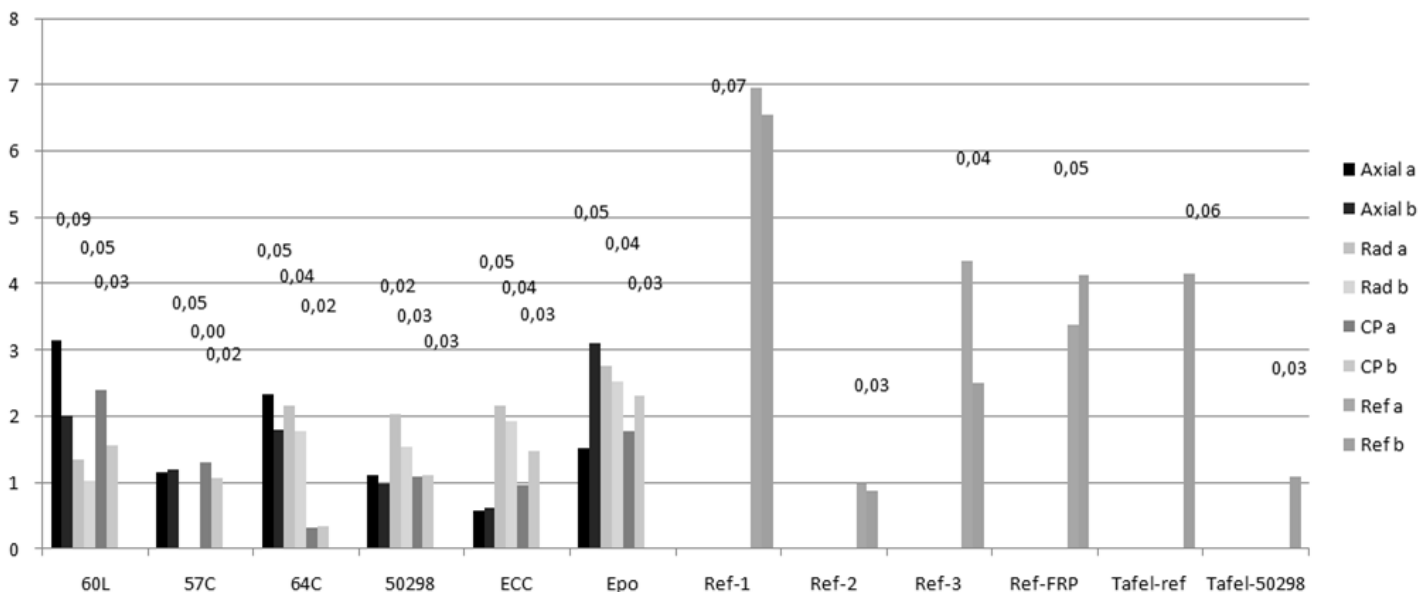
Geleidende epoxies uit de handel

Vier epoxies met verschillende toevoegingen werden aangewend: zilver, nikkel en grafiet. Meer informatie is te vinden in Tabel 1.

III. Monstervoorbereiding

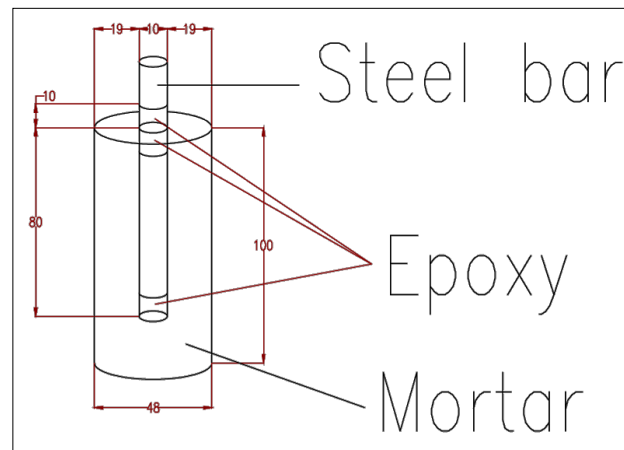
Mortelproefstukken

Kleine mortelcilinders met diameter 48mm en hoogte



Figuur 2: Resultaten. Staafdiagrammen weergeven I_{corr} verkregen via LP metingen van axiale, radiale, vezelloze (“CP”) en referentie proefstukken, voor beide LP sessies (“a” and “b”). De labels weergeven de procentuele massaverliezen van resp. axiale, radiale en vezelloze proefstukken.

100mm werden klaargemaakt. Voor versnelde corrosie initiatie werd NaCl aan de mortel toegevoegd. Een gladde staalstaaf werd over een totale lengte van 80mm ingebed in de as van de cilinder. M.b.v. waterdichte epoxycoatings werd de staallengte, blootgesteld aan corrosie, beperkt tot precies 60mm. De mortelsamenstelling is cem:zand:water:NaCl 1:3:0,65:0,07. De druksterkte van de mortel op 28 dagen bedroeg 34,9N/mm². Figuur 1 weergeeft de algemene geometrie.



Figuur 1: Proefstukgeometrie

CFRP wraps

De CFRP werd in textielvorm op het beton aangebracht ‘wet lay-up’. PC CARBOCOMP PLUS CFRP vezeltextiel van ECC werd hiervoor gebruikt. Voor ieder epoxytype werden drie proefstukken voorbereid. ‘Ax’: axiale vezelrichting, ‘rad’: radiale vezelrichting, gewoon ‘CP’: geen vezels, enkel epoxycoating. Alle proefstukken werden op dezelfde manier van een primaire anode voorzien (voor connectie aan de DC voedingsbron): een bundel carbonvezels met hoogte 10mm werd radiaal aangebracht op

de onderliggende vezels (op de epoxy bij CP-proefstukken).

Drie onbeschermde proefstukken zonder coating werden ter referentie gehouden (Ref-1,2,3), en een vierde referentie kreeg een klassieke niet-geleidende CFRP wrap met axiale vezelrichting (Ref-FRP).

Twee monsters werden bijgehouden voor Tafel experimenten (Tafel-Ref en Tafel-50298).

Een overzicht van alle proefstukken is gegeven in Tabel 2.

IV. KB/onderdempeling programma

Een constante beschermstroom tussen staal (kathode) en CFRP (anode) van alle "CP" monsters werd aangelegd over een periode van 28 dagen. De beschermstroom bedroeg $58,35\text{mA/cm}^2$ gedurende de eerste 14 dagen en $26,53\text{mA/cm}^2$ gedurende de laatste 2 weken.

Tijdens dit programma werden de monsters dagelijks gedurende een uur gedeeltelijk ondergedompeld, tot 20mm van de betonbovenrand, in een NaCl waterbad (1,0m%).

Dit geldt ook voor de referentieproefstukken (Ref-1,2,3 en Ref-FRP).

Zowel KB, onderdempeling als metingen werden ten allen tijde identiek uitgevoerd voor alle betreffende proefstukken.

V. Metingen

Twee lineaire polarisatie sessies (ter bepaling van de polarisatieweerstand R_p) werden uitgevoerd: na 14 en na 28 dagen cyclische onderdempeling. Na 28 dagen werd ook het massaverlies aan corrosieproducten van het staal bepaald, volgens ASTM G1-90. De resultaten zijn te vinden in Figuur 2.

VI. Bespreking

In de meeste gevallen stijgt de open klem potentiaal, als gevolg van de daling van de beschermstroom I_{prot} . De vezelloze proefstukken wijken hiervan af.

De polarisatieweerstanden van KB proefstukken zijn beduidend hoger dan die van onbeschermde referenties, resulterend in lagere corrosiesnelheden I_{corr} (gemiddeld 40 tot 70% lager). De Tafel extrapolatie methode leverde goede correlatie op met LP methode. De bekomen B waarden van de Stern-Geary vergelijking lagen dicht bij 26mV , wat wijst op een gedepasseerde staaltoestand. De I_{corr} berekening uit LP metingen gebeurde met $B=26\text{mV}$.

De radiaal ingepakte monsters tonen een consistente daling in I_{corr} . Dit zou kunnen wijzen op het positieve effect van betonsamendrukking op corrosiesnelheden.

De meest geleidende epoxies (57C and 64C) leveren lage corrosiesnelheden op, en minder evolutie tussen beide metingen. Daarom wordt aangenomen dat naarmate de epoxy meer geleidend is, de vezels minder invloed hebben op stroomdistributie in de anode.

VII. Conclusies

Besluitend kan vastgesteld worden dat Kathodische Preventie (KP) niet bereikt is, wellicht t.g.v. de grote hoeveelheid ingemengde chloriden in de mortel. De KB, daarentegen, was wel effectief. Er kunnen ook enkele conclusies met het oog op verder onderzoek getrokken worden:

- De invloed van geleidende deeltjes op de sterkte-eigenschappen van de epoxylijm moeten onderzocht en geoptimaliseerd worden.
- CB is wellicht niet het ideale middel om oppervlaktegeleidbaarheid te bekomen. Andere mogelijkheden (bvb. carbon nanotubes) moeten verkend worden.
- Mogelijkheden om geleidende deeltjes toe te voegen gedurende het productieproces van prefab CFRP laminaat kunnen ook onderzocht worden.
- Verder onderzoek naar KP kan best zonder ingemengde chloriden gebeuren. Het proefprogramma zal dan verlengd moeten worden. Dit laatste biedt ook de mogelijkheid om meerdere LP metingen uit te voeren, en een betere kijk te verkrijgen op de evolutie van de corrosiesnelheden.

VII. Referenties

- [1] I. WOOTTON, L. K. SPAINHOUR, N. YAZDANI, *Corrosion of Steel Reinforcement in Carbon Fiber-Reinforced Polymer Wrapped Concrete Cylinders*, Journ. Of Composites for Constr., p.339-347, (2003)
- [2] T. EL MAADDAWY, K. SOUDKI, *Carbon-Fiber-Reinforced Polymer Repair to Extend Service Life of Corroded Reinforced Concrete Beams*, Journ. Of Composites for Constr., p.187-194 (2005)
- [3] S. MASOUD, K. SOUDKI, *Evaluation of corrosion in FRP repaired RC beams*, Cement & Concrete Composites, 28, p.3969-977, (2006)
- [4] T. EL MAADDAWY, A. CHAHROUR, K. SOUDKI, *Effect of Fiber-Reinforced-Polymer Wraps on Corrosion Activity and Concrete Cracking in Chloride-Contaminated Concrete Cylinders*, Journ. Of Composites for Constr., p.139-147, (2006)
- [5] S. GADVE, A. MUKHERJEE, S.N. MALHOTRA, *Corrosion of steel reinforcements embedded in FRP wrapped concrete*, Constr. and Building Mat., 23, p.153-161, (2009)
- [6] S. GADVE, A. MUKHERJEE, S.N. MALHOTRA, *Active protection of FRP wrapped reinforced concrete structures against corrosion*, Taylor & Francis Group, London (2009)
- [7] B. WESSLING, *Dispersion as the key to processing conductive polymers*, *Handbook of conducting polymers*, Edited by Skotheim Elsenbaumer and Reynolds, second edition, 1998, isbn 0-8247-0050-3
- [8] M. KUPKE, H.-P. WENTZEL, K. SCHULTE, *Electrically conductive glass fibre reinforced epoxy resin*, MAT Res Innovat, 2, p.164-169, (1998)
- [9] H.S. KATZ, J.V. MILEWSKI, *Handbook of fillers for plastics*, Van Nostrand Reinhold, ISBN 0-442-26024-5 (1987)
- [10] R. SCHUELER, J. PETERMANN, K. SCHULTE, H.-P. WENTZEL, *Agglomeration and electrical Percolation Behavior of Carbon Black Dispersed in Epoxy Resin*, Wiley & Sons, (1997)
- [11] P. WANG, T. DING, *Conductivity and piezoresistivity of Conductive Carbon Black Filled Polymer Composite*, Journ. Of Applied Polymer Science, 116, p.2035-2039, (2010)
- [12] *The fundamentals of Carbon Black*, Cabot Corporation Billerica, electronic version, URL: <http://www.cabot-corp.com/Downloads/DL200808140916AM8680/> (consulted May 2011)
- [13] P.J. MORELAND et al., *Cathodic protection system and a coating composition therefor*, United States Patent, n° 5,364,511, November 15 1994.

Preface

Science is a continuous search for answers to describe reality. If you would have a look at the historical evolution of many scientific theories, you would find it to be an organic process, marked by important milestones and breakthroughs. But mistakes play a central role in this process too. In fact, the right and the possibility to be wrong is probably as crucial as the aim to find right answers. From this point of view, the word “science” may be confusing, because instead of describing what we know, scientific theories describe what we don’t know for sure, or still try to figure out. The mere thought of all of the scientific research that has been done in the past, and that later appeared to be pure nonsense, is somewhat dizzying. However, the smallest scientific work that is written in the past and present (whether it’s wrong or ‘right’), contributes to the level of “science” mankind has reached so far.

For this reason, I feel grateful and humble for the fact that I’ve been given the opportunity to contribute to the world of scientific research, particularly in its most beautiful branch: engineering sciences. Reinforced concrete (RC) has opened many doors in construction engineering. It is impossible to imagine a world today without this wonderful material. However, despite of its vast and monolithic appearances, it has shown some flaws as well, requiring special care. Corrosion of steel in RC elements may be the number one issue regarding concrete buildings, and is certainly the number one financial loss to concrete repair. Every technique that could be valuable for RC construction restoration and conservation, is a welcome gift to the concrete engineering science.

I also feel a certain urge to apologize for the grammatical language use in this work. First, you could notice that English is not my first language, and therefore some sentences might seem artificial, and some words may turn up too often in a sentence (take ‘therefore’ and ‘however’ for instance: those letters have wrecked my keyboard, so to speak). But more importantly, it has become a habit in scientific texts to write down findings and ideas in an impersonal, so called objective fashion, characterized by complex passive sentences. This may be due to a confusion in objectivity in scientific practice and objectivity in expression and interpretation. In this confusion lays the potential danger of taking things for granted, just because the words sound fair enough. I would *therefore* like to remind you that every word in this text has been written down by a human being, and that there is no such thing as pure objectivity, not even in science.

Acknowledgements

I would like to thank prof. dr. ir. Stijn Matthys and prof. dr. ir. Geert De Schutter, the supervisors of this work, for supporting and promoting my master dissertation.

I would also like to take the opportunity to thank Dorleta Ertzibengoa. She has offered a tremendous help during the past academic year for this dissertation. Her lucid views, feeling for scientific relevance and sense of relativization in stressy periods have made this work possible.

Another word of gratitude is addressed to all of the staff of Magnel Laboratory. It is one thing to learn in theory and read about different subjects, and it's another thing to execute them. They have answered all my questions and helped me with endless patience.

I would also like to thank prof. dr. A. Adriaens extensively for giving me access to her laboratory of electrochemistry, in a busy period of the year. In this laboratory, Alice Elia has offered a great help to execute the measurements, and discuss and interpret the results. This experience has learnt me a great deal on corrosion of metals, in a much more profound way than usual in engineering science.

A special word of gratefulness is dedicated to my parents. In light of the nearing end of my studies, I would like to thank them for giving me the opportunity (amongst many other favours) to study for engineer.

Finally, I would like to thank the persons of the companies that have provided materials for this dissertation. In particular A. Ehrenhart from Evonik, A. De Wildt from Cabot, Y. Van Gorp from Henkel and L. Vasseur from E.C.C.

Contents

Preface	IX
Acknowledgements	X
Contents	XI
List of symbols and abbreviations	XIV
List of figures	XVI
List of tables	XVII
Chapter 1: Corrosion of reinforcement steel in concrete:	1
1.1 Corrosion of a metal	1
1.2 Corrosion of steel reinforcement bars in concrete (RC structures)	3
1.2.1 Carbon initiated corrosion	4
1.2.2 Chloride initiated corrosion	6
1.3 Corrosion rate and measurements	9
1.3.1 Corrosion rate definition	9
1.3.2 Electrochemical corrosion rate measurement	10
1.3.3 Polarization resistance: equation of Stern-Geary (1957) and linear polarization (potentiostatics)	11
1.3.4. Tafel slope measurements, potentiodynamics (PDP)	13
1.3.5 Pulse technique	14
1.3.6 Half-cell or potential mapping	14
1.3.7 Corrosion rate criteria	14
1.4 Cathodic prevention (CPrev) and cathodic protection (CP)	15
1.4.1 Sacrificial (passive) CP	16
1.4.2 Induced Current (active) CP (ICCP)	16
1.4.3 Cathodic Prevention (CPrev)	18
1.4.4 Required protection current	19
1.5 References	21
Chapter 2: FRP use as EBR of RC structures:	23
2.1 Fibre reinforced polymer (FRP)	23
2.2 Polymer matrix	23
2.2.1 General aspects and properties	23
2.2.2 Polymers as FRP matrix	25
2.3 Carbon fibres	25
2.4 Externally bonded reinforcement (EBR) of constructions	27
2.5 FRP for EBR	29
2.6 Passive corrosion protection of steel in FRP wrapped RC structures	30

2.7 Outline of the dissertation	31
2.8 Conductivity of the polymer matrix	32
2.8.1 Conductive polymers: generalities	32
2.8.2. Carbon Black (CB): general aspects, properties and use	33
2.8.2.1 CB as a conductive filler: theories	34
2.8.2.2 Practical issues: viscosity, surface oxidation and influence on mechanical properties	35
2.8.3 Experiment and result for CB filling in epoxy resin	37
2.9 References	39
Chapter 3: Experimental program	41
3.1 Experiment set-up	41
3.1.1 Specimen preparation	41
3.1.1.1 Mortar cylinders	41
3.1.1.2 CFRP wraps	42
3.1.2 Epoxy anodes and specimen matrix	44
3.2 CP program and corrosion initiation	45
3.3 Linear polarization (LP)	47
3.4 Potentiodynamic polarization (PDP)	48
3.5 Preliminary remarks, and discussion CP/immersion program	48
3.5.1 Resistance measurements	48
3.5.2 CP/immersion program	51
3.5.3 Depolarization	53
3.5.4 Wetting condition	54
3.5.4.1 Reference specimens	54
3.5.4.2 CP-specimens	54
3.5.5 Oxidation of the anode connections	54
3.6 Results of electrochemical measurements	55
3.6.1 Results	55
3.6.2 Discussion	58
3.6.2.1 Open circuit potentials (OCP)	58
3.6.2.2 Tafel measurements	59
3.6.2.3 LP measurements	59
3.6.2.4 Conclusions	61
3.7 Mass loss measurement	62
3.7.1 Visual inspection	62
3.7.2 Mass loss	63
3.7.3 Correlation between LP and mass loss measurement	64
Chapter 4: Conclusion	66
APPENDIX A	68
APPENDIX B	69
APPENDIX C	71

APPENDIX D	73
APPENDIX E	74
APPENDIX F	79

List of symbols and abbreviations

50298	Conductive epoxy Eccobond 50298
57C	Conductive epoxy Eccobond 57C
60L	Conductive epoxy Eccobond 60L
64C	Conductive epoxy Eccobond 64C
α	Symmetry factor
ϵ_{fu}	Ultimate strain at failure
ρ	Bulk resistivity, expressed in Ωm
ΔM	Mass or gravimetric loss (g)
ΔN_{react}	Amount of reaction products in mol
ΔN_{reag}	Amount of reacting products in mol
$\Delta V, \eta_{corr}$	Potential difference (V), $\eta_{corr} = E - E_{corr}$
Ω	Ohm
A	Ampère
a_0	activity of oxidator
AR	Anode Reaction
a_R	activity of reductor
B	Stern-Geary constant (V)
b_a, b'_a	Anodic Tafel slope
b_c, b'_c	Cathodic Tafel slope
CB	Carbon Black
CFRP	Carbon Fibre Reinforced Polymer
CoRa	Corrosion Rate
CP	Cathodic Protection
CP-ax-...	Experiment specimen name: Cathodic Protected, Conductive CFRP wrap with axial fibre direction and conductive epoxy adhesive "..."
CP-rad-...	Idem, radial fibre direction
CP-...	Idem, but wrap consists of epoxy "... " only, without fibres
CPrev	Cathodic Prevention
CR	Cathode Reaction
SCE	(saturated) Calomel (reference electrode material)
E	Electrical potential (V)
E_0	Standard potential of a O/R system
E_e, E_{corr}	Equilibrium potential (of a corrosion process)

e^-	electron
<i>EBR</i>	Externally Bonded Reinforcement
<i>ECC</i>	Conductive carbon black filled PC 5800 Carbo epoxy
<i>Epo</i>	Conductive carbon black filled Epo-Tek epoxy
<i>F</i>	Faradays constant (96485 C/mol)
<i>FRP</i>	Fibre Reinforced Polymer
<i>GB</i>	Gewapend Beton
<i>I</i>	Faraday current (A)
<i>I, I_{corr}</i>	(Corrosion) Current density (A/m ²)
<i>I_{prot}</i>	Protection current density A/m ²
<i>ICCP</i>	Induced Current Cathodic Protection
<i>ICP</i>	Intrinsically Conductive Polymer
<i>KB</i>	Kathodische Bescherming
<i>KP</i>	Kathodische Preventie
<i>LP</i>	Linear Polarization
<i>Me</i>	Metal atom or ion
<i>M_m</i>	Molar mass (g/mol)
<i>N</i>	Valence number
<i>O/R system</i>	Oxidation/Reduction chemical system
<i>OCP</i>	Open Circuit Potential (or zero current potential)
<i>Q</i>	Electrical charge, expressed in Coulomb C
<i>R</i>	Ohmic resistance, expressed in Ω
<i>R</i>	Universal gas constant (8,314J/Kmol)
<i>RC</i>	Reinforced Concrete
<i>Ref-...</i>	Reference specimen (experiment)
<i>RH</i>	Relative Humidity (atmospheric), expressed in %
<i>R_p</i>	Polarization Resistance (Ω)
<i>S, S_{corr}</i>	(Corrosion) Surface (m ²)
<i>T</i>	Absolute temperature (K)
<i>Tafel-...</i>	Specimen fabricated for Tafel slope and extrapolation measurement
<i>V</i>	Volt
<i>W/C</i>	Water/Cement ratio (by weight)
<i>wt%</i>	weight percentage (percentage by weight)

List of figures

Figure 1: Typical corrosion cell representation	2
Figure 2: Corrosion system of steel embedded in concrete	2
Figure 3: Faraday current and corrosion current flow [1.22]	3
Figure 4: Typical case of concrete cover spalling	5
Figure 5: Pourbaix diagram of iron in presence of chlorides [1.16]	6
Figure 6: Pit corrosion scheme [1.6]	7
Figure 7: Electro-photomicrographs of passive film breakdown [1.10]	7
Figure 8: Principle of linear polarization (Stern-Geary) [1.14]	11
Figure 9: Correlation study between gravimetric loss and LP measurements [1.13]	13
Figure 10: Tafel slope curve and I_{corr} extrapolation [1.3]	14
Figure 11: Basic idea of cathodic protection: passive (sacrificial) CP (top) and active ICCP (bottom) [1.16]	15
Figure 12: Change in Evans' diagram due to application of ICCP [1.16]	17
Figure 13: Qualitative principle of CPrev [1.20]	19
Figure 14: Graphic result resistivity R measurement of carbon fibre string, vs. string length L	27
Figure 15: σ - ϵ diagram of FRP components, theory (a) and reality (b) [2.5]	28
Figure 16: Qualitative dependence of electrical resistivity on CB. The hatched zone is the "percolation threshold" [2.16].	34
Figure 17: Conductivity course of liquid epoxy resin filled with 0,3vol% CB after dispersion. Mixing between $t=0s$ and $t=105s$ [2.19]	35
Figure 18: Lollypop specimen geometry	41
Figure 19: Axial (ax) and Radial (rad) fibre orientation	43
Figure 20: Schematic CP circuit set-up	47
Figure 21: LP-measurement cell set-up	48
Figure 22: Ohmic resistance of steel/concrete/anode systems for ICCP	49
Figure 23: Resistivity of specimens after CP	50
Figure 24: Typical voltage evolution in time during immersion (= between $t=0$ and $t=60$)	51
Figure 25: One of three aberrant voltage evolutions recorded in the first stage	52
Figure 26: Example of brownish solid product in immersion water	52
Figure 27: Corrosion of the clamps connected to the primary anodes	55
Figure 28: Corrosion rates reference specimens	56
Figure 29: Corrosion rates "ax" specimens	57
Figure 30: Corrosion rates "rad" specimens	57
Figure 31: Corrosion rates fibreless specimens	57
Figure 32: Change in corrosion rate	60
Figure 33: Corrosion products on top part of CP-ECC	62
Figure 34: Corrosion products on reference specimens (Ref-1 top left and bottom, Ref-FRP top right, and Ref-3 middle)	63
Figure 35: Corrosion products on concrete interface	63
Figure 36: Mass losses	64
Figure 37: Assumption I_{corr} evolution	64
Figure 38: Correlation graph LP and mass loss	65

List of tables

<i>Table 1: Corrosion rate criteria</i>	15
<i>Table 2: Recommended strength paramters for conductive paints</i>	18
<i>Table 3: Protection current: practical values [1.22]</i>	19
<i>Table 4: PC 5800 CARBOCOMP epoxy resin properties</i>	25
<i>Table 5: Strength parameters of different types of fibres for FRP [2.3]</i>	26
<i>Table 6: PC CARBOCOMP PLUS fibre properties</i>	26
<i>Table 7: Carbon black properties</i>	37
<i>Table 8: Composition of CB added ECC epoxy</i>	38
<i>Table 9: Composition of CB added Epo epoxy</i>	38
<i>Table 10: Mortar specifications</i>	42
<i>Table 11: Names of specimens</i>	43
<i>Table 12: Conductive epoxies</i>	44
<i>Table 13: Specimen overview</i>	45
<i>Table 14: Epoxy conductivities</i>	49
<i>Table 15: Relative potential drop after depolarization</i>	53
<i>Table 16: Results LP measurements</i>	56
<i>Table 17: Results from Tafel slope measurements</i>	58
<i>Table 18: Average corrosion rate drops between both LP sessions</i>	61

Chapter 1: Corrosion of reinforcement steel in concrete:

General aspects, measurements and cathodic protection

1.1 Corrosion of a metal

The general corrosion process of a metal can be defined as the destruction of the metal at its free surface due to an interaction with its environment at a certain temperature. The emphasis is put on the gradual but continuous destructive aspect: e.g. the chemical formation of a protective oxide layer on the metal surface (avoiding further metal destruction) should actually not be called “corrosive”.

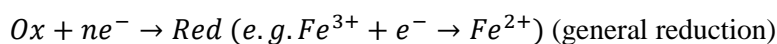
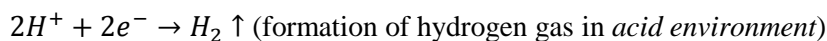
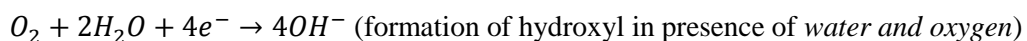
Corrosion can be subdivided in 3 processes that form the necessary conditions for a corrosive process to occur:

- the dissolution of metal ions into the environment: the anode reactions (AR)
- the consumption of electrons: the cathode reactions (CR)
- the mass transport of negative and positive particles: electrolyte solution

A general representation of an AR could be (general oxidation):



where “*Me*” stands for “metal atom or ion”, “*e*” for electron and “*n*” is the number of valence electrons being left behind by the ions. There are different types of cathode reactions (every kind of electron consumption could be a CR), some typical CRs are (reduction) [1.1,1.2,1.3]:



A classic theoretical representation of a stable corrosion process is the ‘electrochemical macrocell’, see Figure 1:

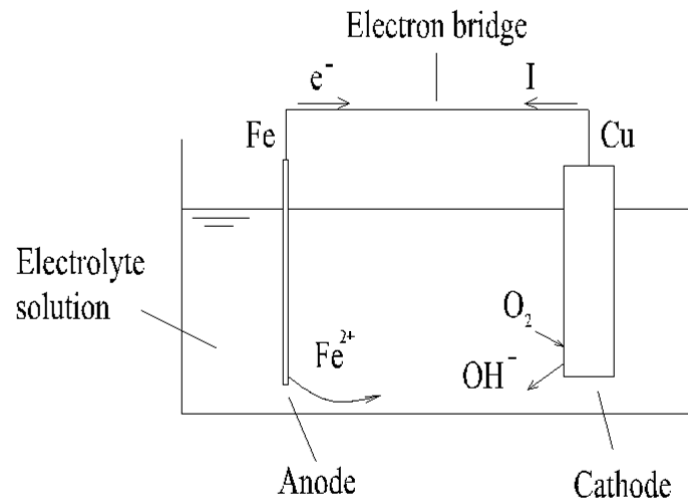


Figure 1: Typical corrosion cell representation

The difference between micro- and macrocell, is the relative long distance between cathode and anode in the latter case. If all reactions take place relatively close to the metal surface the system is called a microcell.

Conventionally, the direction of a movement of positive charges is associated with the direction of a current. Thus, the three processes mentioned before, form a closed current circuit as depicted in Figure 2. This current, called ‘Faraday current’, always involves a chemical transformation. A corrosion process is therefore an **electrochemical process**. An electrochemical process is “a reaction that includes a transfer of electrical charges – usually electrons – through the surface of an electrically conductive material (electrode) and an ion-conductor (mostly electrolyte solution)” [1.4]. It is important to notice that in a corrosion system part of the Faraday current consists of positive ion displacement (“electro-migration”). The Faraday current is directly related to the chemical activity (the amount of ions that has been formed, but also the rate at which the reaction occurs).

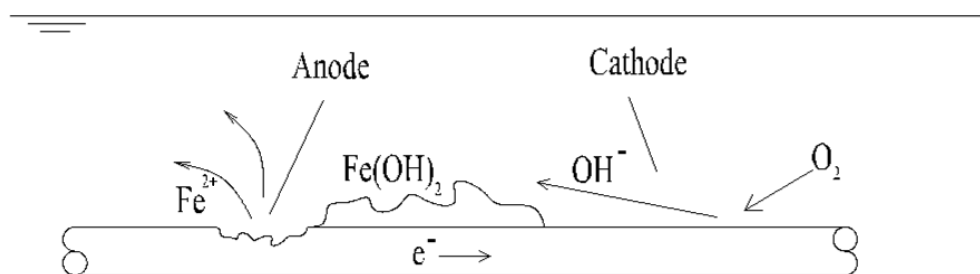


Figure 2: Corrosion system of steel embedded in concrete

Another important characteristic of corrosion processes is the electrical potential: when positive ions move away from the metal surface, they leave this surface behind negatively charged, and form a positive area near the surface. Between these two zones (cathode and anode) an electrical field is established.

The more the corrosion process takes place, the higher the relative potential drop between cathode and anode will be. Both processes (AR and CR) influence each other, and are strongly influenced by their

environment (e.g. some CR are accelerated in an acid environment, or wet/dry cycled environment). Eventually, it will become more and more difficult for metal ions to dissolve, because of the inversely oriented electrical field: a (dynamic) equilibrium will be established and further metal destruction stops: the “corrosive” process in its specific definition shuts down (in practice this is often a safe situation). Some environmental change (e.g. a facilitated CR or AR, or the swift movement of ions through the environment) can cause a shift in potential: the equilibrium will move to another equilibrium potential. A continuous “corrosive” process is therefore characterised by an electrochemical disequilibrium.

This is only a narrow view on general corrosion processes, and its many parameters. Instead of getting into detail on electrochemistry in general, this short introduction will immediately focus on corrosion of steel reinforcement bars in a concrete environment. Specific problems or measurement techniques of electrochemical processes will also be discussed in this specific domain.

1. 2 Corrosion of steel reinforcement bars in concrete (RC structures¹)

In spite of the protective concrete surrounding, steel reinforcement bars can corrode too. The anode reactions consist of different dissolutions of iron atoms into the concrete mix (oxidation):

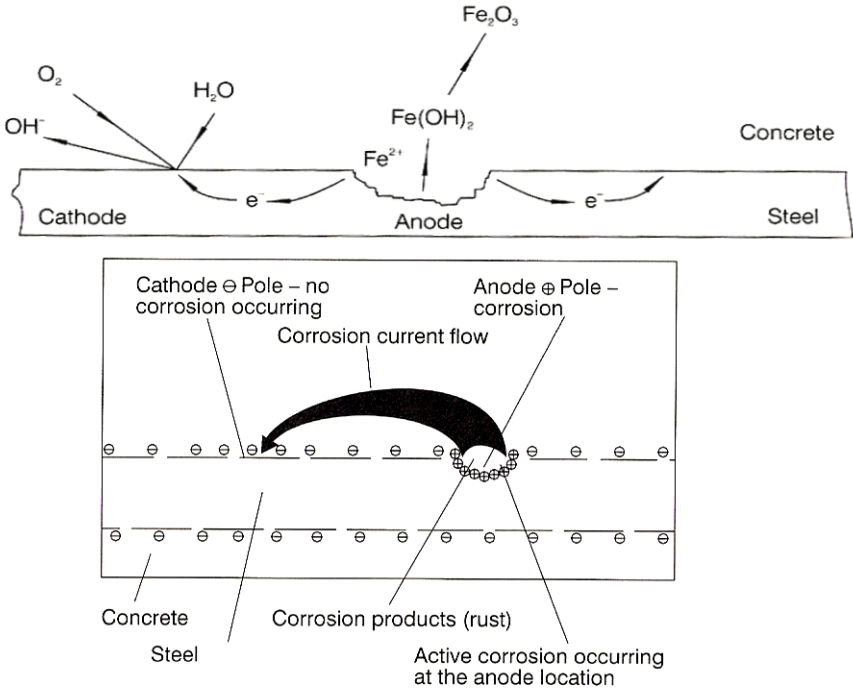
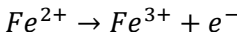
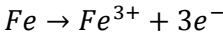
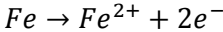


Figure 3: Faraday current and corrosion current flow [1.22]

¹ Reinforced Concrete structures

Figure 3 depicts the Faraday current in a RC structure. The current flow of ions through the concrete is called “corrosion current flow”. The figure shows some necessary ingredients for an ongoing corrosion process. In absence of water or oxygen, for instance, a corrosion process cannot continue².

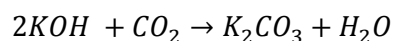
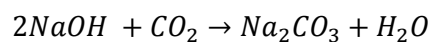
For steel reinforcement of RC structures two main mechanisms of corrosion initiation are distinguished: carbon initiated corrosion and chloride initiated corrosion.

1.2.1 Carbon initiated corrosion

This mechanism is caused by a dealcalization of the concrete surrounding the steel bar. Some soluble alkaline products, a.o. NaOH, KOH and Ca(OH)₂, are formed during the hydration process of cement in concrete. These hydroxides are responsible for the high alkalinity of young concrete mixtures, resulting in pH values possibly higher than 13 [1.3,1.5, 1.6,1.22].

This alkaline environment is a safe situation for steel reinforcement: the initial corrosion products form a dense and impenetrable film around the steel surface. This phenomenon is called “**passivation of the steel**”, because as soon as the film totally encloses the steel surface, a continuous and destructive corrosion process is inhibited³. The higher the alkalinity of the concrete, the greater the protective quality of the passive film [1.22]. Oxygen (and water) necessary for this initial process is believed to be sufficiently present in the mixed water [1.5]. The passive film is thought to consist of several layers of different ferrous oxides (Fe₂O₃, Fe₃O₄) [1.7, 1.23], and probably some minerals originated from the cement paste. It is also generally accepted that the passive film is in a dynamic equilibrium with the concrete: i.e. continuously dissolving in it and re-establishing. Furthermore it is likely that a passive oxidation film allows a small stray current discharge from the passivated steel without mass loss, depending on the resupply of alkalinity [1.22], contrary to the earlier public opinion that stray currents were the main cause of reinforcement bar corrosion.

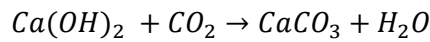
The penetration of acids into the concrete will neutralize the alkaline environment, and allow the destructive corrosion process to start. A typical threshold pH value for overall depassivation of the steel is 8 to 9 [1.2,1.3]. The most important acid causing this corrosion is atmospheric CO₂ (about 0.3% in air)⁴. The process of CO₂ penetration through the concrete after drying out is called “**carbonation**”. The alkaline elements in the concrete mentioned before (Na(OH), Ka(OH), Ca(OH)₂) will form their respective carbonates:



² A typical example is the low corrosion rates, measured in permanently submersed RC structures in aggressive environments like saline seawater [1.22]: low oxygen concentrations and low oxygen diffusion rates in permanently submersed structures.

³ This is often seen as the most important protective role of concrete against corrosion. [1.10] also mentions a thin aggregate-free film of portlandite (Ca(OH)₂) around the steel bar with inclusions of Calcium Silicate Hydrate gel (CSH) – being a less secure protection due to its discontinuity.

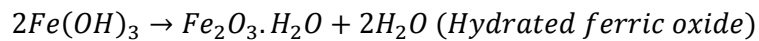
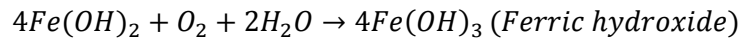
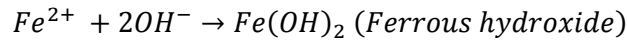
⁴ Corrosion damage due to specific acids from fabrication processes, inorganic fertilizers silos etc. have also been recorded: HCl and H₂SO₄ react with CSH from the cement gel to form a strong silicic acid. Sewage water typically contains high amounts of sulfates and sulfites. Anaerobe bacteria transform these sulfur containing elements into H₂S. Sewage pipes with a free water surface contain enough oxygen to form H₂SO₄ [1.2]. In atmospheric air CO₂ is the most important acid, and to a much smaller extent SO₃.



Calciumsilicates and calciumaluminates are also transformed [1.3].

Several small cathodic and anodic regions form on the steel surface, which are alternated in time, resulting in a more or less uniform corrosion [1.1,1.2].

One of several chemical processes in pH lower than 8-9 circumstances is shown below [1.6]:



This is the well known red to brown coloured corrosion product: a mixture of ferrous and ferric hydroxide and ferric oxide (rust). It has a much more porous structure, allowing water and oxygen to penetrate more easily to the undamaged steel. Furthermore, these products have a much larger volume compared to the undamaged steel or passive layer (about 2 to 6 times the volume of the steel [1.6]). The depassivation of steel is therefore characterized by an important **volume expansion**. In a further stage this volume expansion will induce forces in the surrounding concrete cover. If these forces exceed the tensile strength of the concrete cover, cracks will form and spalling of the concrete cover may occur. Cracks and spalling expose the steel to the environment and thus increase the vulnerability of the concrete against water and oxygen penetration and increase the corrosion rate. The concrete cover thickness is an important protection parameter against corrosion in two ways: firstly to slow down the carbonation process, and secondly a thicker and better protection against cracking and spalling.

In most cases the uniform corrosion process is rather slow and secure: no local steel destruction (diameter reduction of steel rods), neither significant corrosion rates occur, especially in stable environments (an average corrosion rate of 0.13mm/year has been estimated for steel structures unprotected by concrete [1.1]). E.g. concrete inside buildings dries out rather quickly, possibly causing a swift carbonation process. If the concrete remains dry, no significant corrosion damage will occur. However, as soon as the concrete cover cracks and spalling occurs (Figure 4), the risk for structural damage to the RC element increases.



Figure 4: Typical case of concrete cover spalling

A corrosion process is always characterized by a certain potential difference between cathode and anode. In electrochemistry the potentials are expressed in absolute terms, with regard to a certain

reference potential (electrochemical measurement methods always use a ‘reference electrode’⁵). In a Pourbaix diagram (sometimes called pH-diagram) a realistic range of possible metal potential values are plotted against pH-values (see Figure 5). The diagram shows different zones of metal conditions. These diagrams are analytical deductions of the Nernst-equation⁶, and give information about thermodynamically “possible” situations. Additionally they are highly dependent on every specific situation (many other environmental parameters, besides alkalinity). For these reasons Pourbaix diagrams are only used for theoretical comprehension and explications, rather than corrosion rate measurements [1.4,1.9].

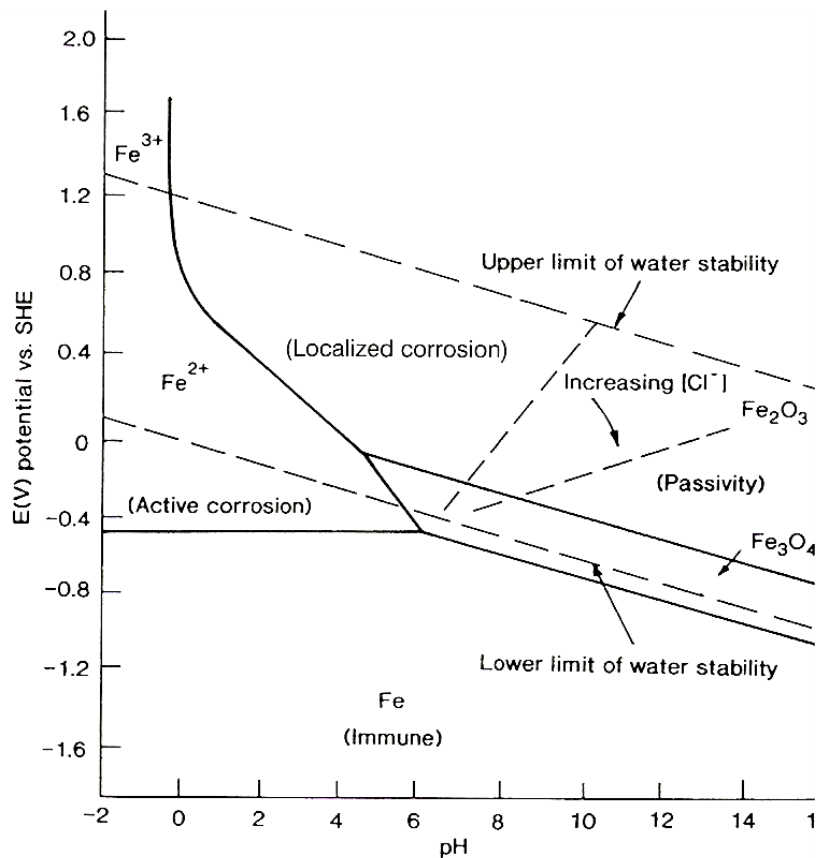


Figure 5: Pourbaix diagram of iron in presence of chlorides [1.16]

1.2.2 Chloride initiated corrosion

A much more local, quicker and potentially more dangerous way of depassivation is *chloride initiated corrosion*. Chlorides and in general aggressive negative ions are able to destroy the passive film very locally, creating acid corrosion pits (‘pit corrosion’). Thus, this mechanism should be seen as a **local breakdown of the passive film**, rather than an overall depassivation (it is not necessarily accompanied by a drop in pH value).

⁵ Different types of reference electrodes (RE) are commonly used. They are supposed to have a constant absolute potential and relative potential difference between each other. Some typical examples are included in APPENDIX A.

⁶ See section 1.3.2 Electrochemical corrosion rate measurement on electrochemical corrosion rate measurements.

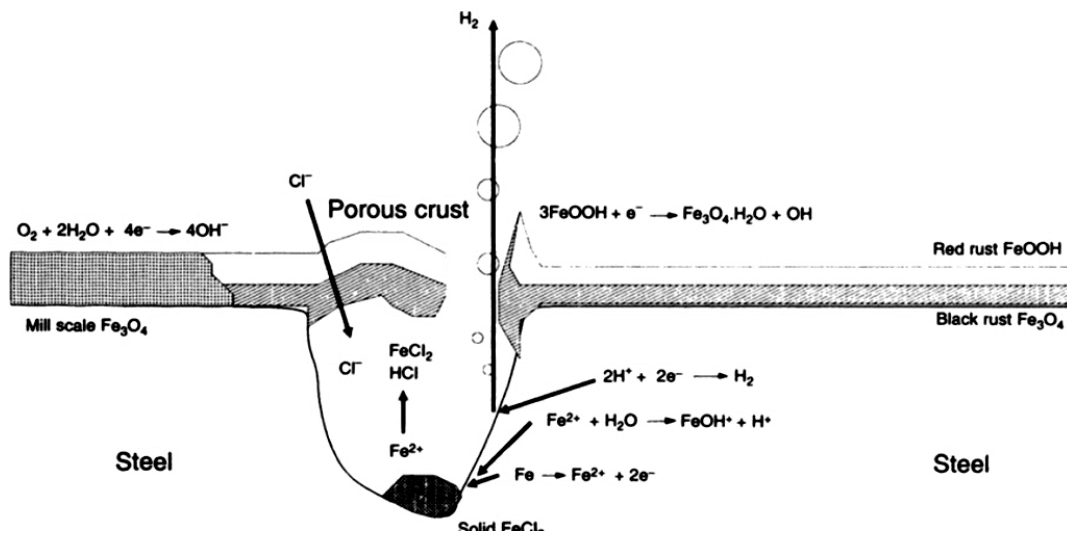


Figure 6: Pit corrosion scheme [1.6]

Research has been done to determine the precise influence of chlorides. Some researchers state that chlorides should be seen as catalysts of the depassivation process [1.6,1.22]. Others [1.10] state that chlorides penetrate through the film, resulting in a bond break between the film and unharmed steel. Electro-photomicrographs of the corrosion pits in this research show torn and curled bits of film, comparable to an old layer of paint coming off a wall (see Figure 7).

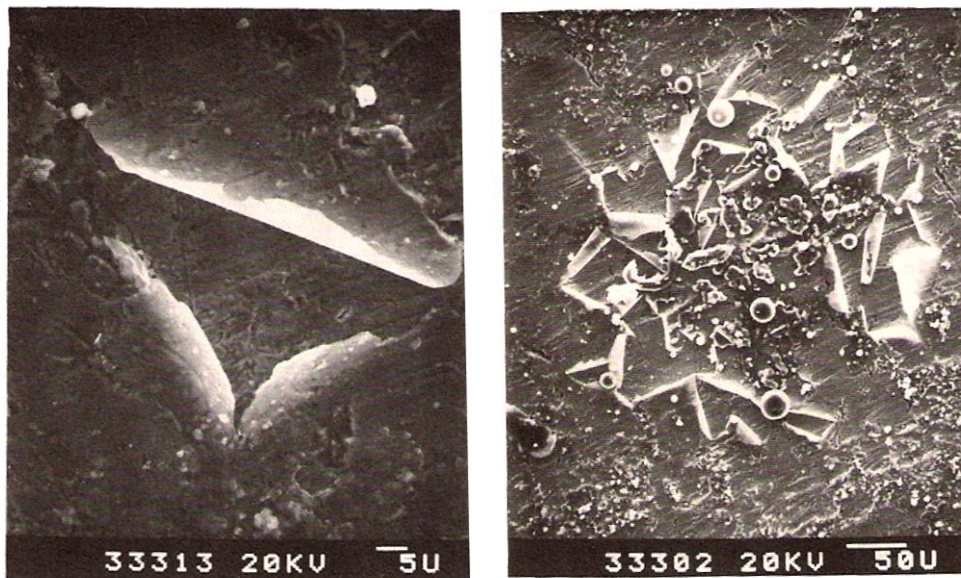


Figure 7: Electro-photomicrographs of passive film breakdown [1.10]

In the same research [1.10] it is confirmed that there is a change in composition from Fe_2O_3 (tending to $\text{Fe}(\text{OH})_2$), towards $\text{Fe}_2\text{Cl}(\text{OH})_4$ or $(\text{Fe}(\text{OH})_2)_2\text{Cl}$ and HCl . Moreover, it distinguishes no difference in internal chloride attack (chlorides mixed in mortar) and external attack (chloride penetration in sound mortar), besides the slower initiation process in the latter situation. About 75-90% of the chlorides mixed in the mortar are 'stocked' in chloroaluminates (depending on the chloride concentration and degree of hydration), but remain in dynamic equilibrium with the chlorides in

solution (so they can resupply chlorides in pore water solution) [1.3,1.22]. The formation of FeCl_2 in this process might explain the green to brownish colour of the concrete surrounding the bar (and sometimes visible at the concrete surface) [1.2,1.3,1.6,1.22]. [1.3] resumes, compares and refers to different theories regarding the breakdown of the passive film.

In old RC structures chlorides were often mixed in the mortar to accelerate the hydration process, mostly in the form of CaCl_2 (this was done up to the 1970s according to [1.2] and [1.3], and prohibited in Belgium afterwards). Nowadays chloride contamination still forms a threat in marine structures (saline water environment) and due to the usage of de-icing salts [1.2,1.6,1.22].

Another important and much discussed subject, regarding chloride initiated corrosion, is the **threshold chloride concentration**: the process only starts from a certain chloride concentration. [1.11] distinguishes different manners of expressing the critical chloride content:

- Total chloride content by weight of the concrete sample
- Total chloride content by weight of cement (or binder)
- Water soluble chloride (or ‘free chlorides’) content by weight of the concrete sample
- Free chloride content by weight of cement
- Cl^-/OH^- ratio

Although the last form is regarded as the most rigorous expression (because it also accounts for the alkalinity), it is difficult to obtain exact concentration values of OH^- . The same can be said about free chloride contents. Therefore, in this work it has been decided to work with the total chloride content by weight of cement.

Many researchers have studied the critical concentration value, and about as many different values have been concluded. [1.3], [1.11], [1.12] and [1.22] sum up values from different researches. They range from 0,10 to 0,40% by weight of the cement according to [1.22], from 0 to 17 Cl^-/OH^- ratio according to [1.11]. [1.2] is only one of many normative documents suggesting a simple rule to avoid chloride initiated corrosion, in this case 0,3% by weight of cement in concrete mixtures. However, in many corrosion research articles in which accelerated corrosion tests are done by mixing chlorides in the concrete mix, much higher values are often used (3 to 5% and higher of chlorides by weight of cement added). It is of much greater interest to briefly discuss the influencing parameters causing this wide ranges of critical concentrations. Amongst those parameters are such diverse elements as [1.3,1.6,1.11]:

- Type and amount of cement (binding capacity of cement paste)
- Presence of air voids near steel surface (mortar compaction)
- W/C ratio (amount of water)
- Temperature
- Type of cation accompanying the chlorides (typically Na^+ or Ca^{2+})
- Oxygen content in pore water solution
- Chemical composition of the steel
- Surface roughness and presence of rust
- The electrical potential of the steel
- The electrical resistivity of the concrete, relative humidity and other aspects influencing the rate of chloride penetration [see literature]

- The corrosion initiation criterion can depend on the type of measurement done in situ on existing RC structures, or in laboratory conditions (in the latter case experiments can be done either in an artificial pore water solution, on mortar samples and concrete samples)

Because of the high number of parameters, preference is given to a statistical approach of the problem in [1.12].

All of these elements immediately suggest the worst case scenario for chloride initiated corrosion to take place, besides the presence of chlorides: a cyclic wet-dry alternation in saline water, preferably in ill-compacted concrete with low cover. This situation allows water, oxygen and chlorides to access easily to the concrete. Furthermore it is noted by different authors that Portland based cement types have a higher initiation threshold, but are more easy for chlorides to penetrate. Thus the influence of cement type is dependent on the specific situation.

It is worthwhile to notice that marine structures exposed to tidal waves (or wave spray) are therefore particularly sensitive to chloride initiated corrosion.

1.3 Corrosion rate and measurements

1.3.1 Corrosion rate definition

The corrosion rate, CoRa, is defined according to [1.13] as ‘the amount of metal loss due to corrosion per unit of exposed surface and accumulated during a certain period of time’:

$$CoRa = \frac{\text{metal loss}}{\text{unit of surface and time}} = \frac{\Delta M}{s \cdot t} \quad (1.1)$$

The gravimetric or mass loss, ΔM , is the weight difference before and after having exposed the metal to a corrosive process. It is an averaged value (assumption of uniform corrosion) [1.13]. In spite of the obvious drawback of this corrosion rate measurement that it is destructive – and therefore mostly limited to laboratory measurements – it is still used in many researches as a robust reference to electrochemical measurements: all of the actual corrosion products weight (taking account of the real history of the steel) integrated over a certain period of time, are measured.

Faraday’s law is the link between weight loss and the electrochemical reaction, translated into an electrical current [1.4]:

$$Q = \int Idt = \pm(\Delta N_{reag})nF = \mp(\Delta N_{react})nF = \frac{\Delta M}{M_m} nF \quad (1.2)$$

Or simplified [1.13]:

$$\frac{i \cdot t}{F} = \frac{\Delta M}{M_m/n} \quad (1.3)$$

Where

i : an electrical Faraday current (Ampère)⁷
 t : time (seconds)
 F : Faraday's constant (96 485 Coulombs/mol)
 ΔM : molar mass loss due to corrosion (g/mol)
 M_m : molecular or molar mass of the metal (g/mol or g)
 n : valence of the metal (2 for steel)

The current i divided by the metal surface area is called 'corrosion current density', or 'corrosion current' I_{corr} , expressed in A/m^2 . The previous equation links mass loss directly to the electrochemical corrosion current. Conversion to $\mu m/year$ of attack penetration is possible through the metal density: $I \mu A/cm^2$ is equivalent to an attack penetration rate of $11,6 \mu m/year$ [1.13].

1.3.2 Electrochemical corrosion rate measurement

The electron transfer process is described as a function of the electrode potential by the Butler-Volmer equation [1.4]:

$$i = i_a + i_c = nFk^0 \left(a_R e^{(1-\alpha)\frac{nF}{RT}(E-E_0^0)} - a_O e^{-\alpha\frac{nF}{RT}(E-E_0^0)} \right) \quad (1.4)$$

Where k^0 is a rate constant, α a symmetry factor, and a the activity of oxidator and reductor. T is the absolute thermodynamic temperature and R is the universal gas constant ($8,314 Jmol^{-1}K^{-1}$). E_0 is the standard potential of the O/R-system⁸. The equilibrium potential of a corrosion system is then described by the equation of Nernst:

$$E_{corr} = E_0 + \frac{RT}{nF} \ln \left(\frac{a_O}{a_R} \right) = E_0 + \frac{RT}{nF} \ln \left(\frac{a_O^\infty}{a_R^\infty} \right) \quad (1.5)$$

In a stable corrosion process both currents at the anode and cathode are equal, which means $i=i_a+i_c=0$. This value of the corrosion current at cathode and anode is the actual corrosion rate as defined. The net current value is zero, and therefore not directly measurable.

This is why in electrochemical rate measurements, the corrosion process is brought to a disequilibrium: the metal surface is deliberately polarized (using an external counter electrode), causing a potential difference with the actual corrosion potential E_{corr} . It is now possible to evaluate the actual corrosion rate i_{corr} combining equation (1.4) and (1.5), evaluated for E_{corr} (for further detail see e.g. [1.3]):

$$i_{corr} = i_{0,a} e^{\alpha f (E_{corr} - E_a)} = -i_{0,c} e^{\alpha c f (E_{corr} - E_c)} \quad (1.6)$$

In this equation $f=F/RT$ and the difference in symmetry is caused by the factor n . Combining this equation with $i=i_a+i_c=0$, gives us i as a function of the change in potential (due to polarization):

$$i = i_{corr} (e^{\alpha a f \eta_{corr}} - e^{\alpha c f \eta_{corr}}) \quad (1.7)$$

⁷ In literature i mostly stands for 'electrochemical current' (A), whereas I stands for current density (A/m^2), obtained by dividing i by the (mostly initial) metal surface area.

⁸ I.e. the equilibrium potential of the O/R system, at which both activities of O and R are equal.

Or simplified:

$$i = i_{corr} \left(e^{\frac{\eta_{corr}}{b'_a}} - e^{\frac{\eta_{corr}}{b'_c}} \right) \quad (1.8)$$

Where $\eta_{corr} = E - E_{corr}$, and E is the variable. b'_a and b'_c are called ‘Tafel slopes’ (see further).

1.3.3 Polarization resistance: equation of Stern-Geary (1957) and linear polarization (potentiostatics)

If the corroding metal is polarized over very small polarization differences η_{corr} , the relation between η_{corr} and i is linear (see Figure 8).

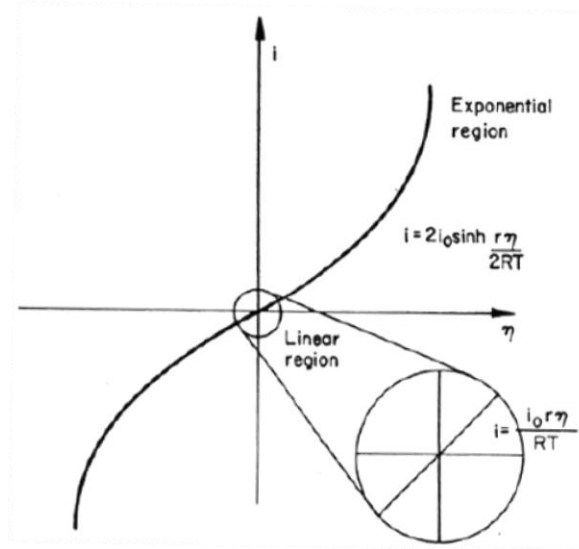


Figure 8: Principle of linear polarization (Stern-Geary) [1.14]

First order differentiation of the previous equation, results in:

$$\left(\frac{\partial i}{\partial E} \right)_{E_{corr}} = i_{corr} \left(\frac{1}{b'_a} + \frac{1}{b'_c} \right) = i_{corr} \left(\frac{2,303(b_a + b_c)}{b_a b_c} \right) \quad (1.9)$$

Where $b_a = 2,303b'_a$ and $b_c = 2,303b'_c$. Equation (1.9) is the slope of the linear region. Stern and Geary inversed this relation, and called it the ‘polarization resistance R_p ’:

$$R_p = \left(\frac{\partial E}{\partial i} \right)_{E_{corr}} \quad (9) = \frac{B}{i_{corr}} \quad (1.10)$$

Where B is a specific constant of the corrosion system (!):

$$B = \left(\frac{2,303(b_a + b_c)}{b_a b_c} \right)^{-1} \quad (1.11)$$

⁹ Sometimes this equation is expressed as a limit for $\eta \rightarrow 0$, meaning the corrosion current and potential are evaluated near the actual corrosion potential.

The essence of a linear polarization measurement (LP measurement) is to measure the slope of the polarization curve. This allows us to calculate the corrosion rate, using the Stern-Geary equation:

$$i_{corr} = \frac{B}{R_p} \text{ or } I_{corr} = \frac{B}{R_p \cdot S_{steel}} \quad (1.12)$$

S_{steel} is the corroding steel surface. In literature the Tafel slopes b_a and b_c (hence value of B) are often estimated (especially for field applications): $B=52mV$ for passive steel and $B=26mV$ for active corrosion, are common values (the exact source is difficult to determine). However, it is possible to determine B for a specific system, using a ‘Tafel slope measurement’ (see paragraph 1.3.4. *Tafel slope measurements, potentiodynamics*).

The above relations may only be used for small polarization potentials, in practice values of $E_{corr} \pm 20mV$ are applied. Typical polarization rates for this technique are of the order of magnitude 0,15mV/s. The reason for the low polarization rates in LP and PDP measurements, according to [1.13] is the so called “double layer”: a layer of electrical charges in direct contact with the metal. This layer has a capacitive effect on the steel. To avoid influences of the layer, the metal should more or less be in a steady state at any time during the measurement, by polarizing slowly.

The most important advantage of LP measurement – besides its remarkable simplicity – is its non-destructive character: thanks to the very small polarization potentials no noticeable disturbance of the corrosion surface takes place.

[1.6] mentions some limitations of the LP testing method. Their first remark states that the instantaneous corrosion rate – at the moment of measuring – is being measured, whilst in practical applications the ‘integrated (averaged) corrosion rate’ over a certain period of time is of more interest. This drawback can be overcome by measuring repeatedly in different conditions (humidity, temperature...).

A second limitation is the risk of errors of factor 10 to 100 in the estimated area of measurements, especially at low corrosion currents. “If corrosion is at a few pits it will underestimate the corrosion rate in the pits and overestimate the general corrosion rate. If it is known that there is pitting corrosion, then corrections can be made based on the fact that corrosion rates in pits are five to ten times that of generalized corrosion.” [1.6]

A third limitation is the fact that the active corrosion zone can possibly be concentrated at the top of the reinforcement bar. In this case the LP-device may only send current to the top steel (this error increases if the total steel surface area – or reinforcement bar length – increases, as remarked in [1.13]).

For this reason correlation studies have been done (e.g. in [1.13]) between LP measurements and gravimetric loss measurements (after an assumption for the change of the corrosion current in time has been made, to integrate I over time), see Figure 9. In this research it has been concluded that the Stern-Geary equation contains an intrinsic error of factor 2.

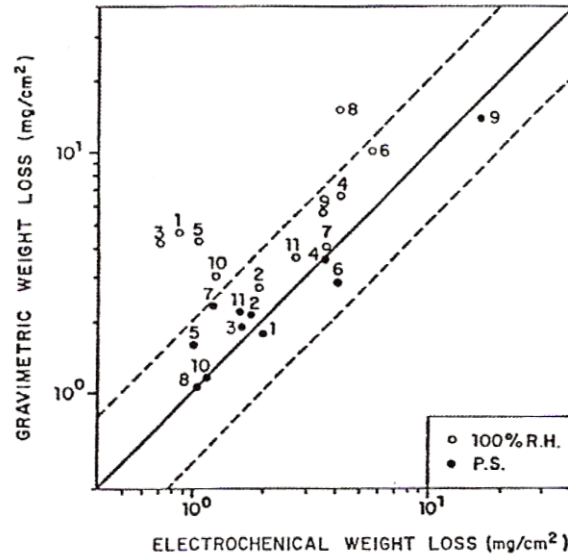


Figure 9: Correlation study between gravimetric loss and LP measurements [1.13]

Indeed, “From these errors”, it is concluded in [1.6], “the best accuracy that can be expected from a LP device is a factor 2 to 4 (Andrade *et al.*, 1995). However, the scale is logarithmic so much errors are less critical than they may seem”.

1.3.4. Tafel slope measurements, potentiodynamics (PDP)

Tafel slope and ‘potentiodynamical’ measurements are very similar. The important difference of these measurements compared to LP-measurements, is the wider polarization potential range: $E_{corr} \pm 250mV$ for Tafel and even higher in potentiodynamics, e.g. $-250mV$ to $+1,5V$. Polarization rates should be lower than $2,5mV/s$ according to [1.3].

If the logarithm of the measured corrosion current is represented as a function of the metal potential, from equation (1.8) a linear relation can be observed:

$$\ln|i| = \ln(i_{corr}) + \frac{\eta_{corr}}{b'_a} \tag{1.13}$$

$$\ln|i| = \ln(i_{corr}) - \frac{\eta_{corr}}{b'_c}$$

Thus, the slopes of the measured anodic and cathodic curve give specific information about the ‘Tafel slopes’ of the corrosion current, enabling calculation of B in the Stern Geary equation. Furthermore the extrapolation of these linear curves points out the actual corrosion current and potential, as depicted in Figure 10.

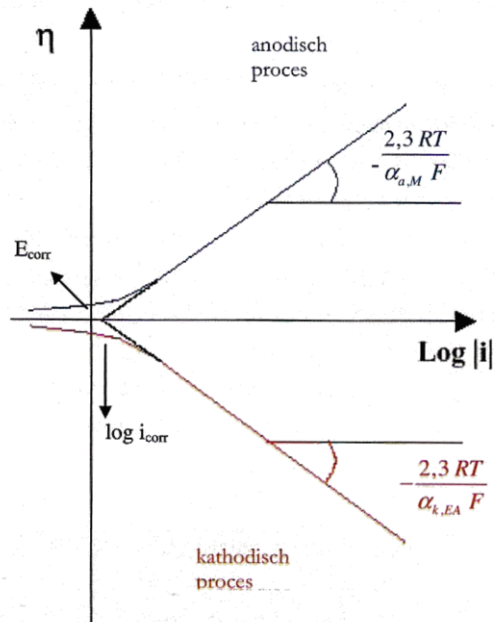


Figure 10: Tafel slope curve and I_{corr} extrapolation [1.3]

1.3.5 Pulse technique

A third and more recent electrochemical corrosion rate measurement technique is based on alternated current (pulse) technique (also called impedance spectroscopy) [1.3,1.8]. The steel/intermittent zone/concrete interface is electrically modelled as a Randles circuit, in which the capacitor represents the double layer at the interface zone. The polarization resistance can be deduced from the potential response (output) to galvanostatic pulses (input).

In this dissertation this technique will not be used, and therefore not discussed into detail.

1.3.6 Half-cell or potential mapping

This technique was first described by Stratfull in 1978 [1.9], and is remarkably simple. It measures the absolute potential of a steel bar underneath a concrete cover surface locally (therefore called ‘mapping’). A reference electrode, connected to a voltmeter, is held against the concrete surface with a wet sponge between both. No current (or potential change) is induced in this system (hence the name ‘half cell’, as a quasi “open circuit”: the device is provided with a high internal resistance). This technique is widely used in field applications to reveal corrosion activity (e.g. in concrete bridges [1.9]). However, actual present corrosion rate can’t be measured with this technique in an easy way [1.1,1.9,1.15], because the net corrosion current of the steel is zero. The results are more of a qualitative significance.

1.3.7 Corrosion rate criteria

Different sources [1.6,1.13,1.19] mention the same criteria to judge corrosion rates obtained from electrochemical measurements (Table 1):

	Criterion	Corrosion condition
I_{corr}	$< 0,1 \mu\text{A}/\text{cm}^2$	Passive condition
I_{corr}	$0,1 \text{ to } 0,5 \mu\text{A}/\text{cm}^2$	Low to moderate
I_{corr}	$0,5 \text{ to } 0,1 \mu\text{A}/\text{cm}^2$	Moderate to high
I_{corr}	$> 1 \mu\text{A}/\text{cm}^2$	High

Table 1: Corrosion rate criteria

Absolute maximum values, according to Andrade et al. [cited in 2.11] range between $100\text{-}200\mu\text{A}/\text{cm}^2$.

1.4 Cathodic prevention (CPrev) and cathodic protection (CP)

As mentioned before, a corrosive protection is characterized by a corrosion current: the cathode/anode interaction form a closed circuit. The *Faraday current* is the electrochemical activity at the steel/concrete interface. The *corrosion current flow* is the ionic flow movement of dissolved metals through the concrete (moving towards a zone where CRs (e.g. formation of oxides, hydroxides etc.) take place). The (very) basic idea of cathodic protection or prevention is to slow down the corrosion process (after depassivation) or avoid depassivation, respectively, by introducing an inverse current to the corrosion current system.

This can either be done by introducing a sacrificial anode, or by active current impression (see Figure 11).

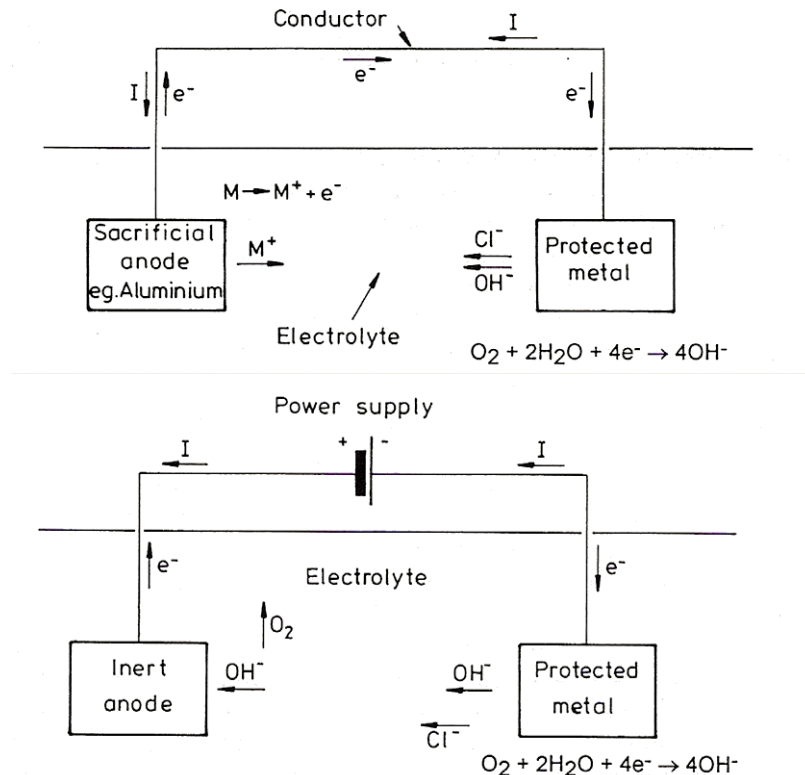


Figure 11: Basic idea of cathodic protection: passive (sacrificial) CP (top) and active ICCP (bottom) [1.16]

1.4.1 Sacrificial (passive) CP

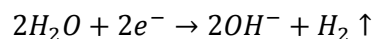
For the first system, the anode consists of a sacrificial metal: this metal will sacrifice itself by taking part of the anode reactions (“corrode”), rather than the protected metal (for the given corrosion system the anode has a lower equilibrium potential than the steel bar). Some kind of electrical connection between both metals has to enable the electrons, left behind by the dissolved sacrificial ions, to move towards the protected steel. The protected steel is thus “provided of enough electrons”, so its anode reactions are slowed down. A well known application of sacrificial CP is the usage of Zinc-blocks attached to ship hulls, to protect them against corrosion (in aggressive sea water conditions).

1.4.2 Induced Current (active) CP (ICCP)

The experimental program in this dissertation tries to prove and discuss the feasibility of active cathodic protection by induced currents (ICCP) of steel reinforcement bars, using externally bonded carbon fibre reinforcement as an anode. Therefore emphasis will be put on this system in the following. In ICCP an ‘inert’ anode is used as an electrode. The protected steel bar is the second electrode. Both electrodes are connected to a DC power supply, creating a potential difference and giving a more negative potential to the protected steel. In this situation the anode is also destabilized, with increased risk of corrosion; the more this material is inert against corrosion in acid environment, the more sustainable the CP system is.

It is interesting to go further into detail on the electrochemical background of this principle, for full understanding of ICCP [1.16]. Under normal corrosion circumstances the metal surface supports both AR and CR (Figure 2). In this system the net current is zero ($i_a+i_c=0$). Figure 12 depicts the linear plots of both AR and CR in a E versus $\log(i)$ graph (“Evans’ diagram”). The point where both lines meet (point A), is the actual stable corrosion state (since both currents are equal in this point).

ICCP lowers the corrosion potential and thus current (rate), by applying a certain current I_{app} . Part of this current will slow down the AR (slope ‘C’), while another part will accelerate the CR - which is normally no problem for the corrosion system. The system has a lower (read: safer) potential, called “protection potential E_{prot}^{10} ”. If the steel bars are overprotected, some CRs may be activated, causing a potential harm to the steel-concrete interface. For instance the somewhat forced reduction of water into hydrogen gas may cause this degradation[1.16]:



This overprotection is also a waste of energy.

It is theoretically possible to ‘shut down’ the AR (see I_{app} ” in the figure), but this is also economically not justifiable.

¹⁰ This term is sometimes also used for thermodynamically immune potential zones in Pourbaix diagrams.

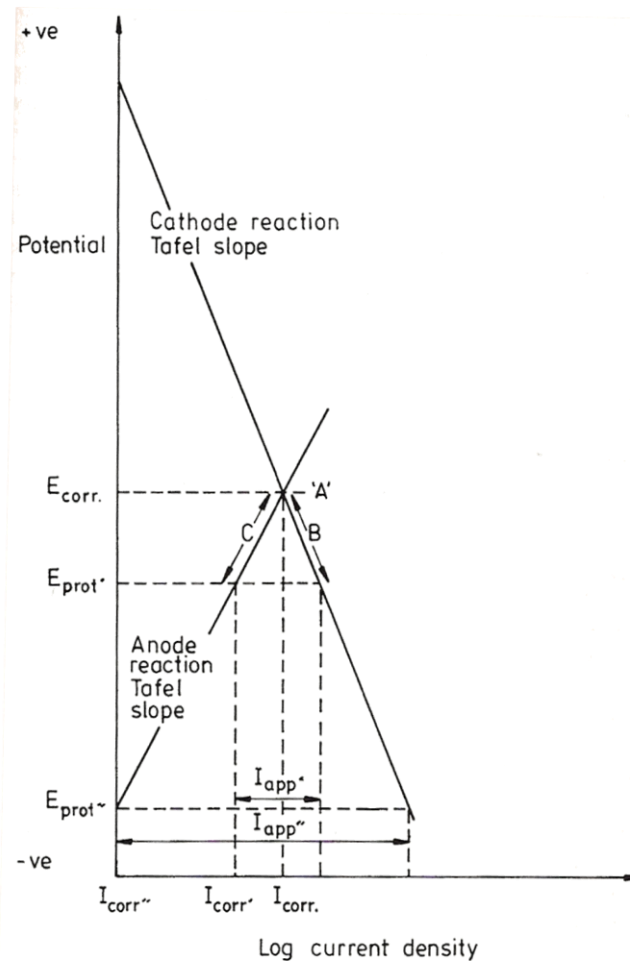


Figure 12: Change in Evans' diagram due to application of ICCP [1.16]

A diverse range of anode types for ICCP is available in the market [1.17,1.22,1.26]. They can be subdivided in three main principles:

- Conductive mortars and coatings
- Anode strips and grids (mostly metallic, sometimes carbon fibre grids) applied onto the concrete surface
- Bored wire or strip anodes

An extended overview is given in [1.26]. The anode type that is being investigated in this work, rather tends towards a conductive coating type. It consists of primary anodes (typically strips or wires, embedded in the coating), that spread out the current over an extended coating surface. Besides the relatively low cost prices and ease of application, these systems show good current spread and overall CP protection, compared to other systems [1.26]. It may also be noticed that the application of conductive coatings is very similar to the application of epoxy resins of CFRP EBR systems.

For large surface applications some rules regarding maximum length of primary anodes should be respected [1.17].

[1.17] also mentions some recommendations for conductive coating anodes, which are of interest for this dissertation. Primary anodes in combination with conductive coating secondary anodes should be applied on the concrete surface. The distance between the primary anodes depends on the conductivity

of the coating (mostly about a couple of meters). The potential drop between any two points of the coating surface should be at most 10% of the potential difference applied by both electrodes of the power supply.

The resistivity of the coating should stay below $1\Omega cm$. This can be controlled, according to [1.17] by applying a coating strip of $7,5 \times 185 cm^2$ and a thickness of $0,130$ to $0,15 mm$ on an insulating surface. The ohmic resistivity between two conductive wires embedded on both ends into the coating is measured, and should be no more than 25Ω .

The anode surface current density has a short term limit of $35 mA/m^2$, and a long term limit of $20 mA/m^2$. Conductive coating applications in the past decade have shown a service life duration of over 10 to 15 years [1.21].

Two more recommendations are listed in Table 2.

Bond strength	N/mm ²	>1,3 >2 ⁽¹⁾
Water damp permeability	m	<4
⁽¹⁾ for reactive resin components		

Table 2: Recommended strength parameters for conductive paints

Ever since the 1970s and 1980s, CP has become a well spread protection system against corrosion. Many bridge decks in rough climate zones (thus often exposed to de-icing salts) have been successfully protected (e.g. in the United States and Canada [1.18]). Many rules and guidelines regarding CP are based on experience, monitoring and research of field applications.

1.4.3 Cathodic Prevention (CPrev)

Anodes for protective current application can be integrated inside the concrete structure. This is sometimes done for CP (e.g. bored systems, or anode surface net, underneath renewed concrete cover etc.), but mostly in case of CPrev. Anodes for CPrev are often built inside the structure, near steel reinforcement bars.

Practical aspects of CPrev are identical to CP. The goal of CPrev, on the other hand, is to avoid steel depassivation, instead of slowing down ongoing corrosion processes. Although the principle is the same as for CP, CPrev can be achieved more easily: it is easier to prevent pitting corrosion, than it is to suppress ongoing pitting corrosion¹¹. Therefore lower protection current densities are required (see next paragraph, “1.4.4 Required protection current”), and the protection current spreads deeper into the structure. Consequently, less anode material is required and prolonged service life of CPrev can be achieved, compared to CP.

CPrev causes a potential depression below the pitting potential. Electromigration causes chloride ions to move towards the anode, and away from the steel. Electrolysis produces hydroxyl at the steel surface, improving tolerance for chlorides, thus maintaining passivity for higher chloride concentrations.

¹¹ Because of the lower polarization potential of passive steel.

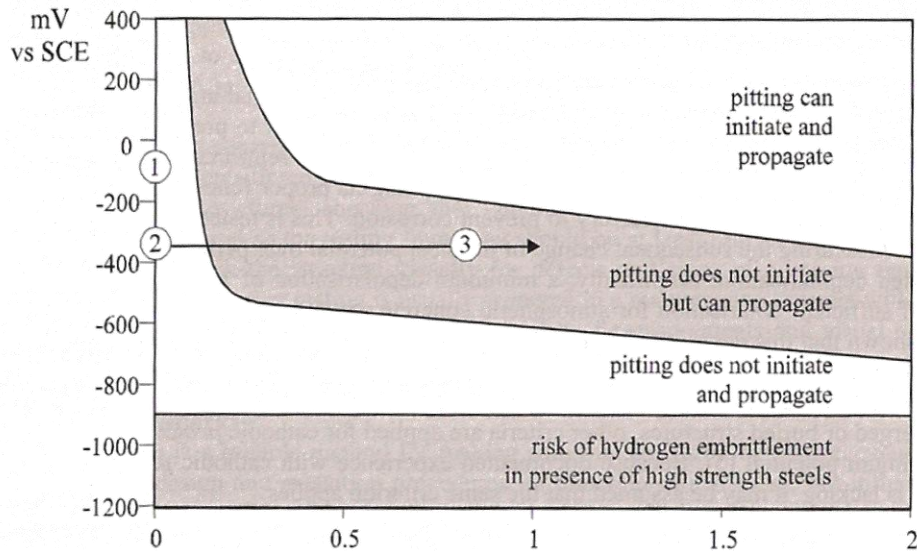


Figure 13: Qualitative principle of CPrev [1.20]

The potential drop due to CPrev (point 1→2) and maintained passivity for higher chloride concentrations (point 2→3) are depicted in Figure 13 [1.20].

CPrev has been successfully applied on the Sydney Opera House, and some motorway bridges in Italy [1.20].

1.4.4 Required protection current

The required protection current I_{prot} is a much discussed subject of cathodic protection applications. In case of CP, the aim is to slow down the process, rather than achieving corrosion immunity of the steel. Whereas the aim of CPrev is to avoid depassivation of the steel. Because the corrosion process has not started off in the latter case, protection currents for CPrev can be lower than for CP, as well as the amount of anode material [1.20,1.21]. A typical range for CP is 2-20mA per square meter of protected steel (around 10mA/m² for activated Ti-meshes and around 2mA/m² for conductive coatings [1.20,1.21]), while values for CPrev range between 0,2 and 2mA/m² [1.25].

However, [1.22] mentions higher values for CP, based on experience (Table 3).

Environment surrounding steel	Current density in mA/m ² of reinforcement
Alkaline, no corrosion occurring, low oxygen resupply	0,1
Alkaline, no corrosion occurring, exposed structure	1-3
Alkaline, chlorides present, dry, good quality concrete, high cover, light corrosion present	3-7
Chloride present, wet, poor quality concrete medium-low cover, wide-spread pitting and general corrosion on steel	8-20
High chloride levels, wet fluctuating environment, high oxygen level, hot, severe corrosion, low cover	30-50

Table 3: Protection current: practical values [1.22]

Other authors confirm the need of higher protection current densities for more aggressive environments and chloride contaminated concrete.

For CPrev, [1.19] mentions values of $0,4$ to $2mA/m^2$ for CP application within construction of RC elements, not yet exposed to aggressive environments, $0,2$ to $2mA/m^2$ for immerse conditions in low oxygen supply and low diffusivity of the concrete. Finally 2 to $5mA/m^2$ for steel surface containing chloride concentrations up to 2 wt% per cement weight. It has also been shown that CPrev systems sometimes need a waiting period to achieve certain level of protection, especially in heavily carbonated situation [1.19].

Higher values may lead to degradation of steel concrete bond and higher risk of alkali-silica reactions [1.19], as mentioned before. Also a waste of energy should be avoided. Some specific CP criteria have been proposed (and are commonly used in field applications) to avoid over- or underprotection of steel in CP systems [1.13, 1.17,1.24] a.o.:

- “100mV depolarization criteria”: 100mV positive potential shift between ‘instant off’ (so IR-drop free) potential and 4 [1.24] to 24 hours after depolarization
- 300mV negative shift in potential between static potential and (IR drop free) potential measurement during operation
- Absolute potential value of -850mV vs. copper-coppersulphate reference electrode (considered conservative regarding overprotection). [1.24] mentions a protective potential from -720 vs. Ag/AgCl on, and risk of overprotection for values more negative than -1100mV (Ag/AgCl).

1.5 References

- [1.1] J. DEFRANCO, *Corrosie van staal*, Ghent University course, Ghent (2009)
- [1.2] Stichting CUR (1998), Betonvereniging Publicatie 172, *Duurzaamheid en onderhoud van betonconstructies*, Gouda, (1998)
- [1.3] K. VAN DEN BERGH, *Studie van de corrosie van wapeningsstaal in beton met behulp van elektrochemische analysemethoden*, doctoral thesis, Vrije Universiteit Brussel, Brussels (2009)
- [1.4] A. ADRIAENS, *Elektrochemische analysemethoden*, Ghent University course, 3rd edition, Acco, Ghent, 2011
- [1.5] A. VOLKWEIN, *Corrosion protection by concrete*, COST 521, p.8-17 (2003)
- [1.6] J. P. BROOMFIELD, *Corrosion of steel in concrete*, E & FN Spon (2003)
- [1.7] M. NAGAYAMA and M. COHEN, *The anodic oxidation of iron in a neutral solution*. J. Electrochem. Soc., 1962, 109, p. 781-790.
- [1.8] C.L. PAGE, *The mechanism of corrosion protection in reinforced concrete marine structures*. Nature, 1975, 285, p. 514-515
- [1.9] E. ESCALANTE, *Effectiveness of potential measurements for estimating corrosion of steel in concrete*, SCI, 1990, p.281-292
- [1.10] D.S. LEEK and A.B. POOLE, *The breakdown of the passive film on high yield mild steel by chloride ions*, SCI, 1990, p. 65-73
- [1.11] C. ANDRADE, *Determination of the chloride threshold in concrete*, COST 521, p.100-112 (2003)
- [1.12] M.C. ALONSO and M. SANCHEZ, *Analysis of the variability of chloride threshold values in the literature*, Materials and Corrosion, 60 No. 8, 2009
- [1.13] C. ANDRADE, *Measurement of polarization resistance on-site*, COST 521, p.82 (2003)
- [1.14] T. LUPING, *Calibration of the Electrochemical Methods for Corrosion Rate Measurements of Steel in Concrete*, NORDTEST Project No. 1531-01, SP Swedish National Testing and research Institute Building Technology, (2002)
- [1.15] C. NAISH, A. HARKER and R.F.A. CARNEY, *Concrete inspection: interpretation of potential and resistivity measurements*, SCI, 1990, p. 314-332
- [1.16] C. NAISH and M. MCKENZIE, *Monitoring cathodic protection of steel in concrete*, Chapter 6 of [1.22] (1998)
- [1.17] BUtgb, Technische goedkeuring sector Burgerlijke bouwkunde, Goedkeuringsleidraad nr. G0016, *Kathodische bescherming door opgelegde stroom van wapening*, LIN-Afdeling betonstructuren (2001)
- [1.18] D.G. MANNING, *Cathodic protection of concrete highway bridges*, SCI, p.486-497 (1990)

- [1.19] D. . KOLEVA, *Corrosion and protection in reinforced concrete, Pulse cathodic protection: an improved cost-effective alternative*, doctoral thesis, Delft University of Technology, Delft, (2007)
- [1.20] R. POLDER, *Cathodic prevention of reinforced concrete structures*, COST 521, p.52-55, (2003)
- [1.21] R. POLDER, *Specific information on Cathodic Protection*, COST 521, p.124-131, (2003)
- [1.22] P.M. CHESS, *Cathodic protection of steel in concrete*, E & FN Spon (1998)
- [1.23] W.E. O'GRADY, *Mossbauer study of the passive oxide film on iron*, J. Electrochem. Soc., 1980, 127, p555
- [1.24] Ø. VENNESLAND, *Monitoring by using embedded sensors*, COST 521, p.60-72,(2003)
- [1.25] CEN, 2000, *Cathodic protection of steel in concrete, part 1: Atmospherically exposed concrete*, EN 12696-1
- [1.26] E. DE MULDER, *Kathodische bescherming van gewapende betonconstructies*, Master Dissertation, Katholieke Hogeschool Brugge-Oostende, (2006)
- [1.27] G.K. GLASS, A.M. HASSANEIN, N.R. BUENFELD, *Monitoring the passivation of steel in concrete induced by cathodic protection*, Corrosion Science 8, vol. 39, p31451-1458, (1997)

General aspects and properties,
conductivity

2.1 Fibre reinforced polymer (FRP)

Fibre reinforced polymers (FRP) consist of high strength organic or inorganic fibres embedded in a polymer matrix. The fibres have high strength characteristics along their longitudinal direction, while the polymer matrix transfers forces between the fibres in different directions (e.g. transversally but also from broken to intact fibres) [2.1,2.2,2.3]. The matrix can also offer some protection against mechanical or environmental attack and abrasion of the fibres. It also increases the toughness of the FRP. Three types of fibres are commonly used for externally bonded reinforcement of construction structures:

- Carbon fibres (ultra high and high modulus fibre and ultra high and high-strength fibre)
- Glass fibres (E-, Z- and S-glass fibre)
- Aramid fibres (aromatic polyamides, Kevlar 49)

The only fibres that are electrically conductive – and therefore of interest for CP anode application – are carbon fibres. This text will therefore immediately focus on carbon fibre reinforced polymers (CFRP). The mechanical properties of CFRP-composites depend strongly on those of the fibres and the quality of the fibre/matrix interface.

2.2 Polymer matrix

2.2.1 General aspects and properties

Polymer research for construction applications started (only) in the 1970-80s. In this domain, the physical and in-service characteristics of the polymer material appear to be of great importance for most CFRP applications, a.o.: the dimensional stability at elevated temperature, the thermal resistance, low water absorption, good chemical resistance high mechanical strength, high stiffness and compressive strength. Polymers used in CFRP are typically organic materials, containing oxygen,

carbon and nitrogen. Resin-like epoxies are polymers of such high quality, most commonly used for FRP (next to vinyl-esters and polyesters).

“**Polymerisation**” is the process of bonding between repeating “molecular building blocks”, called monomers, through all sorts of reaction mechanisms. They form a large chainlike molecule of relatively high molecular mass, called “polymer” [2.1]. If the hardening process is irreversible – i.e. if the plastic is heated no liquefaction occurs – the polymer and polymerisation process are called “thermosetting”¹².

Two kinds of thermosetting polymerisation can be distinguished:

- Addition polymerisation: no by-products are formed. The monomers are dissolved in a solvent, which is later removed.
- Condensation polymerisation: Atoms or groups of atoms are lost during monomer bonding. Usually two or more different kinds of monomers are present.

Resins are ‘crossed linked’ molecular networks, formed at elevated temperature. Epoxy resins used as a building material are usually polymerised or ‘cured’ by addition of a curing agent, in a fix mix ratio. It is then called a two component epoxy resin (although the resin is actually one of both components), cured through *chemical reaction*. Other curing systems are through heat or irradiation [2.4].

The curing of a thermosetting polymer can occur at relatively low temperatures around $10\text{-}30^{\circ}\text{C}$ (mostly for in situ application) or at elevated temperatures of order of magnitude 130°C (mostly in automated production procedures).

Some typical degradation processes of cured epoxy resins are comparable to those of plastics: the influence of temperature, UV-radiation and fire resistance. The temperature below which the polymer acts like a solid material (brittle or glassy), is called ‘**glass transition temperature T_g** ’. Above this temperature the material acts more like a liquid (rubbery, softening). Often T_g is characterised by a temperature range. Polymers for construction applications are mostly amorphous/crystalline polymers (“not entirely amorphous¹³”), and therefore have no ‘melting temperature’. Both during curing and in life service of the polymer the temperature should stay below T_g . The thermal expansion coefficient of polymers are of the order of magnitude of $100E\text{-}6$, thus higher than those of concrete and steel. Polymers are mostly not thermally conductive.

Organic polymer material is **flammable**, and therefore FRP behaviour in fire is an important subject in civil engineering. Even more important than the risk of structural collapse of buildings, is the level of toxicity of the combustion products of polymers [2.1].

Finally **ultraviolet sunlight** is strong enough to break covalent polymer bonds, resulting in embrittlement of the polymer.

Despite these drawbacks, polymers are found to be relatively **sustainable**, compared to other building materials (high resistance against cracking, oxidation, chemical degradation, delamination, wear, ...). Moisture can and will diffuse through organic polymers, leading to change in mechanical properties

¹² Thermosetting polymers have covalent crossed bonds between chains, vs. van der Waals bonds in “thermoplastic polymers”. This is why thermosetting polymers cannot be melted and reshaped. This characteristic makes them stronger than thermoplastic polymers (and more reliable e.g. in construction applications), but impossible to recycle [2.4].

¹³ Amorphous: the opposite of crystalline, in the absence of a repeated molecular structure.

and degradation. Through addition of products (such as silanes and organotitanes) and improving the curing process (thus increasing the degree of cross-linking), however, polymers can be seen as relatively **impermeable materials**, thus forming a ‘barrier’ against moisture ingress (cf. infra). The same can be said of gas or small particle penetration.

2.2.2 Polymers as FRP matrix

Good mechanical, chemical and rheological properties of epoxy resins, make of them the most commonly applied polymer matrix for FRP EBR in construction. The epoxy used in the experimental program of this dissertation is PC® 5800 CARBO of the ECC company. This is a two component, low curing temperature epoxy, specially produced for fibre impregnation. Some characteristics are resumed in Table 4:

PC 5800 CARBO				
Component		A	B	Mixture
Function		Polymer resin	Curing agent	(pot existence)
Colour		yellow	yellow to brownish	yellow
Viscosity (25°C)	(mPas)	700	450	615
Density	(kg/L)	1,15	1,07	1,12

Pot-life (20°C)	(min.)	30
Application temp.	(°C)	5 to 30
Mix ratio	A:B	2:1
Tensile strength¹	(N/mm ²)	61 (DIN 53455)
Compression strength¹	(N/mm ²)	82,6 (EN 12190)
Flexural strength¹	(N/mm ²)	105,3 (DIN 53452)
E-modulus¹	(N/mm ²)	3030 (DIN 5745)
Bond strength¹	(N/mm ²)	>3
Estimated consumption²	g/m ² of treated surface	250-500

¹ 7 days after curing
² Depends strongly on treated surface condition

Table 4: PC 5800 CARBOCOMP epoxy resin properties

Finally, it should be noticed that most polymers (especially high strength thermosetting polymers) are electrical insulators. For FRP anode application, the fibre matrix should be conductive (see “1.4.2 Induced Current (active) CP (ICCP)”). This important shortage will be discussed in further detail in section “2.8 Conductivity of the polymer matrix”.

2.3 Carbon fibres

The base product for carbon fibre production can either be refined petroleum or coal pitch (“pitch fibres”) or polyacrylonitrile (PAN, “PAN fibres”). Pitch fibres are fabricated by passing the pitch through a thin nozzle, and stabilising it through heating. PAN fibres on the other hand, are prepared through carbonation in an inert atmosphere at temperatures above 800°C, followed by a graphitisation

process ($>1200^{\circ}\text{C}$) [2.1,2.3]. Typical diameters of pitch and PAN fibres are, respectively $9\text{-}18\mu\text{m}$ and $5\text{-}8\mu\text{m}$.

The higher the stiffness of the fibre, the lower the tensile strength will be, as illustrated in the table of FIB 14 [2.3] (Table 5):

Carbon fibre type	E- modulus	Tensile strength	ϵ_{fu}
	(GPa)	(MPa)	(%)
High strength	215-235	3500-4800	1,4-2,0
Ultra high strength	215-235	3500-6000	1,5-2,3
High modulus	350-500	2500-3100	0,5-0,9
Ultra high modulus	500-700	2100-2400	0,2-0,4

Table 5: Strength parameters of different types of fibres for FRP [2.3]

Contrary to steel, carbon fibres show a typical linear elastic behaviour until failure. Failure occurs at very low strain, as a result of the high E-modulus. [2.7] recommends a minimal failure strain of 1,0%.

Carbon fibres have low creep characteristics, and – contrary to aramid and glass fibres – do not absorb liquids. This results in a high immunity against alkali or solvent ingress, chloride penetration and other forms of chemical attack [2.1]. It may be concluded that carbon fibres show very appropriate characteristics for anode application.

The fibre material used in the experimental program of this dissertation is *PC® CARBOCOMP PLUS* of the ECC company¹⁴. Some material properties are resumed in Table 6.

Density	(g/cm ³)	1,80
Equivalent thickness	(mm)	0,167
Cross area per unit width	(mm ² /m)	167
Tensile strength	(MPa)	4000
ϵ_{fu}	(%)	1,60
Water absorption	(wt%)	<0,1

Table 6: PC CARBOCOMP PLUS fibre properties

In an early stage of this research, the electrical conductivity of a string of carbon fibres is measured. The string has the average thickness of $0,167\text{mm}$, and width of 5mm . A linear relation between string resistivity and string length is found, as depicted in Figure 14.

¹⁴ E.C.C. n.v. (www.ecc-belgium.be)

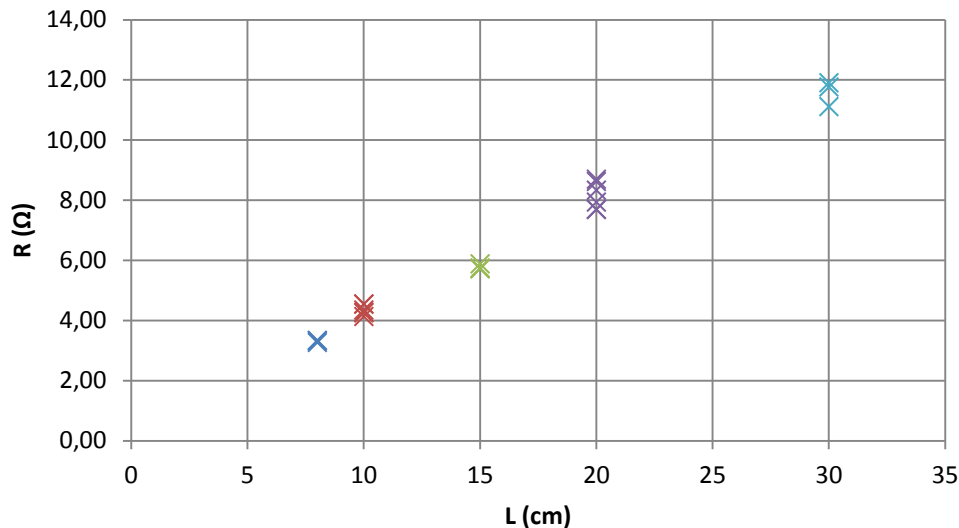


Figure 14: Graphic result resistivity R measurement of carbon fibre string, vs. string length L

It is worthwhile mentioning that for currents higher than about $1,1A$ smoke and heat production occurred along the fibre. For exaggerated currents, the fibres start to glow (white to yellowish light). If the fibres are held in a flame, the same phenomena are distinguished, without flaring (afterwards the fibres are totally embrittled, and pulverize at the mere touch).

The measured root mean square average string resistivity per unit of length is $410\Omega/m$. This value is equivalent to $0,034\Omega cm$ – taking account of the $5mm$ to $0,167mm$ dimensions¹⁵ – which is largely beneath the maximum allowed resistivity for CP anode materials of $1\Omega cm$ [1.17]. This resistivity is measured along the fibre direction. The fibre fabric is not conductive in the transversal direction (even if special effort is done to press the fibres together, only a poor result is obtained). With regard to cathodic protection the ‘maximum current’ of $1,1A$ is interesting for anode current density limitation. The long term anode current density for CP is mostly limited to $20mA/m^2$ in practice (see “1.4.2 Induced Current (active) CP (ICCP)”), to avoid accelerated anode degradation in acid environment. The value of $1,1A$ for a $0,005m$ wide string, accords to a minimal fibre length of order of magnitude $10^{-4}m$. In addition, the values of protection current will be much lower than $1,1A$, so the smoke generation issue is no problem regarding CP applications.

2.4 Externally bonded reinforcement (EBR) of constructions

Externally bonded reinforcement (EBR) is a technique primarily used to enhance the load bearing capacity of structures. Possible structure materials could be concrete, masonry or even steel or wood. The idea is that the EBR should take over a (mostly considerable) part of the load, thus secure the reinforced structure of (further) damage. EBR is often used as a repair technique. An early example of EBR repair techniques is the usage of externally bonded steel plates, e.g. in highway bridges. Much experience and knowledge for FRP EBR has been gained from this technique, ever since the 1980s.

¹⁵ This is a somewhat artificial formulation of volume resistivity of the fibres along their longitudinal direction and considered as a composed volume.

The basic principle is that a strong material is externally glued to the structure at a tensioned face, most often using a strong epoxy adhesive, thus increasing the internal cantilever distance from compression face to neutral axis of the reinforced element. In this way the moment of resistance of the element will increase. Figure 15 [2.5] shows the stress-strain diagram for the three elements in FRP EBR materials, and thus their mechanical role in the EBR system.

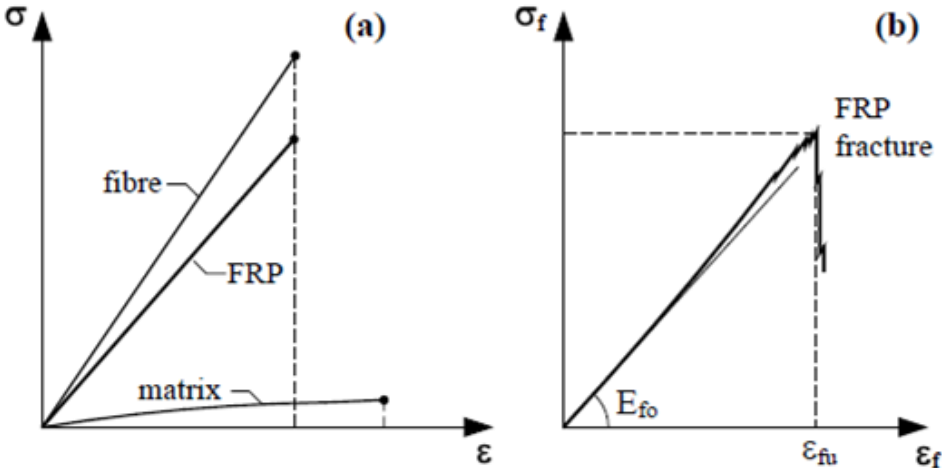


Figure 15: σ - ϵ diagram of FRP components, theory (a) and reality (b) [2.5]

Although the matrix is a much more plastic material, it does not affect the global FRP laminate behaviour significantly. The mechanical behaviour, calculation principles and failure modes of FRP EBR systems will not be further discussed here, but can be consulted in various reference works, a.o. [2.3], [2.5] and [2.7].

Typical reasons to choose an EBR system are restoration of damaged structures or prolongation of service life¹⁶, strengthening in case of design or construction errors or reinforcement in case of functional or structural changes in constructions.

The adhesive obviously takes an important part as stress bridge between the reinforced element and the EBR, and should therefore fulfil some strength requirements. The stresses between the element and the EBR are mostly transferred through the adhesive by shear stresses, although in some cases also peel stresses, normal to the EBR surface, occur. The adhesive can also play a part in ‘holding the element together’, increasing the cohesion, e.g. in masonry constructions or even as bracket reinforcement outside or inside RC structures¹⁷.

Some requirements regarding the adhesive quality are listed in [2.5]:

- Joint quality and adequate **adhesion to the reinforced material** and FRP (wetting ability). Also attachable without the need of temporary fixings.
- **Bond quality** and workability insensitive to limited variations in prepared surface quality or environment.

¹⁶ Several field applications of historical building reinforcement (damaged by earthquakes, environmental attack...) can be found in literature.

¹⁷ Although bond failure at crack bridging can be an important failure mechanism in high shear stress zones, e.g. anchoring zones [2.5].

- Good **moisture resistance, low creep, low shrinkage** (<0.1% recommended by [2.7]), **thermal stability and resistance against alkaline environments**.
- The **glass temperature** T_g should be significantly higher than the service temperature. The minimal application temperature should range between 5 and 10°C according to [2.7].
- The **flexural modulus** should range between 2000 and 15000 N/mm² (also [2.6,2.7]).
- The minimum **shear strength** should be 12N/mm² (at 20°C) [2.5-7]. (it should obviously be ‘at least higher than the tensile strength of the reinforced material’, i.e. about 3N/mm² for concrete). The bond strength should be at least 15N/mm² (20°C), according to NEN-EN 12188 [2.7].
- Low **permeability** and moisture absorption (lower than 3% by weight in specified conditions).

Another important issue regarding the workability is the viscosity of the adhesive product. To optimize application circumstances a thixotropic material is desirable [2.5,2.6,2.7]. The optimum viscosity lays between two extremes: fluid enough for wetting ability of the surface, but viscous enough to enable an “above head” application (for ceilings etc.). These requirements can vary according to the specific situation.

The pot life¹⁸ should preferably exceed 30 to 40 minutes, allowing a decent spreading of the adhesive onto the surface. Between application of the adhesive onto the surface and the application of the EBR material, at least 20 more minutes should be available [2.5,2.7].

2.5 FRP for EBR

Steel plate reinforcement has been a great success for bridge deck reparations, because of the advantageous lack of temporary fixings (scaffolding etc.) during application, thus avoiding traffic disturbance. The same can be said of FRP EBR systems, with some extra advantages to the boot:

- Much lower weight and easier to handle
- Higher tensile strength (high ‘strength to weight ratio’)
- Higher resistance against aggressive environment, water/chloride penetration etc.
- More sustainable
- No added risk of steel corrosion, high acid and alkali resistance
- Nonmagnetic properties
- Higher flexibility for curved surfaces (wet lay-up)
- Little thermal expansion
- Less maintenance

On the other hand FRP have very low failure strains ϵ_{fu} , low ductility, brittle failure, poor shear or transverse resistance and low resistance against fire. The most important disadvantage of FRP with respect to steel plate reinforcement is probably the higher cost. Indeed, the price of FRP reinforcement (both externally as internal FRP rods) remains higher than that of reinforcement steel and prestressing tendons (by weight obviously, but also on the basis of force carrying capacity [2.8]).

¹⁸ Time lapse between preparing the adhesive for application (e.g. mixing of components) and curing.

FRP EBR can typically be applied in two different ways: the prefab FRP laminates or strips and wet lay-up systems. **Prefab strips and laminates** consist of already impregnated and cured fibre fabrics, in its final shape strength and stiffness. The fibre volume fraction will often range between 60-70%. The thickness is about *1mm* (*1,5mm* overall with adhesive). The advantage of prefab FRP fabrics is the high level of quality (only in-situ bonding) and the ease of application.

In **wet lay-up systems**, the dry fibres are not impregnated¹⁹, but form a textile like fabric, with very small thickness (mostly about *0,1mm*). The resulting fibre contents in wet lay-up systems (ca. 30%) is typically smaller than in prefab laminates, but several layers can easily be applied. In these systems the resin serves for bonding and impregnation. To apply a wet lay-up fabric, first²⁰ a layer of epoxy resin is applied on the reinforced surface, afterwards the fibre sheet is put on top of this layer, and pushed against it (using a roller or other appropriate equipment), and finally a finishing epoxy layer for fibre impregnation and finishing is applied.

2.6 Passive corrosion protection of steel in FRP wrapped RC structures

Not only are FRP materials intrinsically resistant against aggressive corrosion conditions, their low permeability and water/gas penetrability enable them to form a protective ‘barrier’ for the underlying RC structure, against all sorts of aggressive environments (wet/dry, chloride, carbon dioxide ...).

The ‘barrier protection’ is sometimes called ‘passive corrosion protection’, comparable to some techniques like anticorrosion coatings of concrete structures [2.14]. The positive influence of FRP wraps on corrosion rates has been shown in several researches (a.o. [2.9-13]).

In [2.9] it is found that FRP wraps affect the absorption of water into the concrete, reducing infiltration at the surface and **limiting water penetration**. This phenomenon is attributed to the hydrophobic nature of the carbon fibres. In addition, FRP wraps can cause a **confinement of the concrete** (increasing strength and ductility, typically in wrapped columns). The wraps also confine the corrosion area around steel bars, slowing down the corrosion initiation and further process. It is believed that the confined corrosion layer is consolidated and compacted, limiting the access of water and oxygen. This phenomenon is studied on small concrete cylinders “lollypops” in [2.9], very much comparable to the ones in the experiment of this dissertation. The effect of confinement was studied through different fibre orientation (radial, axial and bias). The effects were measured in different ways: time until failure²¹, steel mass loss, potential readings and chloride contents near the steel surface. It was concluded that the confinement had a very effective protection influence against corrosion initiation and slowing down the further process upon cracking failure of the concrete. After cracking, a substantial acceleration can take place, due to steel exposure and corrosion product expansion in the cracks. In addition, it appeared that **the type of epoxy** has an important influence too: a better result is obtained through applying a thicker epoxy layer, until *2mm* (above this value the influence was negligible). More importantly, the application of high moisture- and corrosion resistant epoxies showed a much better result. A similar study [2.12] showed the influence of the **cover-to-bar diameter** ratio c/d : increasing the ratio decreases the circumferential expansion, due to corrosion. This

¹⁹ Or sometimes impregnated in non-cured resin, called “prepreg”.

²⁰ After concrete surface preparation for FRP application (e.g. roughening, rounding corners, clean...).

²¹ The corrosion process was accelerated in [2.9] through inducing an anodic current into the steel, a fast and effective technique

effect was found to be more pronounced in unwrapped specimens. It was also concluded that the average summation of **crack widths** of unwrapped specimens was much higher than in wrapped specimens.

In [2.13], an experiment on pre-corroded and cracked cylinders, the cell voltages of the steel were found to increase right after the wrapping procedure, leading to the conclusion that the (non conductive) **corrosion products were entrapped and filled up the cracks**, thereby increasing the systems resistivity. It was concluded that FRP wrapping can also have a positive influence on already (severely) corroded concrete structures.

A similar research has been done on beams in [2.10], with special attention to the influence of corrosion in wrapped (with and without confinement) on the **mechanical aspects** of the beam (yield and ultimate load, strength, deflection stiffness). It was concluded that wrapping and confinement had a positive influence here too. [2.11] also discusses the influence of FRP wraps on corrosion activity of reinforcement steel in RC beams. In this research the barrier effect of FRP against water and oxygen penetration is discussed. Confinement through wrapping was not researched. It was found that **GFRP wraps showed a better passive protection** against corrosion. This result was also found in [2.13]. A possible explanation is the electrical resistivity of GFRP, although it is also noted that glass fibres sheets have a higher thickness, which may have an influence as well [2.13].

The protection results in the experiments mentioned above were in general better for research on cylinders, compared to beams (order of magnitude 30% against 15% respectively better mass loss results compared to unwrapped specimens). This is another indication that better confinement conditions in cylinders can play an important part in the corrosion process of FRP wrapped RC structures.

It is worthwhile mentioning now that the experiment conducted in this research does not aim to measure the effects of confinement. On the contrary, the ability of FRP wraps to serve as anodes for CP is researched. From this point of view, as much other protective effects of the wraps as possible should be avoided, to have a clear view on the anode effectiveness. For this reason some reference specimens were made to compare the results, and some other measures were taken – as will be discussed in the next chapter, “Chapter 3: Experimental program”.

2.7 Outline of the dissertation

The aim of this dissertation is to check the technical feasibility of using CFRP wraps as anode material for induced current cathodic protection. As mentioned before, CFRP can perform as a corrosion inhibitor and slow down an ongoing corrosion process. Furthermore, FRP strengthening is often used as a concrete repair technique for severely corrosion damaged RC structures²². This explains the interest of combining both CP and FRP: in addition to the strengthening capacity and *passive* protection, the FRP could be used for *active* protection to the boot.

FRP is also increasingly used as an initial construction material, rather than only for repair in a later stage of the constructions service life. In these cases, the FRP could be used for CPrev instead of CP.

²² Typically in case of pitting corrosion the steel bar diameter decreases locally, affecting the bearing capacity of the RC element.

An experimental program was set up to try out the combined system on small concrete cylinders (see “Chapter 3: Experimental program”).

The effect of the CP program is measured, to determine to what extent the specimens were effectively protected, and the influence of the fibres on current spread is investigated. Other positive influences of CFRP wraps on corrosion systems (barrier, confinement) are not the primary aim of this work.

The idea of CFRP use as a cathode, has already been studied by Gadve, Mukherjee and Malhotra in [2.23]. In this experiment chloride contaminated concrete lollypop samples were precorroded through anodic current induction. Afterwards, the specimens were kept in a NaCl mist chamber for 60 days, some of them being cathodically protected ($I_{prot}=50mA$). During this period the CP program was monitored. After this period destructive pull-out tests were executed, followed by bar mass loss due to corrosion measurements. The active protected specimens showed lower pull-out strengths than the specimens in FRP wrap without CP. The proposed explanation, given by the authors of [2.23], is the softening of CSH gel after Sodium migration towards the steel bar. Mass losses were much higher (400%) for non protected samples.

2.8 Conductivity of the polymer matrix

As mentioned before (in “1.4.2 Induced Current (active) CP (ICCP)”), the resistivity of the anode should be approximately $1\Omega cm$ (preferably not higher than this value). It has been showed in paragraph “2.3 Carbon fibres” that the fibres are abundantly conductive enough along their longitudinal direction to fulfil this requirement. But in order to obtain a good CP system in an externally reinforced element, the matrix and adhesive should be able to transfer the current to the concrete surface as well.

Consequently, prefabricated FRP laminates are excluded a priori, because of the low conductivity of traditional matrix materials. However, this does not exclude the future possibility of preparing conductive laminates for this specific application²³. In this dissertation it has been decided to choose a wet lay-up fabric for the experimental research.

The matrix and adhesive polymer material should now form the conductive bridge between secondary FRP anode and concrete surface. However, epoxy resins typically have – like many other polymers – very low electrical conductivity properties.

2.8.1 Conductive polymers: generalities

Some **intrinsically conductive polymers** (ICP) do exist²⁴. The conductivity of these materials is originated from their chemical and crystalline structure or morphology. But the stability of these conductors is noted to be very unreliable. In [2.15] it is noted that, when stored in an inert atmosphere, complexed polyacetylenes, for instance, “lose their excellent electrical properties after a short time”.

²³ The preparation of a “prepreg” (fibres that are impregnated with a thermosetting polymer in a “flexible” intermediate stage before curing, prepregs can be stored for later use, and are cured through heating [2.5]) has been done in a research [2.16] on antistatic polymer (by addition of CB) for airplane construction panels. The obtained resistivity was of the order of magnitude of $10k\Omega cm$.

²⁴ E.g.: polyacetylenes, polypyrroles, polythiophenes, polyphenylenes and polyanilines [2.15].

These phenomena are attributed to oxidative degradation and cross-linking. In [2.16] a lack in ageing is also noted. A second shortcoming of ICPs for EBR applications is their poor mechanical properties.

Another possibility to overcome this problem, is making the existing epoxy resin conductive, by adding conductive particles to the mixture; this is called “filling” the polymer with “fillers”. **Metal fillers** are frequently used for this purpose (e.g. for electrical junctions). However, in the long run, these metal particles can corrode as well, and it should be kept in mind that anode materials for CP have to survive aggressive (acidic) corrosion environments. for this reason it did not seem the most intelligent solution for the conducting issue.

A much more sustainable material that can be used as a conductive filler is **carbon**. Carbon materials exist in different structures: diamond and graphite being commonly known. Diamond is a highly crystalline form of carbon, whereas graphite is amorphous. A direct consequence of the latter structure is the anisotropy of graphite: it has no strong or weak direction, no preference failure mode etc. A third – less known – structure is the so called “black carbon”, typically in a powder form (often called “carbon black (CB) powder”).

2.8.2. Carbon Black (CB): general aspects, properties and use

Amorphous CB particles consist of planal hexagonal nets of carbon atoms, similar to (but less extensive than) those in graphite. The layers are also further apart from each other ($3,5\text{\AA}$), compared to graphite. CB can be considered as paracrystalline in nature.

Carbon blacks are added to polymers for various reasons:

- Stabilization against UV light
- Reinforcement for improved mechanical properties (like graphite fibres)
- Colouring and opacifying (e.g. in inkjet)
- Cost-reduction as a filler
- Changing electrical conductivity
- Changing thermal conductivity

Furnace-produced blacks²⁵ have the best conductivity characteristics, ranging from a couple of $100\Omega\text{cm}$ to a small fraction of $1\Omega\text{cm}$ for more conductive blacks. Several parameters influence the conductivity of CBs [2.18]:

- “Small particle size: to provide more particles per unit volume, thus reducing the interparticle distance
- High structure: to increase the conductive path the electrons have to travel through the carbon and reduce the number of gaps in the network
- High porosity: to yield more particles per unit weight than compact solid particles. This will reduce the interparticle distances
- Low volatiles²⁶ content: (...) volatiles tend to inhibit [the tunneling effect, see further]”

²⁵ “In the oil furnace process, CB is produced in a refractory lined reactor. In the reactor, a flame is produced from air and natural gas. The CB feedstock is atomized in the flame, and the CB formation reaction takes place. Downstream from this reaction zone, water is sprayed into the reactor, to stop the CB formation reaction.” [2.21]

2.8.2.1 CB as a conductive filler: theories

The conductivity of a compound filled with CB, will not increase in a linear fashion with the percentage of added CB. On the contrary, poor results are obtained beneath a certain critical CB concentration, called “*threshold concentration*”. Addition of CB after this point once again brings only a gradual increase. The most widely accepted and researched theory used to explain this phenomenon, is the “*percolation theory*” [2.15-16,2.18-21] (Figure 16).

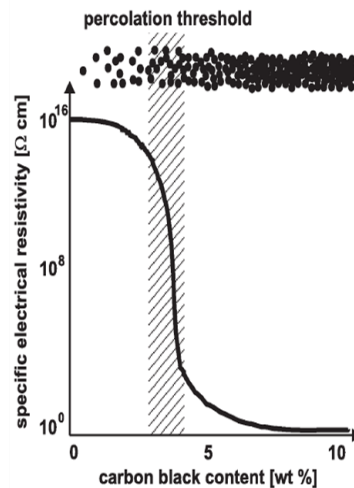


Figure 16: Qualitative dependence of electrical resistivity on CB. The hatched zone is the "percolation threshold" [2.16].

Because of the very high surface content of CB materials, strong adhesion forces between the particles force them to agglomerate. This happens at several levels (primary agglomerates form secondary agglomerates etc.). In earlier theories it was assumed that in order to obtain good conductivity results, the CB particles should form a close network covering the complete polymer matrix, allowing electrons to travel through the network from one end to another (therefore called “percolation” theory); in this explanation the threshold concentration accords to the concentration needed to form such an overall network. In this theoretical reasoning, the length of the CB chains²⁷ that can be built up, is considered the most influencing parameter for conductivity.

However, more recent research showed [2.15,2.18] that not the length of the chains, but the width of the gaps in the network is of greater importance²⁸. Electrons are able to “jump” over gaps – provided that the gaps are small enough. This is called electron “**tunneling effect**”. The percolation of electrons should therefore not be understood as a travel through a closed network, but jumping from one conductive agglomeration to another, resulting in an overall conductivity of the bulk material. Thus, the threshold value must be understood as the CB concentration, above which the gaps become small enough for electron tunneling (order of magnitude millimicrons). CB concentrations to obtain

²⁶ Various combinations of carbon with oxygen and hydrogen, present on the surface of the CB particles, are referred to as “volatiles”. Typical volatile content of CB range between 1 (more conductive CBs) to 10% by weight.

²⁷ The agglomeration happens in a linear fashion; thus the CB particles form chainlike agglomerates.

²⁸ This was deduced in a theoretical way: statistical modeling of dispersion of spherical particles in a polymer, resulted in threshold values much higher than real values (about 27 to 52vol% in theory, versus 20vol% for CBs with poor surface characteristics and 10vol% for extremely conductive CBs) [2.15].

resistivities as low as $1\Omega cm$, using “extremely conductive CB” (as in this research), range between 10-20wt%.

Different ways of adding the CB to a polymer are commonly used, a.o.: ultrasonic vibration, melt blending, pultrusion, high speed mixing... However, it is found that high speed mixing techniques result in poorer conductivity. Contrarily, slow **internal mixing and shear mixing** improve the conductivity. This is explained in [2.18] by the higher interparticle distance, resulting from high speed mixing.

It has also been shown that during the mixing procedure the polymer does not become substantially more conductive (Figure 17). Only after mixing, the agglomeration starts to form.

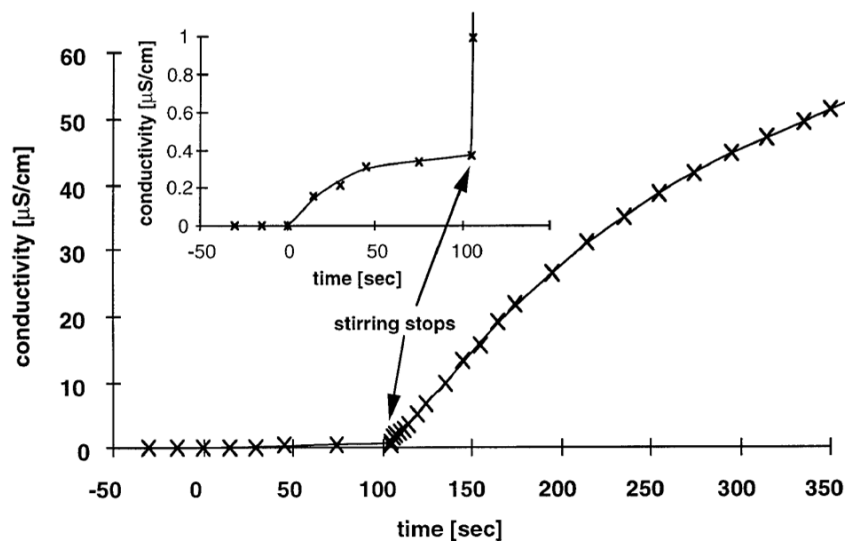


Figure 17: Conductivity course of liquid epoxy resin filled with 0,3vol% CB after dispersion. Mixing between $t=0s$ and $t=105s$ [2.19]

The improvement of CB dispersion and lowering the threshold value through shear mixing or adding chloride ions to the polymer (to increase ionic concentration), together with the theory of colloids, prove – according to [2.19] – that the dispersion of CBs into polymers is characterized by a “**potential barrier**”. The interfacial energies play an important part in the dispersion of CBs: adhesion (CB-polymer) and cohesion (CB-CB), van der Waals interaction, Coulomb forces etc. These phenomena are not accounted in the percolation theory (which is a mere statistical theory, based on the geometry of particles that are statistically dispersed). In the potential barrier point of view, the threshold concentration, is the value above which it is energetically (thermodynamically) advantageous to form more and more CB-CB interfaces; a network with a predominantly linear network, is built up. This also explains why CBs with a larger surface area (m^2/g) have lower threshold concentrations: because they possess a larger accessible wettable surface, they reach their maximum of adhesion interface energy earlier (CB-polymer), after which other structures are formed (CB-CB) [2.15].

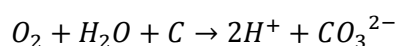
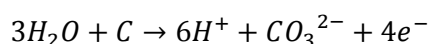
2.8.2.2 Practical issues: viscosity, surface oxidation and influence on mechanical properties

Whatever the threshold value (and the theory behind it) may be, a more important inconvenience regarding CB dispersion is of interest here: the influence of CB on the mixtures **rheology**. Whilst adding CB to a polymer, the viscosity will increase nonlinearly (exponential equations are mentioned

in [2.15]). According to the same article it may be assumed that “it is largely, if not completely, *the size of the specific surface area* of the disperse phase, rather than the nature (strength) of the interaction between dispersed phase and matrix that causes the change in viscosity”. The high surface area per weight of CB has a positive influence on conductivity, but increases the problem of viscosity.

High speed mixing or special vibration techniques can help to keep the viscosity low enough during mixing and even for application. As mentioned before, fast mixing techniques improve the dispersion of CB, but impede the formation of a percolation network. Therefore this techniques were not used in this work. Heating is another possibility (‘melt-blending’) to keep the polymer fluid. It is important to stay below the glass transition temperature, or other temperature limitations according to the product distributor²⁹. A third method consists of adding a solvent to the mixture. The influence of solvents on the polymer properties (chemical resistance, mechanical properties...) is noted to be unreliable and strongly dependent on both the polymer and solvent type. Therefore, this technique was not tried out in this dissertation.

A third remark on CB use as conductive filler is the problem of **oxidation of the CB particle surfaces**. Furnace blacks contain small quantities of chemisorbed oxygen on their surfaces. The oxygen exists in organic functional groups, such as phenols and carboxylic acid. This so called ‘surface oxidation’ can improve the rate of dispersion and dispersion stability, typically interesting for coating (e.g. coating against UV deterioration) and printing ink applications. The surface oxygen reduces the filled polymer viscosity [2.21]. On the other hand, the surface oxidation of carbon blacks is fatal for their conductivity. In [2.22] the use of carbonaceous conductive particles as fillers for anode coatings in CP systems is discussed. It is stated that the acidic conditions prevailing in and adjacent the coating – used as an anode – enhances the degradation process of the carbon particles:



According to this document, this degradation of the carbon particles, leads to deterioration of the anode conductivity. This might be an important shortcoming of CB fillers for CP anode coating applications. Further research in this domain is still to be done. The proposed solution in [2.22] is to coat the CB particles with a conductive metal of a type possessing a natural passive and in itself conductive oxide film, such as: nickel, cobalt, platinum and silver.

Finally, the influence of CB on the polymers **mechanical properties**, according to [2.15,2.18]: massive increase in the modulus of elasticity, decrease in percentage elongation at break, breaking strength and notched bar impact strength. Although there is no exact explanation for the mechanical consequences, it is stated in [2.15] that some influences of different polymers on CBs show different forms of CB complexes, compared to “seams” in a matrix. The curvature of these seams might play a role in the mechanical deterioration: if the curvature would increase, the seams would eventually form tubes, insulating parts of the polymer matrix, thus affect its mechanical properties.

In [2.16], however, small amounts of carbon black were added to a (glass fibre reinforced) epoxy resin to obtain (low) electrical conductivity. They found that the tensile strength (and E-modulus) of non-

²⁹ The technique of ‘post curing’ through heating is noted to improve conductivity of high temperature curing epoxies, filled with metallic powders [2.17].

filled was lower than the 1,3wt% and 1,5wt% filled resins. It is assumed that at nanoscale ($d_{CB} \approx 30nm$) the CB act as a reinforcement phase.

As specified in section “2.7 Outline of the dissertation”, the scope of this research is limited to the technical feasibility of CP with anodic FRP EBR material. Therefore it was decided to try out the addition of CB to the epoxy resin anyway, **regardless of the effects on mechanical properties. Further research for this particular issue should be done to determine the consequences for the EBR system.**

2.8.3 Experiment and result for CB filling in epoxy resin

To obtain a conductive epoxy resin for anode purpose in a CP program, it was tried to fill the epoxy resin **PC 5800 CARBO** (described in “2.2.2 Polymers as FRP matrix”).

The CB powder used for this purpose was PRINTEX®XE2, super conductive CB used for electrically conductive coatings, plastics and rubbers from DEGUSSA (Evonik) company³⁰ in Germany. Some technical data are resumed in Table 7:

Property	Unit	Actual value
Ash content (650°C)	%	0,4
Volatiles (105°C)	%	0,1
pH-value		8,1
Cloride content	ppm	25
Sulfur content	%	0,1
Particle size	nm	35

Table 7: Carbon black properties

Different trials to obtain excellent conductivity, were done; most of them had very poor results. The high viscosity of the polymer after adding the CB was the most important issue: concentrations higher than 8 to 10wt% were practically impossible to mix in a decent way. After polymerisation it would seem that not all of the components were polymerized. Several techniques were tried out:

- Different mixing speeds: slow manual up to intermediate automated mixing speeds
- Different mixing times: 30 sec up to 10 minutes
- Heat mixing: at temperatures of 70° to 80°C
- Different CB concentrations: all orders of magnitude between 1 and 20wt% were tried out. As mentioned before, concentrations higher than 8wt% became very difficult to mix
- Gradual versus instant CB addition
- CB addition in epoxy resin component (‘A’), or hardener (‘B’), or both
- Instant mixing of both epoxy components with CB (maximum mixing time about 30 minutes, before curing), or a priori CB mixing in epoxy components, and curing after “resting period”

All of these attempts failed to achieve their goal. This is the main reason why for the experimental program some commercial conductive adhesives were used.

The answer of the CB-mixing issue was much simpler: because of the very high surface structure of the CB, the polymer would typically adhere to the filler (‘wetting the CB particles’), causing very high

³⁰ www.corporate.evonik.de

viscosity, but also poor curing of the polymer. So the answer to the problem was to simply change the mixing ratio of the polymer components. In this research, (much) more hardener was added to the mixture, than the prescribed mix ratio 1:2. Once again a variety of mass ratios (component A:component B:CB) were tried out, and it appeared that there was a maximum amount of hardener (comp. B) that could be added. For higher wt% of hardener, the curing procedure suddenly failed to create a consistent solid compound. The epoxy remained more or less fluid. It is assumed that bits of cured epoxy resin were floating around in the residual unused hardener.

The optimum conductivity/rheology of the filled polymer mixture is described in Table 8

Component	mass [g]	wt%
A	16,6	51,23
B	12,6	38,89
CB	3,2	9,88

Table 8: Composition of CB added ECC epoxy

The CB was gradually mixed by hand in component A, while component B was also gradually added to the mixture, to keep a more or less fluid substance. The final rheology was a thick and wet paste (good wetting ability).

This technique was also applied on an antistatic epoxy: **Epo-Tek 353ND** of the Epoxy Technology company³¹. This two component epoxy is in fact a high temperature curing epoxy, which can also be cured at low temperatures. Its intrinsic conductivity (for antistatic application) is higher than $1,8 \cdot 10^{13} \Omega cm$. Its lap shear strength is $14 N/mm^2$. No specific information about bond strength is found. The mix ratio of the components (A:B) is 10:1.

The optimum conductivity/rheology mixture found for the Epo-Tek epoxy is mentioned in Table 9

Component	mass [g]	wt%
A	10	54,05
B	6,1	32,97
CB	2,4	12,97

Table 9: Composition of CB added Epo epoxy

Both conductivity and viscosity were found to be better than the added ECC epoxy.

Finally, this technique was tried on a third epoxy *paint*: **ICOSIT® 277** of the Sika® company³². The expected improvement of rheological conditions, was not obtained. Furthermore, the epoxy paint had good protective coating properties, but very poor bond strength, so it was decided not to try this epoxy in the experimental program.

³¹ www.epotek.com

³² www.sika.com

2.9 References

- [2.1] L.C. HOLLAWAY, *A review of the present and future utilisation of FRP composites in the civil infrastructure with reference to their important in-service properties*, Constr. And Building mat., 24, p. 2419-2445, (2010)
- [2.2] A. PALMIERI, unpublished doctoral thesis
- [2.3] FIB, CEB-FIP, bulletin 14, *Externally bonded FRP reinforcement for RC structures*, (2001)
- [2.4] Wikipedia online encyclopedia: www.wikipedia.com
- [2.5] S. MATTHYS, *Structural behaviour and design of concrete members strengthened with externally bonded FRP reinforcement*, doctoral thesis, Ghent University, Ghent (2000)
- [2.6] R. VAN BOECKEL, *Enhancing the efficiency and safety of FRP reinforcements*, TRADECC
- [2.7] Stichting CUR (2002), Aanbeveling 91, *Versterken van gewapend-betonconstructies met uitwendig gelijmde koolstofvezelwapening*, (tweede, herziene uitgave), (2007)
- [2.8] A.E. NAAMAN, *FRP reinforcements in structural concrete: assessment, progress and prospects, FRP reinforcement for concrete structures*, proceedings of the sixth international symposium on FRP reinforcement for concrete structures (FRPRCS-6), Singapore, (2003)
- [2.9] I. WOOTTON, L. K. SPAINHOUR, N. YAZDANI, *Corrosion of Steel Reinforcement in Carbon Fiber-Reinforced Polymer Wrapped Concrete Cylinders*, Journ. Of Composites for Constr., p.339-347, (2003)
- [2.10] T. EL MAADDAWY, K SOUDKI, *Carbon-Fiber-Reinforced Polymer Repair to Extend Service Life of Corroded Reinforced Concrete Beams*, Journ. Of Composites for Constr., p.187-194 (2005)
- [2.11] S. MASOUD, K. SOUDKI, *Evaluation of corrosion in FRP repaired RC beams*, Cement & Concrete Composites, 28, p.3969-977, (2006)
- [2.12] T. EL MAADDAWY, A. CHAHROUR, K. SOUDKI, *Effect of Fiber-Reinforced-Polymer Wraps on Corrosion Activity and Concrete Cracking in Chloride-Contaminated Concrete Cylinders*, Journ. Of Composites for Constr., p.139-147, (2006)
- [2.13] S. GADVE, A. MUKHERJEE, S.N. MALHOTRA, *Corrosion of steel reinforcements embedded in FRP wrapped concrete*, Constr. and Building Mat., 23, p.153-161, (2009)
- [2.14] M. RAUPACH, *Concrete Repair According to the new European Standard EN 1504*, electronic version, URL: http://www.ibac.rwth-aachen.de/fileadmin/user_upload/forschung/docs/84841_Raupach.pdf (consulted in May 2011)
- [2.15] B. WESSLING, *Dispersion as the key to processing conductive polymers*, Handbook of conducting polymers, Edited by Skotheim Elsenbaumer and Reynolds, second edition, 1998, isbn 0-8247-0050-3

- [2.16] M. KUPKE, H.-P. WENTZEL, K. SCHULTE, *Electrically conductive glass fibre reinforced epoxy resin*, *MAT Res Innovat*, **2**, p.164-169, (1998)
- [2.17] MOSCICKY A., SOBIERAJSKI T., FALAT T., FELBA J., *The post-curing technology for conductivity improvement of low-viscosity electrically conductive adhesives*
- [2.18] H.S. KATZ, J.V. MILEWSKI, *Handbook of fillers for plastics*, Van Nostrand Reinhold, ISBN 0-442-26024-5 (1987)
- [2.19] R. SCHUELER, J. PETERMANN, K. SCHULTE, H.-P. WENTZEL, *Agglomeration and electrical Percolation Behavior of Carbon Black Dispersed in Epoxy Resin*, Wiley & Sons, (1997)
- [2.20] P. WANG, T. DING, *Conductivity and piezoresistivity of Conductive Carbon Black Filled Polymer Composite*, *Journ. Of Applied Polymer Science*, **116**, p.2035-2039, (2010)
- [2.21] *The fundamentals of Carbon Black*, Cabot Corporation Billerica, electronic version, URL: <http://www.cabot-corp.com/Downloads/DL200808140916AM8680/> (consulted May 2011)
- [2.22] P.J. MORELAND et al., *Cathodic protection system and a coating composition therefor*, United States Patent, n° 5,364,511, (1994).
- [2.23] S. GADVE, A. MUKHERJEE, S.N. MALHOTRA, *Active protection of FRP wrapped reinforced concrete structures against corrosion*, Taylor & Francis Group, London (2009)

3.1 Experiment set-up

3.1.1 Specimen preparation

3.1.1.1 Mortar cylinders

For the experiment that was conducted in this dissertation, mortar cylinders of height *100mm* and diameter *48mm* are fabricated. The cylinders are reinforced with a smooth steel bar, diameter *10mm*, placed in the axis of the cylinder to obtain a constant circumferential concrete cover of *19mm*. The total length of an embedded rod is *80mm* – starting at *20mm* distance from the bottom side of the mortar cylinder, see Figure 18. At the top side of the cylinder the steel rod sticks out of the mortar, with a length of *80mm*. This form of sample is sometimes called “lollypop sample”. Lollypops are often used in corrosion related researches (sometimes even lower concrete cover, often higher), because of their controllable and symmetrical geometry (e.g. in [1.3, 1.19, 2.9, 2.12 and 2.13]).

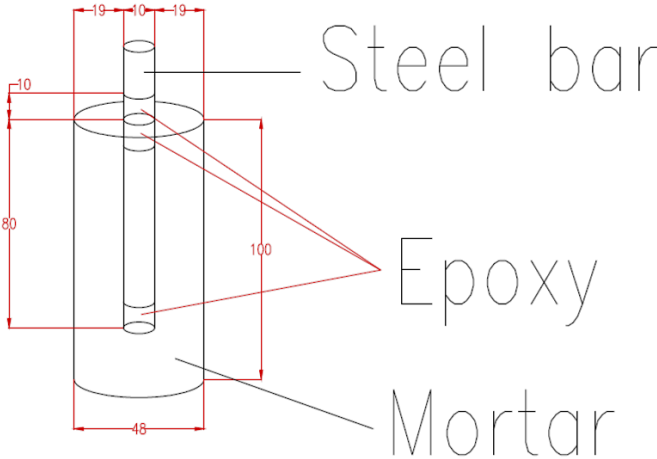


Figure 18: Lollypop specimen geometry

Before casting the specimens, all corrosion products are removed from the steel rod surface, by polishing. The removed corrosion layer consisted of a very thin blackish film. Geometrical ‘end effects’ at both ends of the steel-in-concrete surface (bottom and top interface) may cause some irregular corrosion rate distribution on the steel surface. To avoid this irregularity both locations on the steel bar are sealed from the mortar through epoxy coating: the bottom end over a length of *10mm*, the interface location over a total length of *20mm*, of which *10mm* are embedded in the mortar. The epoxy used for the seals was PC® 5800 of ECC company (mentioned and described in “2.2.2 Polymers as FRP matrix”). If the epoxy impregnation is applied in a close airtight film, it should form a good protection against corrosion³³. Before casting the specimens all of the rods were weighed.

Chlorides are added to the cement mix (dry mix) to accelerate the corrosion initiation. Because of the short experimental program duration, the rather high chloride concentration of 4,25% per weight of cement was added³⁴. Moreover a high water content (water:cement W/C-ratio of 0,65) was applied to weaken the concrete structure (porous structure) and provide a high pore water content for corrosion activity. Some technical information about the mortar mix is given in Table 10.

Mortar properties		
Volume of 1 specimen	(L)	0,2
Volume density	(kg/m ³)	2186,5
Cem:Sand:Water:Nacl	(-)	1:3:0,65:0,07
W/C-ratio	(-)	0,65
Cl- content	(wt% of cem)	4,25
Air content	(vol%)	2
Compr. strength (28 days)¹	(N/mm ²)	34,9
¹ NBN EN 12390-1		

Table 10: Mortar specifications

After casting, the specimens are cured for 1 week in a wet environment (90% relative humidity at 20°C). During the two following weeks (and the rest of the test program, see further) the specimens were kept in a dry environment (RH 60%, 20°C).

3.1.1.2 CFRP wraps

The “protected specimens” are wrapped in CFRP wraps. 6 different conductive epoxy adhesives were used (see further section “3.1.2 Epoxy anodes and specimen matrix”). For each type of conductive epoxy two wrapping directions are applied: axial and radial fibre direction (see). A third specimen per epoxy is prepared for CP, on which only the epoxy (without any fibres) was used as an anode. The specimens wrapped in CFRP with conductive epoxies will be cathodically protected and cyclically immersed for corrosion initiation (see further).

³³ The science behind reinforcement bar coating against corrosion will not be discussed here; but it is a well known fact that the smallest damage to the coating may cause pit corrosion. Therefore the epoxy coating application is done with high care.

³⁴ The reader might remember the short discussion on chloride threshold values in previous chapter. The added concentration is a bit higher than typical values for these conditions.

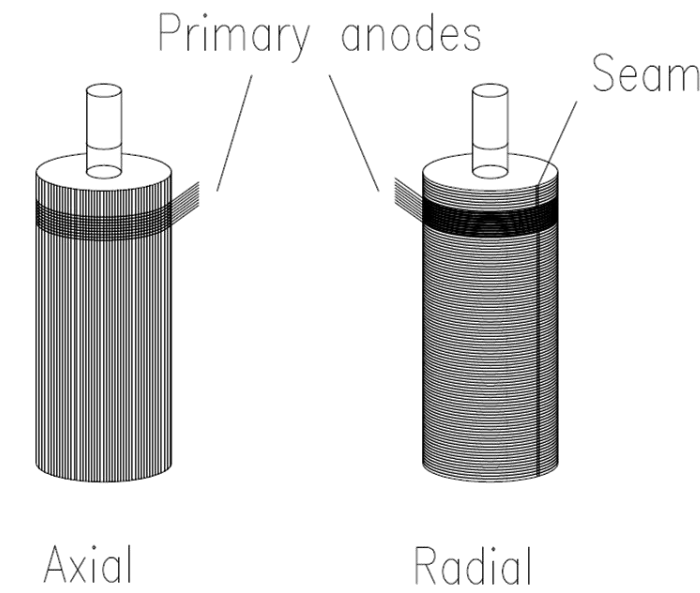


Figure 19: Axial (ax) and Radial (rad) fibre orientation

Besides the 18 specimens included in the CP program (“CP” specimens), 4 more specimens are subjected to the cyclic immersion (“Ref” specimens). Three of them being unwrapped (unprotected steel in chloride contaminated mortar and wet dry chloride cycles), and one being wrapped in traditional CFRP, using insulating epoxy and with axial fibre direction.

Two more specimens are made for Tafel slope measurements (“Tafel” specimens), to obtain specific values of the Stern-Geary constant B (see “1.3.3 Polarization resistance: equation of Stern-Geary (1957) and linear polarization (potentiostatics)”). **Tafel-50298** is wrapped in CFRP along the longitudinal direction, using ECCOBOND 50298 as a conductive epoxy. **Tafel-ref** is kept unwrapped. Both of these specimens are not cyclically immersed: the value of B is a characteristic of the steel in concrete situation, but does not depend on the actual rate of corrosion. Therefore it was chosen not to immerse these samples.

The agreed names in this text are summarized in Table 11, where “CP” stands for cathodic protection, “ax” for axial and “rad” for radial CFRP fibre orientation.

Specimen name	Wrap	Fibre orientation	CP	Chloride immersion	Tafel slope measurement
Ref-1,2,3	no		no	yes	No
Ref-FRP	yes	axial	no	yes	no
CP-ax	yes	axial	yes	yes	no
CP-rad	yes	radial	yes	yes	no
CP	yes	no fibres	yes	yes	no
Tafel-ref	no		no	no	yes
Tafel-50298	yes	axial	no	no	yes

Table 11: Names of specimens

All of the CP specimens need a “primary anode” to connect to the DC power supply. A string of carbon fibres (5mm wide) is used for this purpose, and applied directly onto the other CFRP fibres (without intermediate epoxy layer). They are applied in radial direction at 1cm of the top concrete surface, with an overlap for better attachment. At least 3cm of the string isn’t glued to the specimen to

make the connection (with a conductive clamp). The radial orientation of the primary anode is also applied on the specimens with radial fibre direction. This is done to study the influence of the fibres on current spread. As mentioned in “2.3 Carbon fibres”, the fibres are not expected to transfer electrical loadings in the transverse direction.

Besides the fibre direction, the wrapping procedure for each epoxy is identical in both fibre directions. First, the epoxy is spread out on the concrete surface. Second, the fibres are applied onto the primary epoxy layer. Finally a finishing layer of the epoxy is spread onto the fibres. The wrapping procedure is depicted in APPENDIX B. However, wrapping is sometimes done differently for different epoxy types, because of the different rheological conditions (see further).

In the transversally wrapped specimens, no overlap of the CFRP sheet is created, to avoid the effects of concrete confinement. In addition, no epoxy coating was applied on the bottom concrete surface, to allow chloride penetration during chloride “bathing” through this surface, thus minimizing the effect of the passive CFRP protection against chloride ingress.

3.1.2 Epoxy anodes and specimen matrix

The two carbon black (CB) filled epoxy resins (PC 5800 and Epo-Tek 353ND) were used for CFRP wraps. Additionally, four conductive epoxies distributed by Henkel company³⁵, and produced by Emerson & Cuming were used (Table 12):

Adhesive	Company	Filler	Filler content (wt%)	Bond strength [N/mm ²]	Resistivity [Ω .cm]
Eccobond 50298	Emerson & Cuming	Ni	74-76	>12	0,5
Eccobond 64C	Emerson & Cuming	Ni		5,52	0,02
Eccobond 60L	Emerson & Cuming	graphite		>10	50
Eccobond 57 C	Hysol	Ag	>50	<4,8	6x10 ⁻⁴
ECC PC 5800 Carbo	ECC	CB	9,88		(119,04)
Epo-Tek 353ND	EpoTek	CB	12,97		(78,72)

Table 12: Conductive epoxies

It can be noticed that the minimum bond strength according to NEN-EN 12188 of $15N/mm^2$ is not always respected. The resistivity of the graphite filled epoxy (Eccobond 64C) is about $50\Omega cm$, which is higher than the advised minimum of $1\Omega cm$, but – compared to other epoxies – still relatively acceptable (other epoxies easily range from 100 to $10^3\Omega cm$ and much higher for antistatic coating applications). The silver filled 57C epoxy is the most conductive anode, but has a very inappropriate rheology. It is applied as a hard pasty substance (comparable to a chewing gum), and has very bad wetting and bonding ability on the concrete (comparable to a foil, which is easily removed before curing). Only after good application it bonded more or less to the concrete, resulting in a relatively

³⁵ www.henkel.de

acceptable CFRP wrap. Epoxies 60L and 64C were rather creamy³⁶, and had good wetting ability. Epoxy 50298 was a paintlike substance, very comfortably applied to the concrete – although maybe a bit too runny for “above-head-application”.

Tafel	Ref	Ref-FRP	CP-ax	CP-rad	CP
Tafel-Ref, Tafel-50298	Ref-1,2,3	Ref-FRP			
			CP-ax-60L	CP-rad-60L	CP-60L
			CP-ax-57C	CP-rad-57C	CP-57C
			CP-ax-64C	CP-rad-64C	CP-64C
			CP-ax-50298	CP-rad-50298	CP-50298
			CP-ax-ECC	CP-rad-ECC	CP-ECC
			CP-ax-Epo	CP-rad-Epo	CP-Epo

Table 13: Specimen overview

Notice: the names “ECC” and “Epo” refer to the respective *carbon black added* epoxy resins.

It could be overall concluded that epoxy 50298 has the best fitting characteristics for bond strength, rheology and conductivity.

The small amount of 57C that was provided, didn’t allow the preparation of all three samples. It was decided to leave out specimen **CP-rad-57C**.

All of these epoxies are two component epoxies, cured at low temperatures. The mixing ratios differ strongly. In most cases the filler addition is done in both components: 57C, ECC, Epo and 60L.

The two CB added epoxies were used as anode on 6 samples as well (epoxy “ECC” and “Epo”). The application of these two epoxies was somewhat more difficult. In spite of the relatively good rheology and wetting ability of these mixtures, it appeared that the carbon black paste didn’t adhere to the concrete surface (every striking movement would rip the CB/epoxy mixture off). Therefore it was decided to press the fibres against the first epoxy layer, in order to obtain a well spread CB network. The result was much better than any attempt made by hand. The confinement pressure was created by using the moulds that were used for casting the concrete specimens.

3.2 CP program and corrosion initiation

At the age of 3 weeks the specimens were subjected to a **wet/dry cycle** to accelerate corrosion initiation: 1hour of immersion in a chloride bath (1,0% of NaCl by weight) every 24 hours. The specimens were kept in the same dry environment (RH 60%, 20°C) during this period.

This immersion was repeated for 28 days, and was done at a constant water level beneath the upper concrete face, at a distance of 20mm.

³⁶ The vocabulary about rheology is sometimes dubious in technical datasheets: creamy, pasty, fluid, more or less viscous; the same description is sometimes used for different rheologies. Therefore in this text it is agreed that “paintlike” means that it can be applied with a brush (more or less fluid, good wetting ability). “Creamy” is used for a paste with good wetting ability and bonding. “Pasty” is used for a dry and hard paste, bad wetting ability, difficult to apply to the surface.

The choice of **corrosion acceleration technique** was influenced by the cathodic protection program. Besides some general question marks regarding the reliability of the impressed current technique, the combination of this technique with CP would become rather artificial: the applied potential field between steel rebar and its surrounding for corrosion initiation would have been opposite to the one applied for CP. To study and measure their respective influences would have been impossible. Therefore the more “natural” corrosion acceleration through cyclic bathing was chosen.

During the immersion program, the test samples were **cathodically protected**, with exception of the unprotected reference specimens. The CFRP wrap and primary anode were used as anode material, the steel rod as cathode. The protection current was kept constant at $0,11mA$ during the first two weeks. It was then lowered to $0,05mA$ for the two remaining weeks. Between both fazes a first Linear Polarization (LP) measurement was done (this measurement took three days, not included in the 28 days of bathing cycles). After the second period a second LP measurement was effectuated, to study the evolution of the corrosion process.

Taking account of the epoxy coatings on the steel bars to avoid irregular end effects, the total length of the bars exposed to corrosion is $60mm$. The corrosion surface is then calculated through:

$$S_{corr} = \pi D l = \pi \cdot 10 \cdot 60 \approx 1885mm^2 \quad (3.1)$$

The corrosion protection current density is calculated as follows:

$$I_{prot} = \frac{i_{prot,abs}}{S_{corr}} \quad (3.2)$$

Resulting in $I_{prot}=58,35mA/m^2$ for the first period and $26,53mA/m^2$ for the second period.

To ensure an equal protection of all of the samples, it was decided to build up the **electrical circuit in series**. This means that the anode of the first specimen, was connected to the cathode of the second sample etc. The cathode of the first specimen was connected to the negative pole and the anode of the last specimen to the positive pole of the DC power supply. This set-up is schematically depicted in Figure 20, and a photograph is enclosed in APPENDIX C.

Because of the different resistances of the specimens (see further) and the series circuit, the anodes have relative potential differences with respect to each other. If the specimens are immersed in one chloride bath, currents through the water would level up these differences, resulting in an energy loss and more or less a parallel system (equal voltage of the anodes). The specimens were therefore immersed in **individual chloride baths** (beakers).

After a certain period of CP, a potential difference between anode and cathode is built up. This potential difference remains unharmed immediately after switching off the CP. This means that the specimen acts like a small battery. To avoid increased depolarization after switching off the CP in the serial circuit between a cathode and the anode of the next specimen, all connections between the specimens should be disconnected immediately.

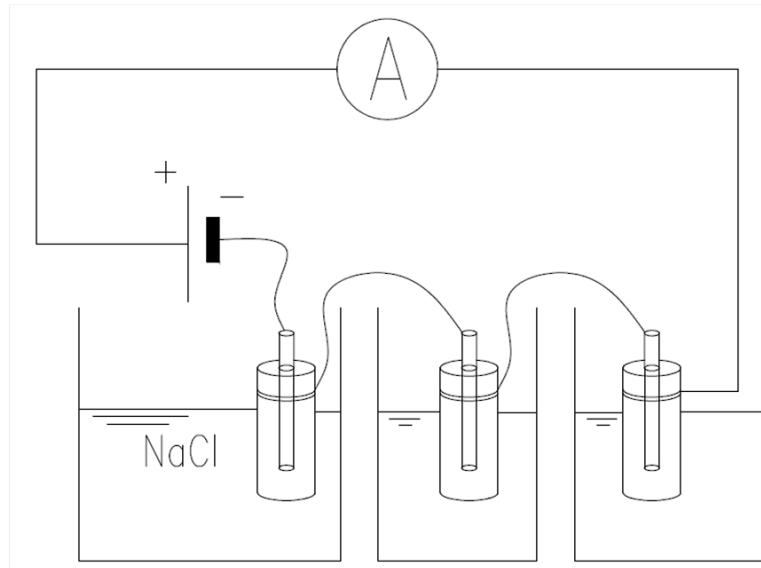


Figure 20: Schematic CP circuit set-up

During the bathing and CP period a logbook was kept of demanded potentials, and different recorded phenomena, which will be discussed later.

3.3 Linear polarization (LP)

The equipment used for this measurement was EcoChemie AUTOLAB PGSTAT 20 of the Electrochemical and Surface Analysis laboratory in De Sterre 12, Ghent³⁷.

The LP-measurements were executed in the same electrolyte solution as the bath-immersion (1,0wt% NaCl in water), to avoid effects of chloride migration or diffusion.

A cylindrical Titanium mesh was used as counter electrode. The specimen was placed inside the mesh. Between both specimen and counter electrode, the reference electrode was placed. The material used as a reference was saturated Calomel (SCE). The cell set-up is depicted schematically in Figure 21 and a photograph can be found in APPENDIX C.

The steel bars were polarized over a range $\pm 20mV$ around the open circuit potential (OCP), so an absolute polarization of $40mV$ was achieved. The potential step was $0,15mV/s$. This means that one LP measurement took about 5 minutes. Before every measurement was done, however, the OCP had to be determined. To do so, every lollypop was stabilized in the cell set-up in an open circuit (OC or 'zero current'), while potential versus reference electrode is recorded. This stabilization period took 30 minutes per specimen. To improve the stabilization process, the specimens were **submersed** completely at least **12 hours** in advance, to a water level comparable to the level in the cell set-up³⁸.

³⁷ With the kind permission and assistance of prof. dr. A. Adriaens of the *Electrochemistry and Surface Analysis research group* of the science department of Ghent University.

³⁸ It was found that the water level of submersion had an influence on the OC situation: a higher level induces higher water pressures, resulting in faster saturation of the concrete. The potential evolution in OC was found to be either increasing or decreasing towards a stable situation. However, the important part is that the samples are stabilized when the polarization starts.

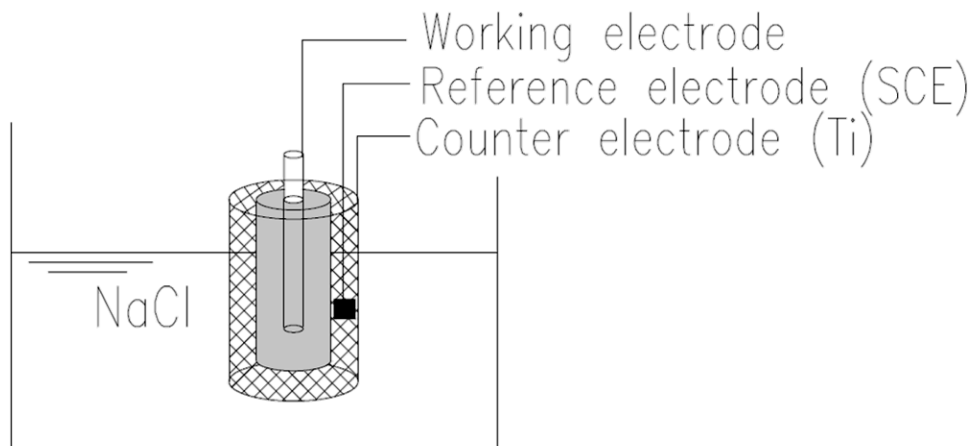


Figure 21: LP-measurement cell set-up

The cathodic protection was switched off **36 hours** before this permanent submersion (48 hours before the first LP measurement).

The specimens were measured in the same order for the two performed LP-measurement sessions.

3.4 Potentiodynamic polarization (PDP)

Specimens **Tafel-ref** and **Tafel-50298** were polarized over a range of $-0,200V$ to $+1,5V$ vs. OCP, at a polarization rate of $0,5mV/s$ ³⁹. The same cell set-up as for Linear Polarization was used for this measurement.

3.5 Preliminary remarks, and discussion CP/immersion program

3.5.1 Resistance measurements

For every **type of conductive epoxy**, the Ohmic resistance was determined. Because of the relatively small amount of every epoxy that was provided, the criterion mentioned in paragraph 1.4.2 for conductive paints for ICCP (obtained from [1.17]) could not be verified. A similar test was done however, with a much smaller surface.

A coating of $5,5cm \times 5,5cm$ of each epoxy was applied on a wooden surface. At both ends conductive wires (silver alloy) are embedded in the material, as prescribed in the aforementioned recommendation document. The results of the resistivity measurements are summarized in Table 14.

	S cmxcm	t mm	R Ω	ρ Ωcm
60L	5,5x5,5	1,50	299,4	44,91
57C	5,5x5,5	0,5	3,2	0,16

³⁹ Lower than $2,5mV/s$, as advised in [1.3], and same value as in [1.19].

64C	5,5x5,5	1	9,1	0,91
50298	5,5x5,5	0,5	38,5	1,925
ECC	5,5x5,5	3	396,8	119,04
Epo	4x3	2	295,2	78,72

Table 14: Epoxy conductivities

The measurement was done for low voltages ($0,5V$) and currents (mA). In some trials epoxy “Epo” showed much higher conductivity, of the same order of magnitude of 57C. This is not found in this measurement. The ratios between the 60L/64C/50298 conductivities accord more or less to the datasheets.

A second resistivity measurement was done on the finished concrete specimens. Before starting the CP program, the induced protective current of $0,12mA$ was tried on every specimen individually. Out of the required voltage to obtain this current, an **equivalent Ohmic resistance** of the steel/concrete/anode system could be calculated⁴⁰. A small scatter in the results was anticipated, because the resistance of the concrete mortar was expected to be much higher than both steel and anodes. Very scattered resistances were found between different kinds of epoxies, whereas specimens with the same epoxy material showed very similar results.

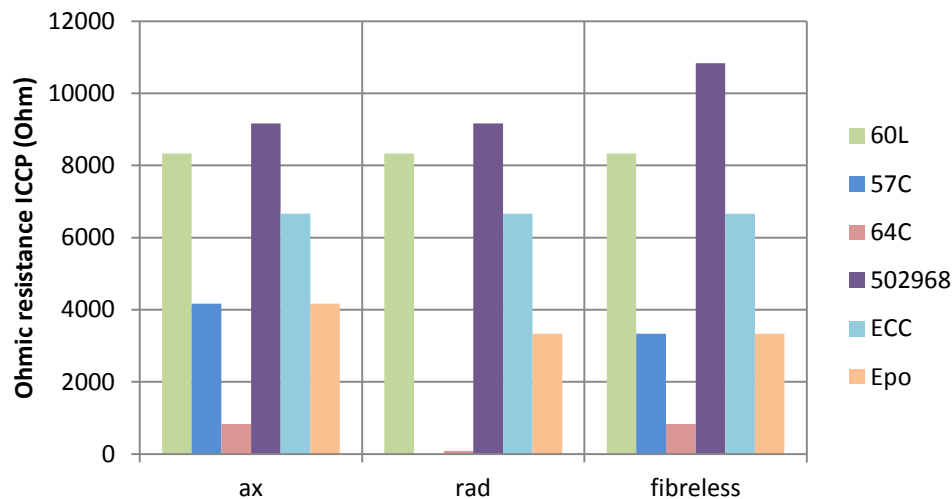


Figure 22: Ohmic resistance of steel/concrete/anode systems for ICCP

Because of the correlation between epoxy type and ohmic resistance that is found out of Figure 22, it can be concluded that in this stage the epoxy type is an important parameter for ohmic resistance. However, it is found that 64C has a lower resistance ($0,02\Omega cm$ according to datasheet, against $6 \cdot 10^{-4} \Omega cm$ for 57C) than 57C. This may be the influence of the anode current distribution: 57C was a lot more difficult to apply to the concrete surface.

The influence of fibre orientation appears to be minimal.

⁴⁰ It may be noticed that this “Ohmic” resistance is somewhat artificial: inside the concrete an ionic current system is induced.

During the CP program, the potential difference between C and A in every sample was measured (during ICCP) both in and out of the water. The results are summarized in APPENDIX D. No conclusion is drawn regarding Ohmic resistance, because the capacitive characteristic of the samples should be taken into account to do so.

A second Ohmic resistance measurement has been done **after the CP program** (1 week of depolarization and drying). The results are shown in Figure 23.

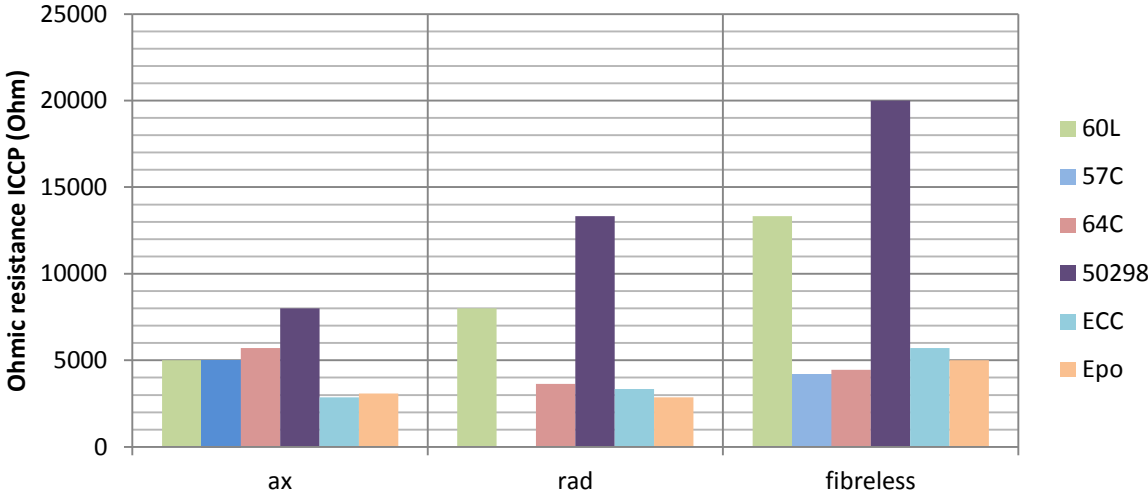


Figure 23: Resistivity of specimens after CP

The graph now shows more scattered results, even for each epoxy. No important change was measured for ECC and Epo. 64C and 57C have an overall increased resistivity. Epoxies 60L and 50298 show an upward trend in resistivity from axial to fibreless. These are the most resistant commercial epoxies (compared to 57C and 64C).

It should be kept in mind that these resistivities result from the combination of steel, mortar and anode.

The increasing trend for 60L and 50298 between specimen types might indicate the influence of the fibres: the fibres enhance the conductivity of the wrap, the axial orientation has the best surface current spread, thus lowest resistivity. However, this has not been recorded in the first resistivity measurement.

Another possible explanation could be the increased resistance of the anode (due to oxidation of the filler component). However 50298 is a Ni filled epoxy, whereas epoxy 60L is graphite filled, and therefore not expected to corrode fast.

A third, more consistent, explanation is a resistance increase due to resistant corrosion products, insulating the steel bar from the mortar environment. However, it could be a combination of these phenomena.

In case of the CB added epoxies (ECC and Epo), the presence of the fibres seems to have a positive influence (ca. 3000Ω vs. 5000Ω), although the fibre orientation does not seem to differentiate this influence.

The invariability of 57C and 64C regarding carbon fibres can be explained by the high intrinsic conductivities of these epoxies. It is believed that for high epoxy conductivity, the fibres influence on anode current spread is minimal.

3.5.2 CP/immersion program

The total voltage required to maintain a constant protection current density for the entire series circuit during a dry cycle was about $15V$ for $0,11mA$ and $11,5V$ for $0,06mA$ (second stage).

During each immersion the protection current was also kept constant. The voltage to maintain this current would typically drop right after the immersion started (about $5V$), to evolve to a steady state situation. This means that the total resistance is lower during the immersion. The abrupt drop can be explained by the instant conductivity increase of the wetted anode.

After taking them out of their chloride baths, an instant voltage increase would follow, although smaller than the initial drop (around 1 to $2V$). Followed by a slow evolution to the dry steady state situation.

Figure 24 shows a typical voltage evolution plotted against time (the two vertical lines indicate the immersion).

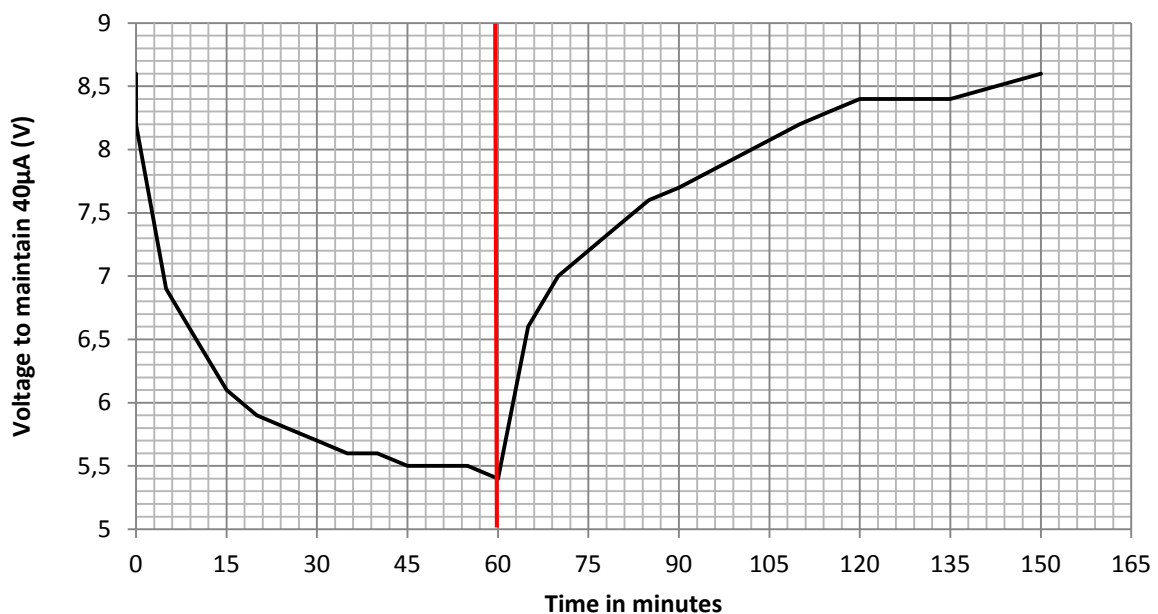


Figure 24: Typical voltage evolution in time during immersion (= between $t=0$ and $t=60$)

Three immersions during the first stage of the program showed an aberrant behaviour: right after the instant voltage increase, after taking the specimens out of their baths, the voltage would go down again to a value even lower than during the immersion. Followed by a very slow evolution to the dry cycle voltage (Figure 25). No exact explanation is found for this phenomenon. It might be related to the depassivation of some specimens: the formation of one (or several) corrosion pit, would concentrate the protection current in this sample at the pit(s) location, and result in a lower Ohmic resistance of these specimens. A simpler explanation could be a delayed water penetration that reaches a steel bar, thus creating a conductive bridge between A and C.

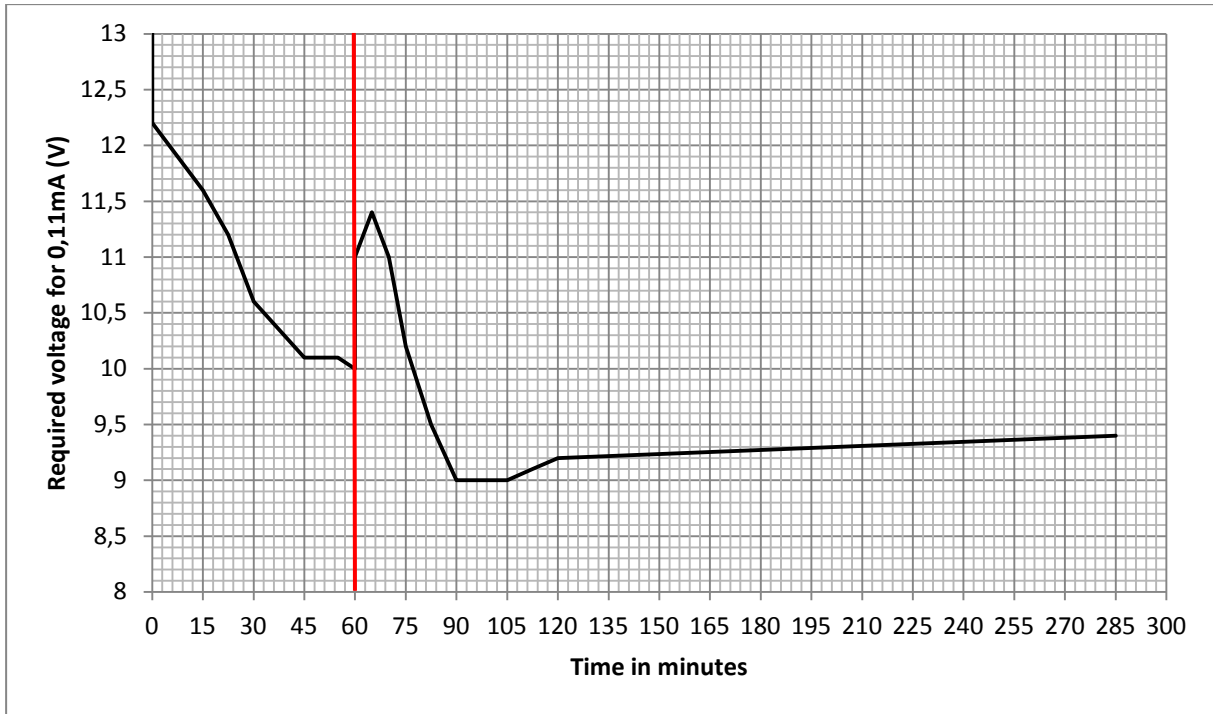


Figure 25: One of three aberrant voltage evolutions recorded in the first stage

After the fifth immersion a brownish solid product was found in the chloride bath of CP-ax-Epo. Two days later the same product was found in the bath of specimen Ref-1, and specimens Ref-2 and Ref-3 the day after that. At the end of the first program stage, several beakers contained brownish water.

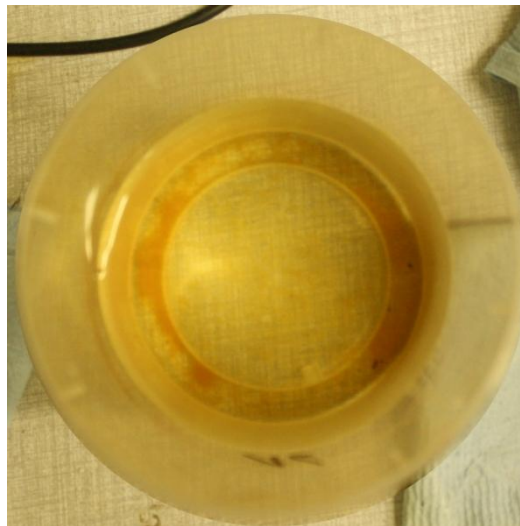


Figure 26: Example of brownish solid product in immersion water

This brown solid product was accompanied by a higher pH value. The fresh water (initial water and added daily to level up the beakers) had a $pH=7,5$ (slightly alkaline). About half way the first stage (9th immersion), the pH values for all the CP specimens was found to be 9 and 9,5 for the Epo samples⁴¹. It may be remembered that the anode in ICCP attracts chloride ions and hydroxyl groups.

⁴¹ The ones that showed the brown product first. The pH values were measured right after immersion.

The unprotected samples showed *higher* values for the unwrapped specimens (**Ref-1,2,3**) $pH > 10$ (⁴²) and $pH = 8,5$ for the traditional CFRP wrap (**Ref-FRP**). After the first stage the water was completely refreshed, and a much faster pH evolution was found: in a couple days only the pH went up from 7,5 to > 10 in all the beakers, except for **Ref-FRP**. This sample had a slower evolution. The recorded difference between specimen Ref-FRP (CFRP) and the other wrapped specimens (CFRP+CP) may be explained by the accelerating influence of the protection current on OH^- expulsion.

3.5.3 Depolarization

During the first stage of the CP/immersion program, a depolarization was carried out, to study the behaviour of the samples. It must be noticed that no reference electrodes were present at the time, so no absolute potentials could be measured, only the relative difference between cathode (steel) and anode (CFRP). The $100mV$ depolarization criterion (mentioned in paragraph “1.4.4 Required protection current”) was verified.

The results are summarized in Table 15. Some specimens showed an unstable instant off⁴³ relative potential difference, which is also noted in the table.

	instant off ΔV		ΔV (24 hours)	Difference
	(mV)		(mV)	(mV)
CP-ax-60L	-491		-179,1	-311,9
CP-ax-57C	-417		-286,4	-130,6
CP-ax-64C	-130,6	unstab.	-193,3	62,7
CP-ax-50298	-26,5	unstab.	-30,1	3,6
CP-ax-ECC	-75	unstab.	-78	3
CP-ax-Epo	-65	unstab.	-233,3	168,3
CP-rad-60L	-111,9	unstab.	-153,7	41,8
CP-rad-64C	-45,1	unstab.	-179,3	134,2
CP-rad-50298	-50,7		-111,9	61,2
CP-rad-ECC	-456		-176,4	-279,6
CP-rad-Epo	-489		-173,3	-315,7
CP-60L	-632		-211,4	-420,6
CP-57C	-431		-356	-75
CP-64C	-277	unstab.	-137,3	-139,7
CP-50298	-125	unstab.	35,8	-160,8
CP-ECC	-472		-90,8	-381,2
CP-Epo	-517		-273,4	-243,6

Table 15: Relative potential drop after depolarization

All of the specimens were found stable after 24 hours. CP-57C shows a too small potential drop (less than $100mV$). Specimens CP-ax-64C, 50298, ECC, Epo and CP-rad-60L, 64C, 50298 show an

⁴² $pH = 10$ is the highest value that could be measured.

⁴³ Right after switching off the CP.

unexpected increase in potential difference. There is no apparent correlation between these specimens and the ones that showed an increased potential difference in APPENDIX D. There is also no relations to the epoxy type: e.g. epoxies 60L and 57C show a normal behaviour in axial fibre orientation, but an increased potential difference in radial orientation. **The only thing that can be said is that all of fibreless specimens show a normal behaviour.**

This depolarization should be done with a reference electrode, to study the absolute potential drops of the steel. It seems plausible that the anode depolarization affected the conducted measurement. The fibres might have an influence on anode (de)polarization, which would explain the good behaviour of the fibreless specimens.

3.5.4 Wetting condition

As mentioned before, the immersion level was kept at a distance of *20mm* beneath the upper cylinder surface. A different wetting condition of the non-immersed upper *2cm* was recorded.

3.5.4.1 Reference specimens

During immersions, the unprotected samples (both wrapped, Ref-FRP, and unwrapped, Ref-2,3) remained dry at their upper surface. This means that 1 hour of immersion was not long enough for the capillarity to wet the entire specimens. It should be noted that for Ref-2 and 3 it was a ‘close call’, mostly the circumferential cylinder surface was wetted upon a couple of millimeters distance from the top surface.

A slight damage to Ref-1 somehow improved capillarity until the upper surface. This sample was more or less entirely wetted after each immersion.

3.5.4.2 CP-specimens

Some of the actively protected samples showed a *completely* wetted upper surface, implying that the wraps of these samples had a hydrophilic behaviour, thus enabling the water to wet the concrete sample more easily. This concerns epoxy 60L, 57C, 64C and Epo. However, this improved wetting only concerned the fibre reinforced specimens (ax and rad). This might mean that the fibres played a role in enhancing the wetting ability.

The passive “barrier” protection of the CFRP wrap seems to be weakened by the conductive epoxies. The “moisturizing” epoxies thus increase the risk of corrosion to their steel bars. It may be noticed that the ECC epoxy is a strong hydrophobic behaviour for concrete protection, and that epoxy 50298 had the best fitting rheology for CFRP application (coating ability, formation of a watertight coating).

3.5.5 Oxidation of the anode connections

After 1 week of CP/immersion, the connection clamps of the anodes started to corrode, resulting in corrosion stains both on the CFRP primary anodes and secondary epoxy coating. This can be seen in the pictures in Figure 27.



Figure 27: Corrosion of the clamps connected to the primary anodes

3.6 Results of electrochemical measurements

3.6.1 Results

The graphical results of the linear polarization measurements can be found in APPENDIX E

The corrosion rates found using the Stern-Geary equation, with $B=26mV$ are listed in Table 16. “*a*” stands for the first LP-measurement session and “*b*” for the second one.

Specimen	$I_{corr,a}$ ($\mu A/cm^2$)	OCP _a (mV vs SCE)	$I_{corr,b}$ ($\mu A/cm^2$)	OCP _b (mV vs SCE)
CP-ax-60L	3,142143	-468	2,01522	-358
CP-ax-57C	1,155475	-427	1,201683	-419
CP-ax-64C	2,322813	-502	1,789008	-444
CP-ax-50298	1,119888	-401	0,98223	-397
CP-ax-ECC	0,576979	-388	0,610497	-387
CP-ax-Epo	1,518656	-547	3,092487	-530
CP-rad-60L	1,356997	-511	1,032852	-440
CP-rad-64C	2,154534	-516	1,78487	-457
CP-rad-50298	2,024875	-568	1,539347	-477
CP-rad-ECC	2,157292	-527	1,918666	-471
CP-rad-Epo	2,768341	-551	2,532473	-514
CP-60L	2,401436	-359	1,554519	-443
CP-57C	1,311065	-427	1,06706	-471
CP-64C	0,323042	-306	0,33256	-281
CP-50298	1,095336	-371	1,118095	-394
CP-ECC	0,972299	-412	1,482794	-460

CP-Epo	1,772456	-426	2,299365	-564
Ref-1	6,949129	-639	6,544982	-628
Ref-2	0,993541	-479	0,874227	-402
Ref-3	4,338033	-573	2,509025	-482
Ref-FRP	3,389045	-488	4,125614	-482
Tafel-ref	-		4,153201	-642
Tafel-50298	-		1,079612	-422

Table 16: Results LP measurements

These results are graphically represented in the following figures.

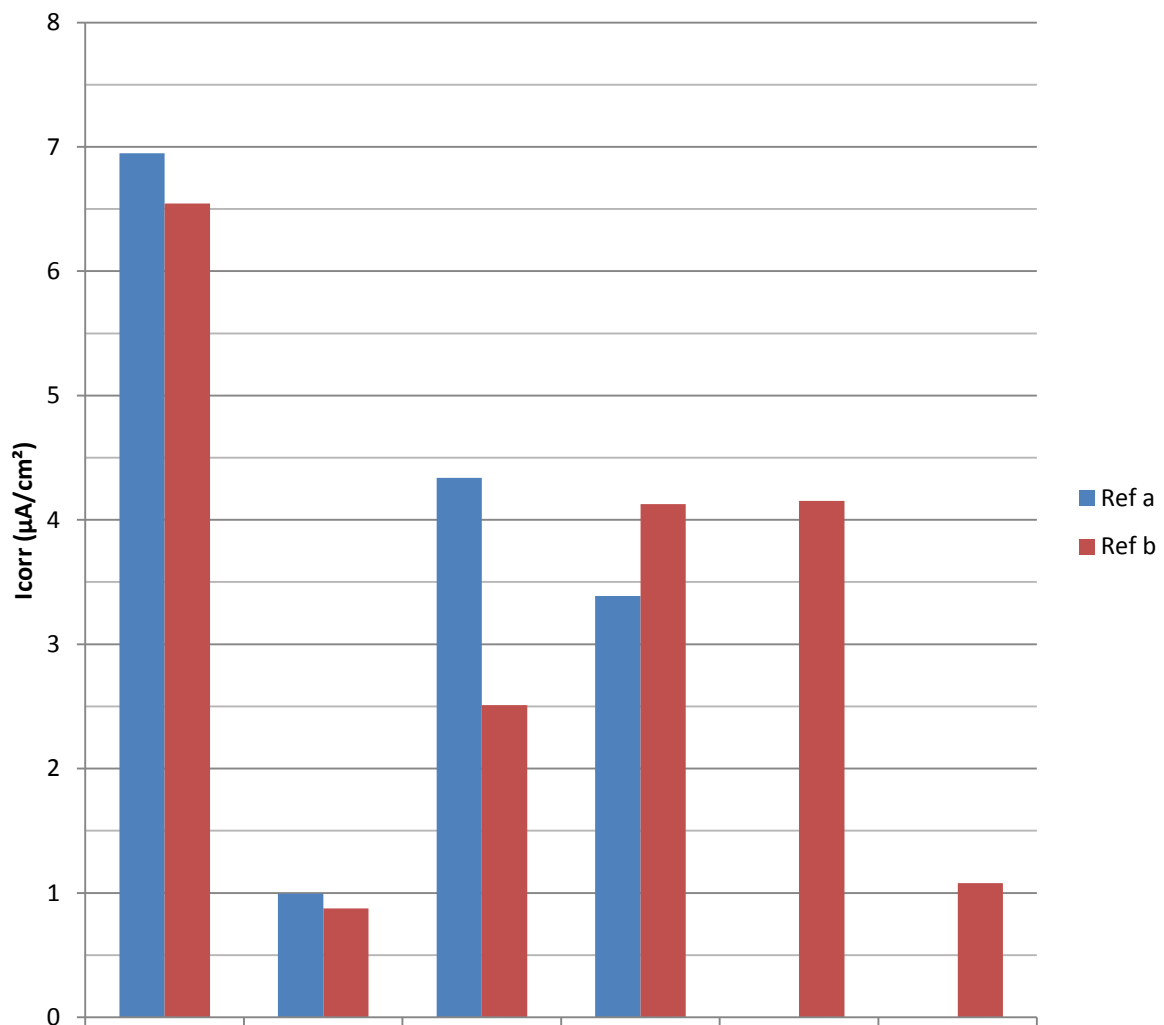


Figure 28: Corrosion rates reference specimens

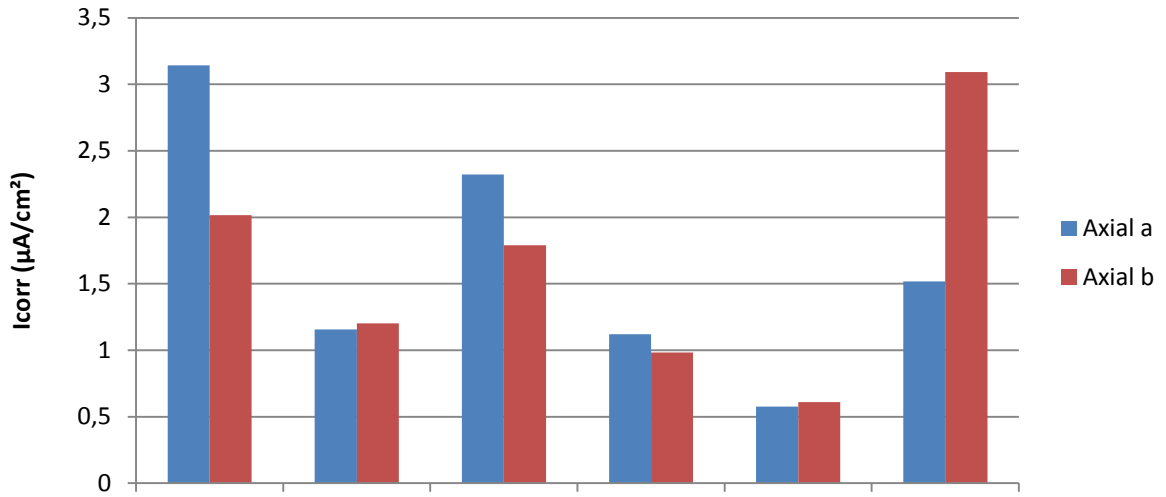


Figure 29: Corrosion rates "ax" specimens

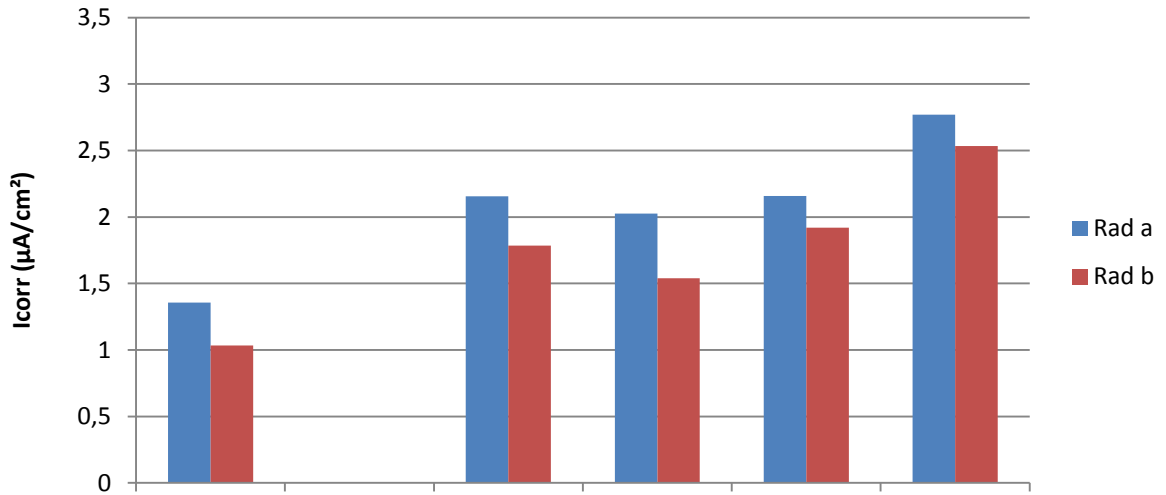


Figure 30: Corrosion rates "rad" specimens

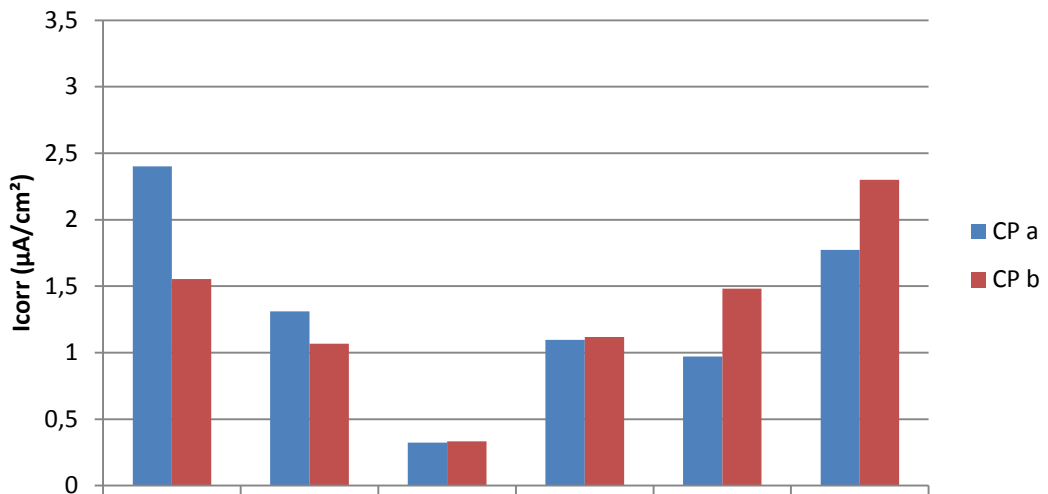


Figure 31: Corrosion rates fibreless specimens

The corrosion rates and B values of the Tafel slope measurements are resumed in Table 17.

Tafel slope measurements					
Tafel-ref	i_{corr}	6,725	E	-5	A
	I_{corr}	3,567723			$\mu A/cm^2$
	b_c	0,062			V/dec
	b_a	0,111			V/dec
	R_p	4,479	E	1	Ω
	B	0,017273			V
Tafel-50298	i_{corr}	1,521	E	-5	A
	I_{corr}	0,806916			$\mu A/cm^2$
	b_c	0,15			V/dec
	b_a	0,095			V/dec
	R_p	3,42	E	2	Ω
	B	0,025255			V

Table 17: Results from Tafel slope measurements

3.6.2 Discussion

3.6.2.1 Open circuit potentials (OCP)

None of the OCPs reach the safe zone, according to “1.4.4 Required protection current”, of $-765mV$ vs. saturated SCE electrode. The Tafel measurements confirm that even without the immersion program, the reinforcement steel of the specimens is not in a safe passive situation (see next section). This is probably due to NaCl addition to the mortar. During the first three weeks no CP current was applied, allowing depassivation to occur.

The steel surface was not externally disturbed or changed between both measurements, so the evolution of OCP can give an indication of the change of protection level.

Most specimens show a higher potential (OCP) in the second measurement, as expected. This is the overall response to the lowering of I_{prot} from $0,11mA$ to $0,05mA$.

However, **CP-60L**, **CP-57C**, **CP-50298**, **CP-ECC** and **CP-Epo** show lower OCPs, indicating a positive evolution of the corrosion system. Despite of the lower protection current, the steel evolved to a safer potential. It's interesting to notice that this OCP evolution is recorded on almost all fibreless specimens (except for CP-64C, which is probably passive, see further).

Next to the depolarization measurement in “3.5.3 Depolarization”, this is a second indication of carbon fibre influence on potential evolution.

3.6.2.2 Tafel measurements

Both Tafel measurements point out B values close to $26mV$, indicating a depassivated steel situation (“1.3.3 Polarization resistance: equation of Stern-Geary (1957) and linear polarization (potentiostatics”). Since these samples weren’t immersed cyclically and given the relatively high steel OCPs (previous section), it may be concluded that the other specimens are also depassivated.

No Tafel slope measurements were therefore done on the other samples, to subject them to destructive mass loss measurements⁴⁴.

The corrosion rates obtained from LP measurements in Table 16 are calculated with $B=26mV$.

3.6.2.3 LP measurements

A good correlation between I_{corr} obtained from the Tafel extrapolation measurements and LP measurements is found (compare values in Table 16 and Table 17 for Tafel-ref and Tafel-FRP). The graphical figures of the extrapolation method are enclosed in APPENDIX F.

Except for Ref-2, all of the **reference specimens show overall higher corrosion rates I_{corr} than the protected specimens**. Unexpectedly low results are obtained for Ref-2, which may indicate an immune passivity of the steel – despite of the identical immersion program. The second LP measurement on specimen Ref-3 is much lower than the first one, indicating an unexpected improvement of the corrosion situation.

The values of I_{corr} for the protected specimens are mostly higher than $1\mu A/cm^2$ which is equivalent to “high corrosion rates”, according to literature on steel corrosion in RC structures (as mentioned in “1.3.7 Corrosion rate criteria”). Together with the high OCP potentials and Tafel slope measurements (indicating initiated corrosion), **it may be concluded that corrosion was not prevented, despite of the high protection current densities**. The chlorides added to the mortar mix probably initiated corrosion before the CP program was set-up.

CP-ax-ECC and CP-64C specimens show minimal corrosion rates. In case of a passive condition it should be noted that parameter B will be closer to $52mV$, resulting in corrosion rates possibly twice as high for these specific specimens. **This passivity could be the result of a successful CPrev**, or another aberrant result similar to Ref-2 (or a combination of both).

However, **the cathodic protection *did* work on average**. If *all* of the corrosion rates are compared between ax, rad and CP specimens (and Ref-2, CP-ax-ECC and CP-64C are left out of the calculation to exclude uncertain results), then it can be concluded that:

- Axial fibre direction specimen have *on average* 56% lower corrosion rates than reference specimens (61% taking account of CP-ax-ECC)
- Rad-specimens have 53% lower corrosion rates compared to references

⁴⁴ As mentioned in “1.3.4. Tafel slope measurements, potentiodynamics”, the high polarization range introduces accelerated corrosion, disturbing the corrosion process and surface.

- CP-specimens have 64% lower corrosion rates compared to references (68% with CP-64C)

If *all* of the corrosion rates are studied in the same way per epoxy type, then it can be concluded that:

- 60L specimens have 53%
- 57C specimens have 71%
- 64C specimens have 51% (65% taking account of CP-64C)
- 50298 specimens have 68%
- ECC specimens have 61% (69% taking account of CP-ax-ECC)
- Epo specimens have 44%

lower corrosion rates than reference specimens on average.

It is also interesting to study the evolution between both I_{corr} measurements.

If the axial radial and fibreless specimens are compared, the most consistent results are found for the Rad-specimens: an overall improvement for all specimens. The radial specimens also have the highest average I_{corr} improvement of $0,33\mu A/cm^2$.

The highest average decrease in I_{corr} is recorded for 60L. Both CB added epoxies show average higher I_{corr} . The change in I_{corr} between both measurements is shown in Figure 32, thus were more sensitive to the protection current drop.

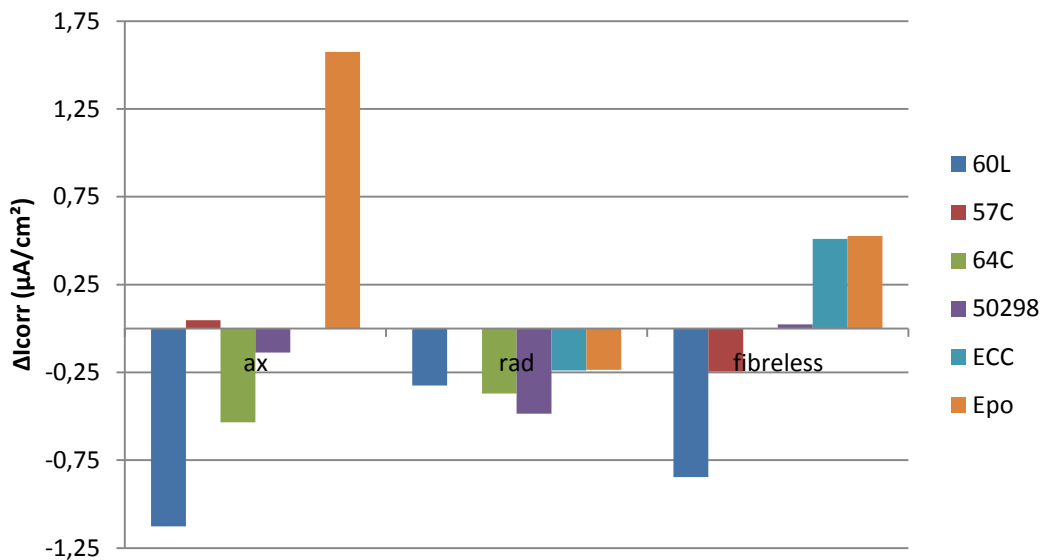


Figure 32: Change in corrosion rate

The average I_{corr} changes are also summarized in Table 18 (with exclusion of CP-ax-ECC and CP-64C).

Only **ECC and Epo** have an average increased corrosion rate.

60L is the only epoxy showing overall improvement. The largest improvement is recorded for CP-ax-60L. Both **64C** and **50298** show stable, low corrosion rates for fibreless specimens, and a positive evolution for fibre reinforced specimens.

Spec. type	ΔI_{corr} ($\mu A/cm^2$)
ax	-0,02972
rad	-0,33077
CP	-0,00513
60L	-0,766
57C	-0,0989
64C	-0,30116
50298	-0,20014
ECC	0,090623
Epo	0,621624

Table 18: Average corrosion rate drops between both LP sessions

Eccobond **57C** has overall low corrosion rates ($<1,5\mu A/cm^2$), which can be attributed to the high conductivity of the epoxy. The axial fibre configuration gives stable results, while the fibreless configuration gives an improvement of $0,24\mu A/cm^2$.

3.6.2.4 Conclusions

- The steel potentials are not found in the safe passive zone (i.e. $< -765mV$ vs. SCE). This is probably due to the high chloride concentration added in the mortar
- The lower protection current in the second experiment phase (from $0,11$ to $0,05mA$) causes a potential increase between both LP sessions. Only the fibreless specimens show lower (i.e. safer) potentials after 28 days.
- The Tafel slope measurements show good correlation with LP measurements (calculated with $B=26mV$). They confirm the aggressive depassivated steel situation, insinuated by the high steel potentials (low B values)
- Active chloride corrosion initiation was not prevented, but the cathodically protected specimens show overall much lower corrosion rates than references (40% to 70% lower). Thus, ICCP was effective.
- Some specimens show very low rates, and are believed to be in passive steel condition: Ref-2, CP-ax-ECC and CP-64C. Although it may also be a combined effect with CPrev for the two latter cases.
- Most of the I_{corr} evolutions are rather scattered. The radial fibre orientation gives the most consistent results: overall improvement. This *evolution* indicates that better concrete confinement due to radial wrapping may have played a role.
- On the other hand, absolute I_{corr} values are lower (on average) for axial fibre orientations than for radial. This can be explained as the positive effect of the current distribution from primary anode to secondary anode in axial fibre configuration.
- Despite of its high resistivity ($50\Omega cm$), epoxy 60L showed the best improvement on all specimen configurations. The resistivity of the anode seems to have an influence on CP: the most conductive epoxies show low change in I_{corr} evolution between both

measurements. In these specimens the fibres are believed to have minimal influence on current surface spread.

- The CB added epoxies show the worst results.

3.7 Mass loss measurement

After the second LP session the specimens were dried for 1 week. Afterwards they were broken, for destructive research.

3.7.1 Visual inspection

The visual inspection of the steel bars showed relative low corrosion products on all protected specimens. No overall passive corrosion layer was found on any specimen.

Two types of corrosion products were found, both visible in Figure 33. The first type was most found on top and bottom part of steel surfaces, near the epoxy seals (greater ellipse in Figure 33). These corrosion products were often mixed with some whitish mortar residues, that were difficult to remove. Underneath the mortar residues a red to brownish material was found.

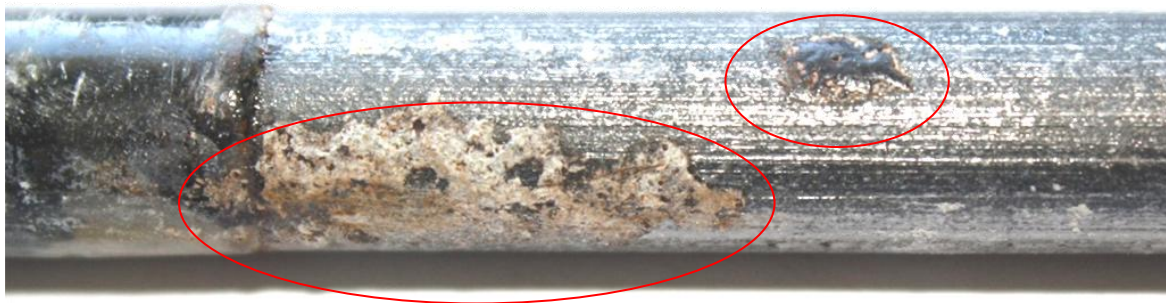


Figure 33: Corrosion products on top part of CP-ECC

The second type of corrosion product was much more local. The product formed small, dense and blackish stains on the surface (small ellipse in Figure 33), that were thicker than the first type. No adhesion to mortar residues occurred with this type of corrosion, and after removal of the black product a small pit in the surface remained. These thick local corrosion bulbs were found on various places (at the ends and middle sections of the steel surface).

The reference specimens showed the same corrosion products, although in slightly higher amounts. Especially Ref-1 was found most heavily corroded. Some close-up pictures are shown in Figure 34. Especially the top middle and bottom pictures show corrosion pitting.



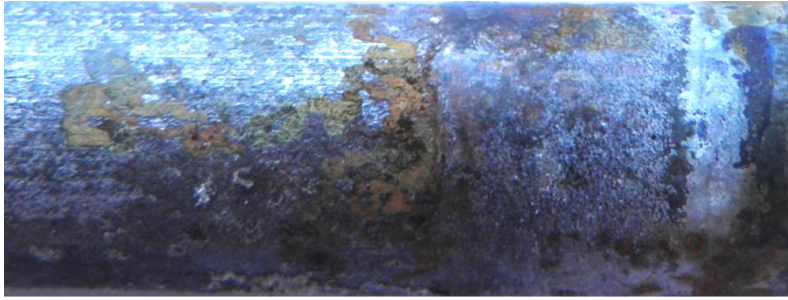


Figure 34: Corrosion products on reference specimens (Ref-1 top left and bottom, Ref-FRP top right, and Ref-3 middle)

Dark brown to black corrosion stains were also detected on the concrete interface after breaking (Figure 35).

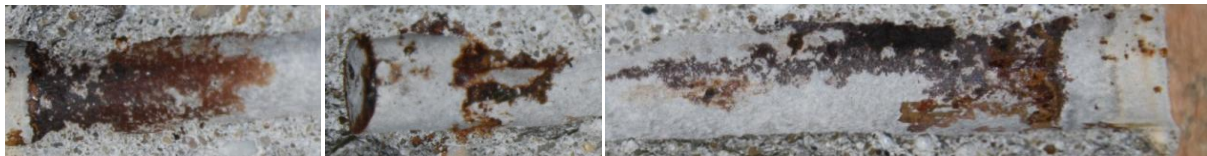


Figure 35: Corrosion products on concrete interface

3.7.2 Mass loss

As much mortar residues as possible were removed before the measurement started. Corrosion products were removed by scraping (mechanically) according to ASTM G1-90. The weighing accuracy was $0,1mg$. The results are shown graphically in Figure 36.

Very low mass loss percentages are found, because of the small amounts of corrosion products. It should be noticed that specimen CP-ax-60L had much mortar residues adhering to the corrosion products. These residues were partly left on the steel for first measurement, because corrosion products were being ripped off with the residues. The mass loss of this specimen is therefore higher than other specimens.

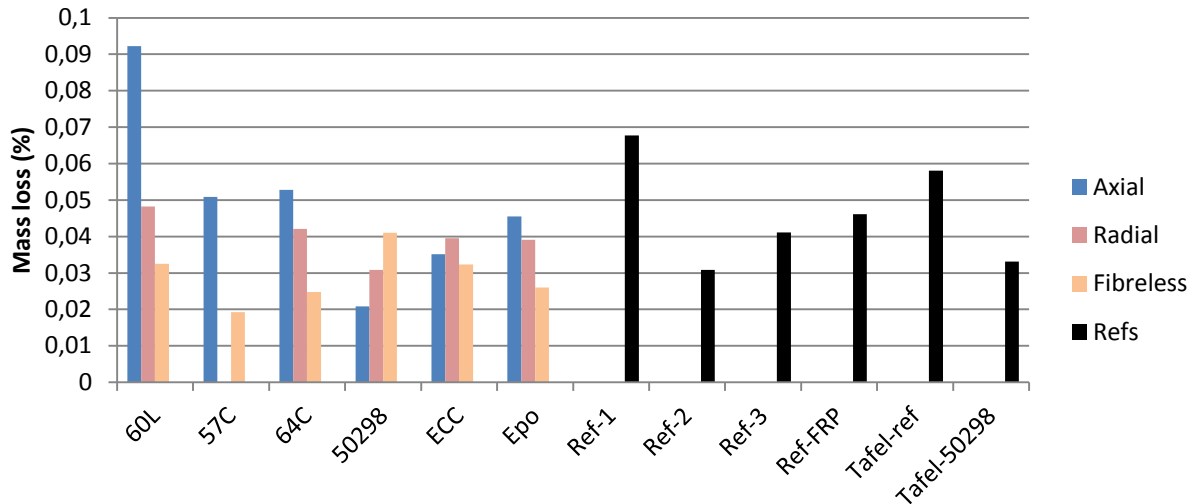


Figure 36: Mass losses

It may be remarked that the low I_{corr} specimens from the LP measurements (Ref-2, CP-ax-ECC and CP-64C) have relatively low mass losses.

3.7.3 Correlation between LP and mass loss measurement

If an assumption is made for the evolution of I_{corr} in time, equation (1.3) can be used to calculate the mass loss. The assumption made in this work, is a linear evolution, using both I_{corr} measurements, integrated over a period of 28 days. Figure 37 shows the calculation principle of $\int I \cdot dt$. Both hatched triangles are equal in surface, so the integral is simplified to $\int I \cdot dt = I_{corr,14} \cdot \Delta t$.

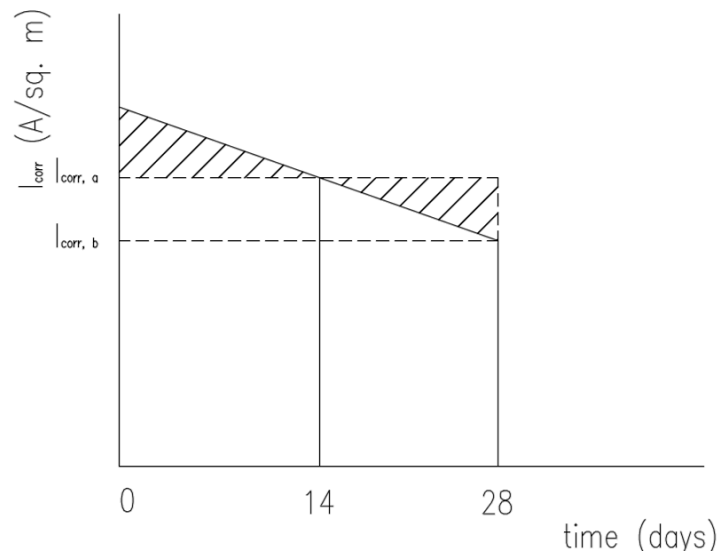


Figure 37: Assumption I_{corr} evolution

The correlation between the actual measured mass loss and calculated mass loss, is shown in Figure 38. This graph is set-up in the same way as Figure 9. Both axes are logarithmic.

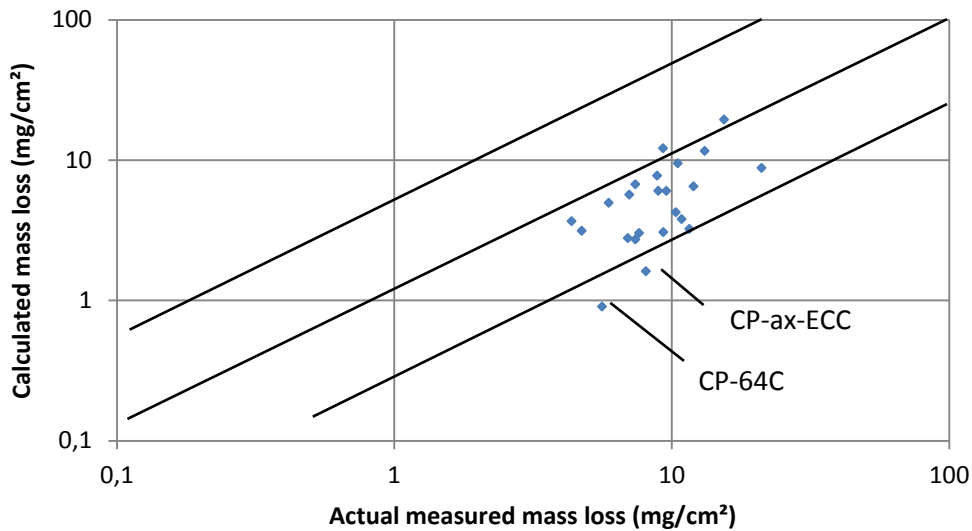


Figure 38: Correlation graph LP and mass loss

It can be concluded that a good correlation between both measurements is obtained, within the error factor 2 boundaries. The calculated ('electrochemical') mass losses underestimate the actual measured mass loss. In case of local corrosion attack, the I_{corr} values obtained through LP underestimate the actual corrosion rate in the pits (and overestimate the global corrosion rate). This explains the higher values obtained from the gravimetric mass loss measurements, where the actual local corrosion is weighed.

The two aberrant measurements in the graph are the results from CP-ax-ECC and CP-64C (the two samples that gave very low I_{corr} in the LP measurements).

Chapter 4: Conclusion

In “Chapter 1: Corrosion of reinforcement steel in concrete:” some general aspects regarding corrosion and corrosion rate measurements of steel bars in concrete were discussed. Some issues regarding corrosion research (accelerated corrosion initiation, chloride threshold values etc.) were also briefly discussed. The principles of cathodic protection and prevention (CP and CPrev) were introduced, and practical guidelines regarding CP of steel in RC structures were mentioned.

In “Chapter 2: FRP use as EBR of RC structures:” some properties of Carbon Fibre Reinforced Polymers (CFRP) for Externally Bonded Reinforcement (EBR) of RC structures that are of interest in this dissertation, were discussed. The link between CFRP and corrosion protection was made in different aspects (e.g. fibre sustainability, passive protection through FRP wrapping etc.). This link showed the relevance of the subject of this dissertation: researching the feasibility of *active* corrosion protection (ICCP) using CFRP anodes, in paragraph “2.7 Outline of the dissertation”.

At the end of the second chapter, a paragraph was dedicated to the conductivity of the polymer matrix (2.8 Conductivity of the polymer matrix). This issue was only partially treated in this work. It was chosen in this dissertation to work with epoxy resins, filled with conductive particles. The strength requirements regarding epoxies for FRP application were only partially respected, and even totally disregarded for the Carbon Black added epoxies. This matter needs more attention in further research.

The possibility of inserting the filler addition process in the fabrication process of prefabricated CFRP laminates is an interesting track, that should also be investigated in future research.

Finally, in “Chapter 3: Experimental program”, much attention is paid to the experimental method that was used in this work. This method is distilled both out of literature study (based on past corrosion and CP researches) and practical aspects (feasibility, equipment limitations etc.), and is certainly open for further improvement. It is impossible to built up an experimental method, taking account and with full notice of all sorts of phenomena: it is only during the experiment that these issues come to the surface. Therefore, some attention is paid to possible experimental method improvements in this conclusive text.

To investigate the feasibility of CPrev, a longer experimental program is needed. The addition of chlorides to the mortar mix will automatically create an “active corrosion” situation, resulting in high steel potentials. It would be better to minimize the chloride contamination, and to gradually increase it afterwards for depassivation and corrosion initiation (e.g. through cyclic immersion, salt mist chamber

etc.). This latter chloride penetration will obviously need much more time. In addition, low corrosion product masses were found in this experiment, even for reference specimens. For the sake of visual inspection and mass loss differentiation between specimens, it may be interesting to prolong the CP/immersion program too.

A second recommendation involves the number of specimens. This experiment was only a modest research for the feasibility. In more extended research, more samples should be produced to create statistically more robust conclusions. Also extra samples for Tafel slope measurements can be helpful. E.g. some specimens in this experiment showed very high polarization resistances, insinuating a passive steel condition. The bad correlation with mass loss measurement, made it difficult to draw a definite conclusion. If more specimens of this kind had been available, a Tafel slope measurement would have brought this definite conclusion.

The integration of a reference electrode inside the mortar specimens – similar to field applications of CP – or an equivalent system that can be used externally, might also improve the understanding of the CP. For instance the depolarization method (discussed in “1.4.4 Required protection current” and “3.5.3 Depolarization”) is a very simple technique to measure the effectiveness and efficiency of the CP system, but it requires a reference electrode. The method was tried without a reference in this work, but no final conclusion could be drawn. The presumption that the fibres had an influence on anode depolarization was expressed, and is certainly interesting for further investigation (e.g. with a reference electrode the depolarization behaviour of the anode can also be recorded).

Finally, it may be noticed that more linear polarization (LP) measurements could improve the result interpretation (in a prolonged CP program). The evolution of the steel in a longer term could be investigated. Also a LP at the beginning or before the CP program is started, could reveal valuable information.

Notwithstanding these recommendations, the effectiveness of the CP was shown at the end of chapter 3. CP specimens showed corrosion rates substantially lower than unprotected reference specimens. A good correlation between the applied test methods (Tafel extrapolation, linear polarization and mass loss measurements) was found.

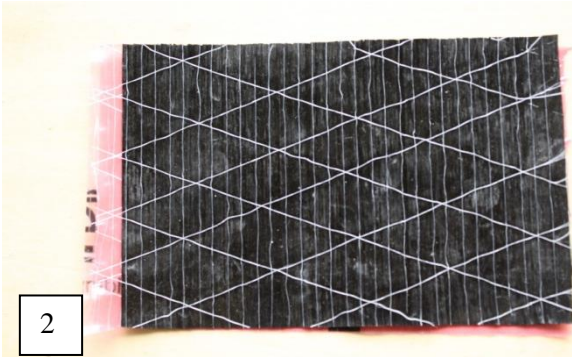
APPENDIX A

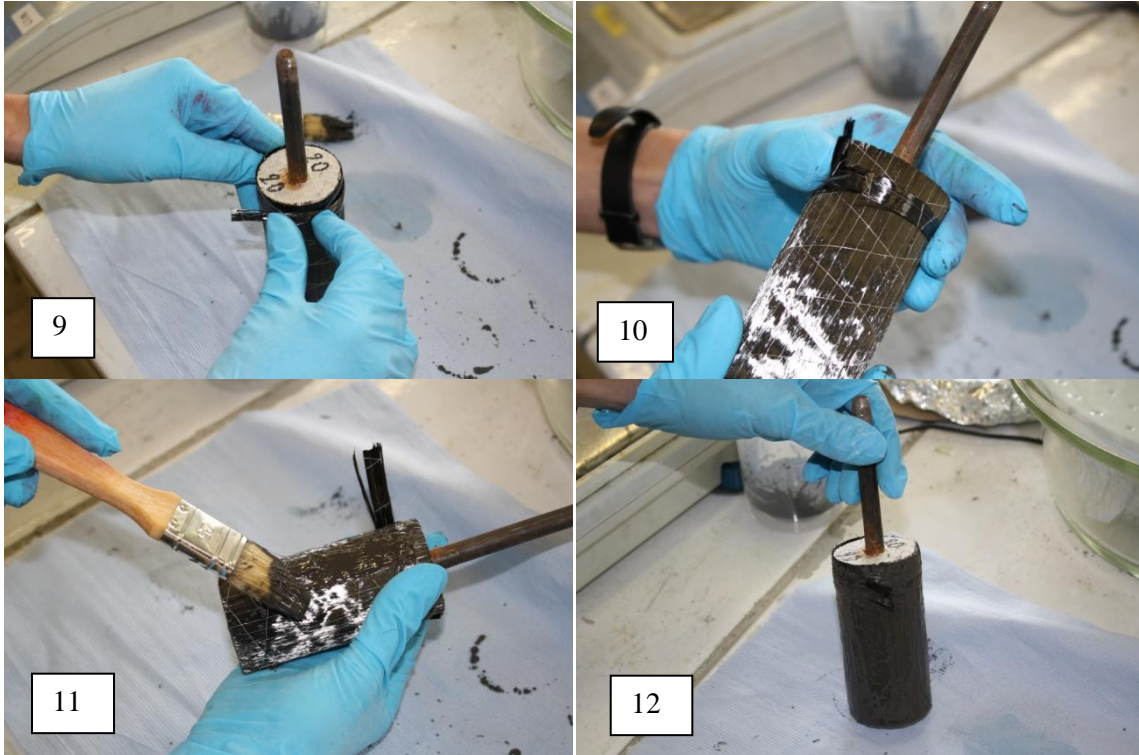
Reference electrode potentials vs. normal hydrogen (NHE) electrode [1.8]

Electrode material	Potential (mV vs. NHE)
Calomel (SCE)	+244
Silver/silver chloride	+199
Copper/copper sulphate	+316
Manganese dioxide	+365
Graphite	+150±20
Activated titanium	+150±20
Stainless steel	+150±20
Lead	-450

APPENDIX B

Wrapping procedure

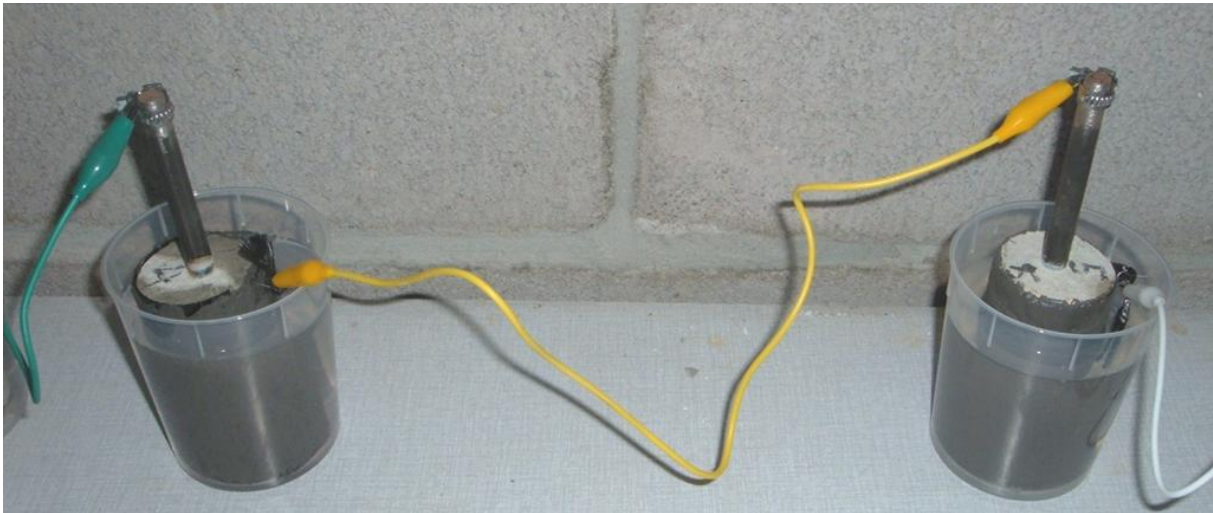




1. Lollypop specimen n°20 and epoxy Eccobond 5028	2. FRP fibres for wet lay-up
3. String of FRP as primary anode	4. Application of first epoxy coating
5. Application of the FRP wrap	6. Manual wrapping
7. Removal of wrap plastic	8. Result of wrapping
9. Positioning of the primary anode	10. (<= idem)
11. Application of top epoxy layer	12. Final result

APPENDIX C

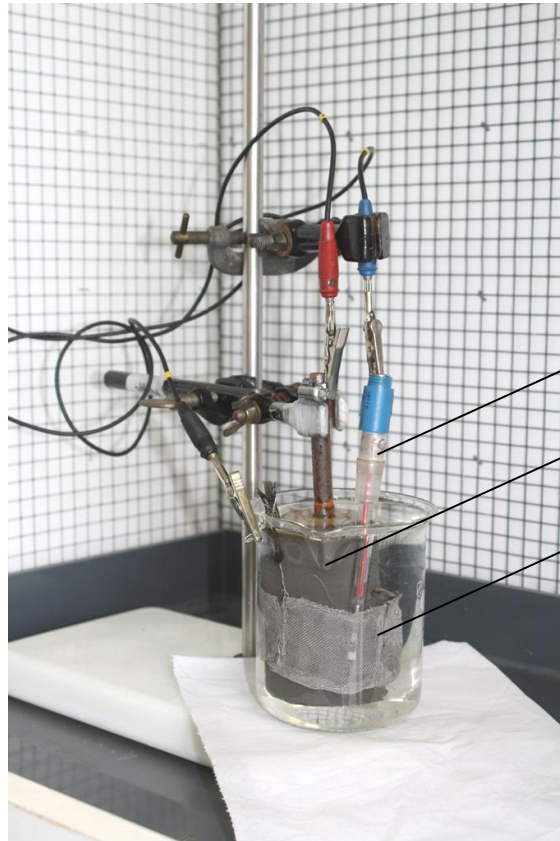
CP-circuit set-up



The specimens were connected in series, to ensure an identical protection current at any time. The pictures are taken during a wet immersion cycle (1 hour per day), at a constant level (20mm of upper surface) in a 1,0wt% NaCl water solution, in a 60% RH and 20°C environment.

In the close-up picture of specimens CP-ax-64C (left) and CP-ax-50298 (right), the difference in wetting condition can be seen: the combination of fibres and Eccobond 64C epoxy result in a better mortar moisturizing condition (wetted upper surface).

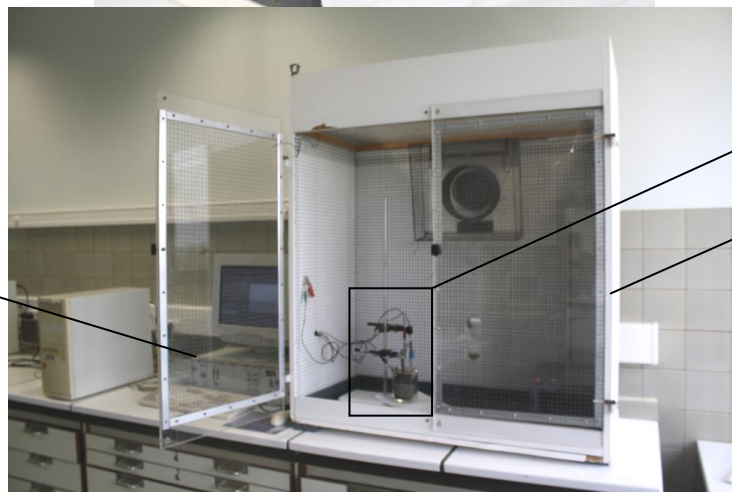
LP cell set-up



Reference electrode

Concrete specimen

Titanium mesh counter electrode



Upper image

Faraday cage

Autolab equipment

APPENDIX D

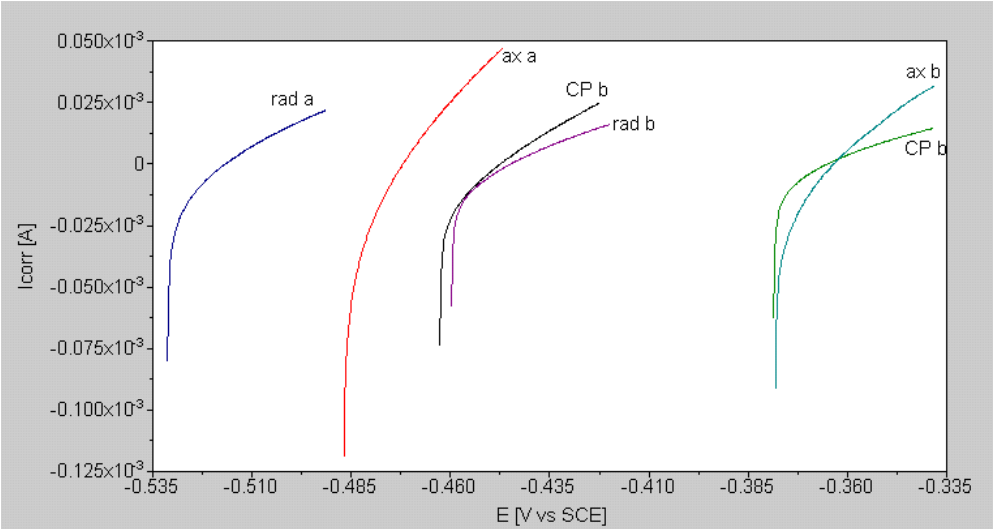
Relative potential difference per specimen. These are the in circuit (ICCP) potential differences between anode (CFRP wrap) and cathode (steel bar). The measurement was done with a high internal resistance voltmeter, connected in parallel between C and A. The protection current during the ICCP was $0,05mA$ at the moment of measurement.

Relative potential difference per sample ($I=50\mu A$)		
	dry (mV)	wet (mV)
CP-ax-60L	488	335
CP-ax-57C	450	433
CP-ax-64C	315	321
CP-ax-50298	315,2	324,3
CP-ax-ECC	471	484
CP-ax-Epo	341	380
<hr/>		
CP-rad-60L	620	286
CP-rad-64C	309	305,7
CP-rad-50298	360	247,5
CP-rad-ECC	445	451
CP-rad-Epo	346	389
<hr/>		
CP-60L	648	219
CP-57C	484	479
CP-64C	393	395
CP-50298	386	260
CP-ECC	558	573
CP-Epo	417,5	329

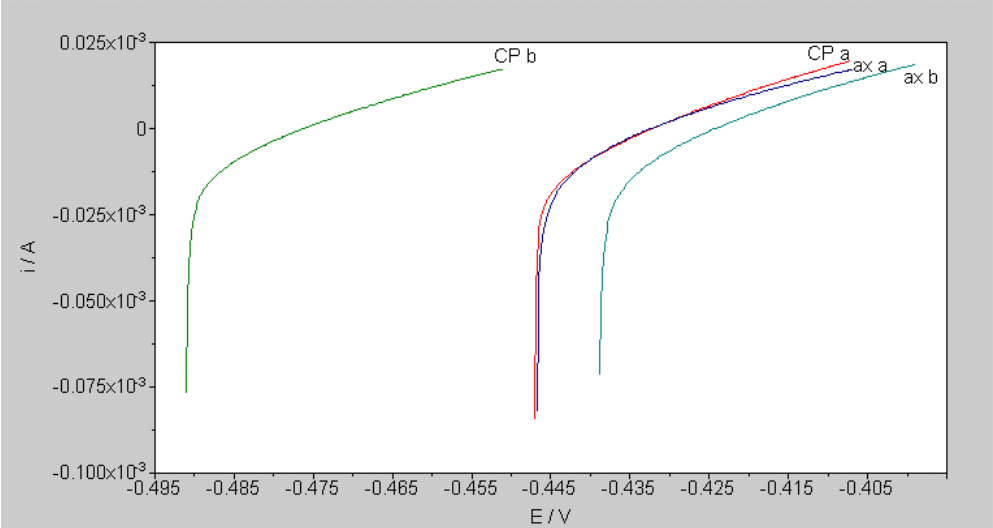
APPENDIX E

Graphical results of the LP measurements. Vertical axis: current (Ampère), horizontal axis potential of steel versus Calomel (Volts). The slope of the linear part of the curves, around the OCP, is a relative measure for corrosion rate: the flatter the curve, the higher the polarization resistance (R_p) and the lower the actual corrosion rate. Visual slope inspection can be done in each graph separately, or between two graphs with identical vertical axis range.

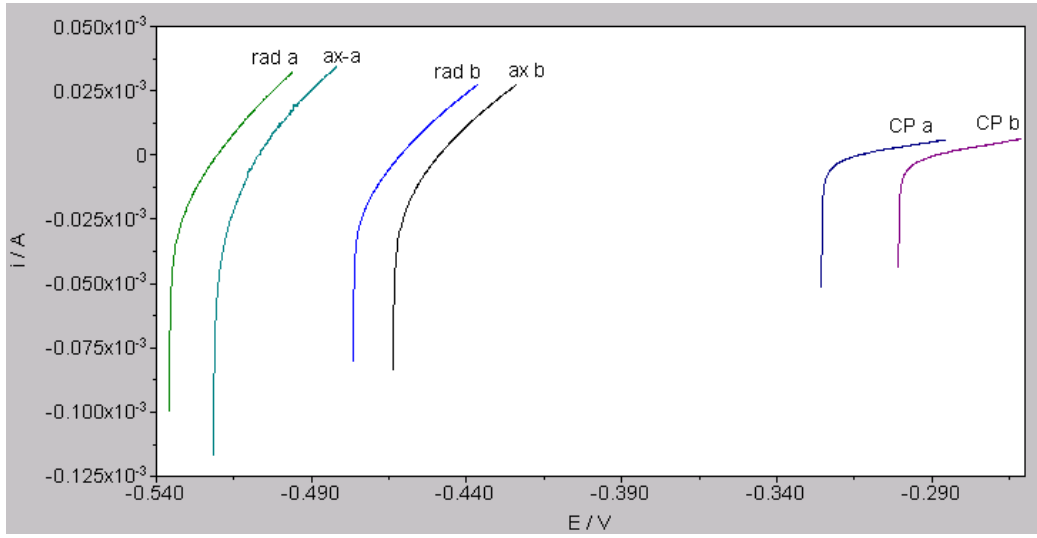
60L:



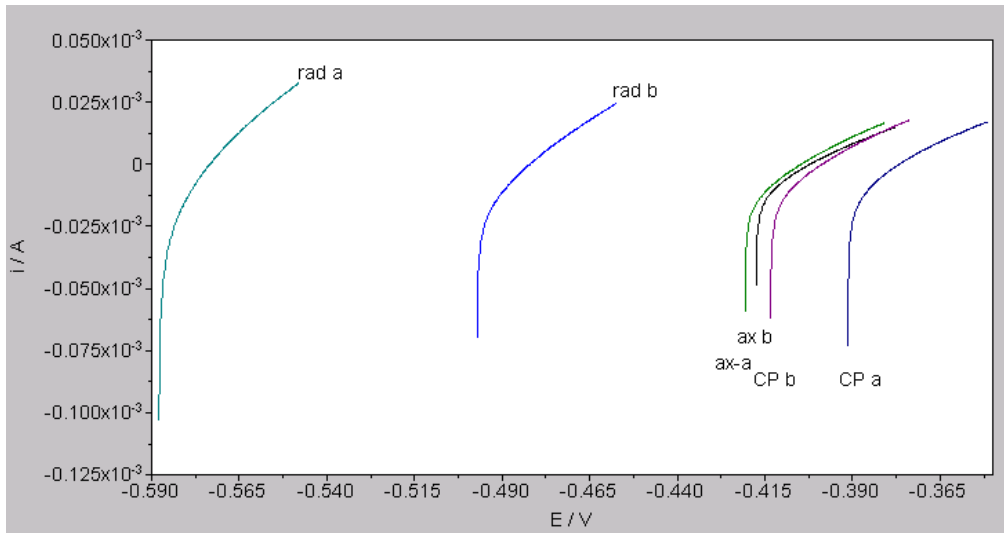
57C:



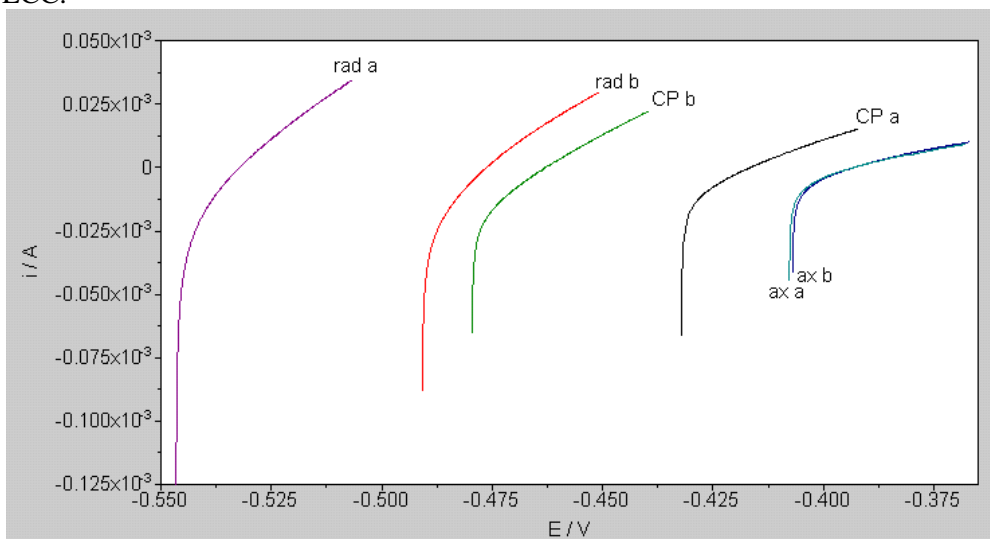
64C:



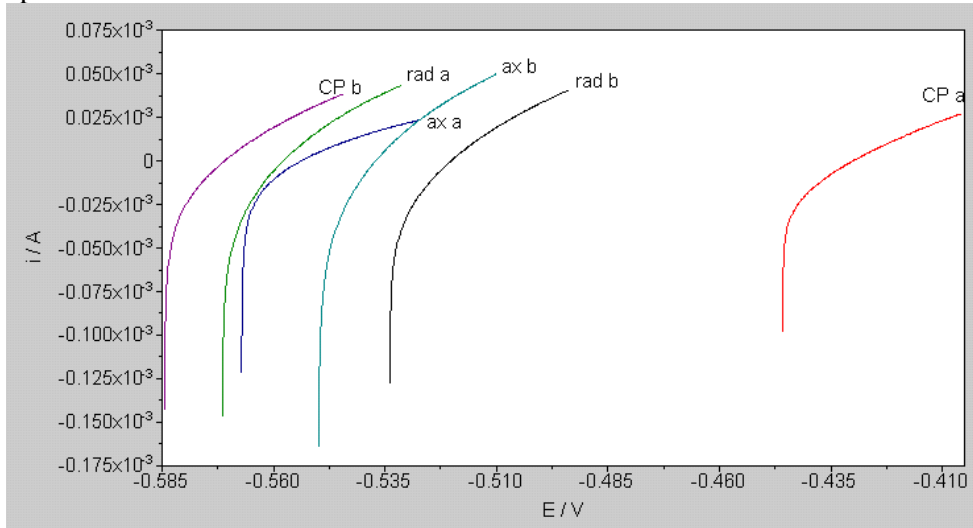
50298:



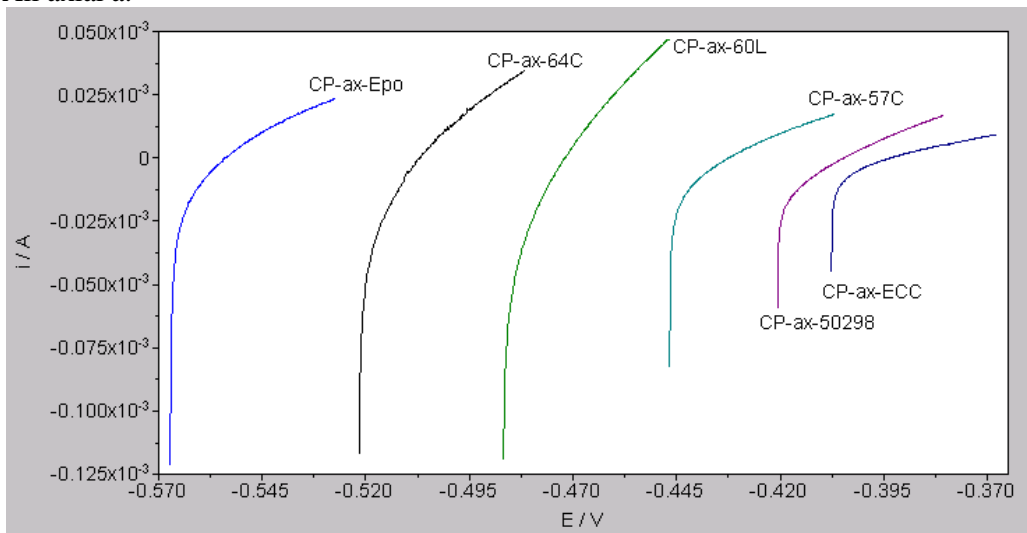
ECC:



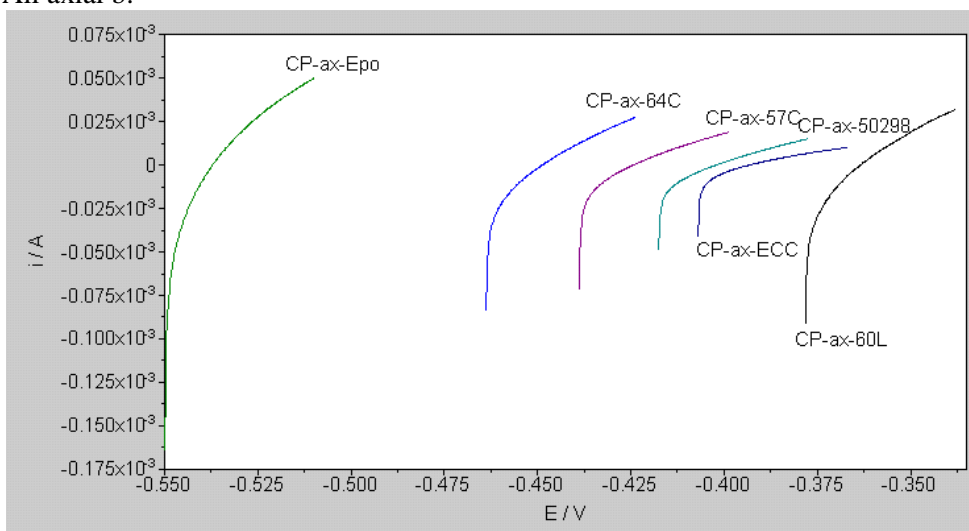
Epo:



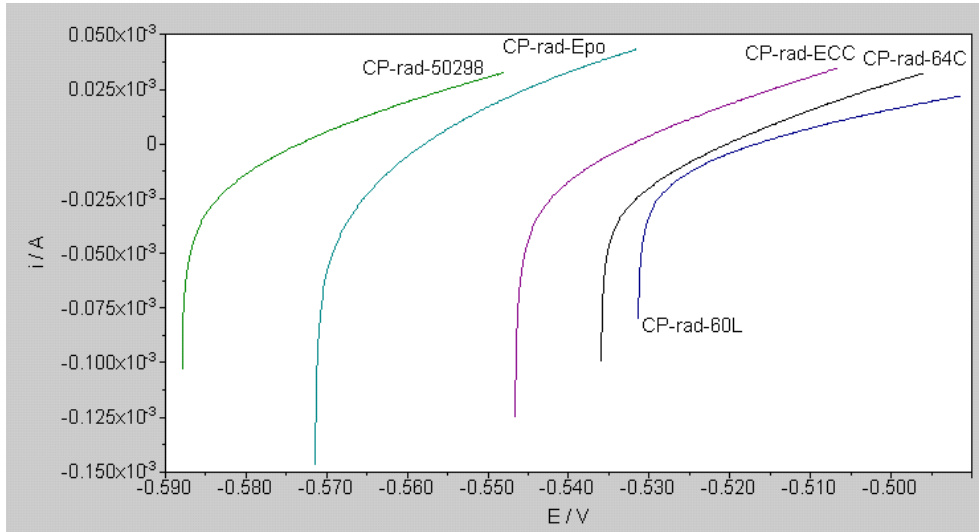
All axial a:



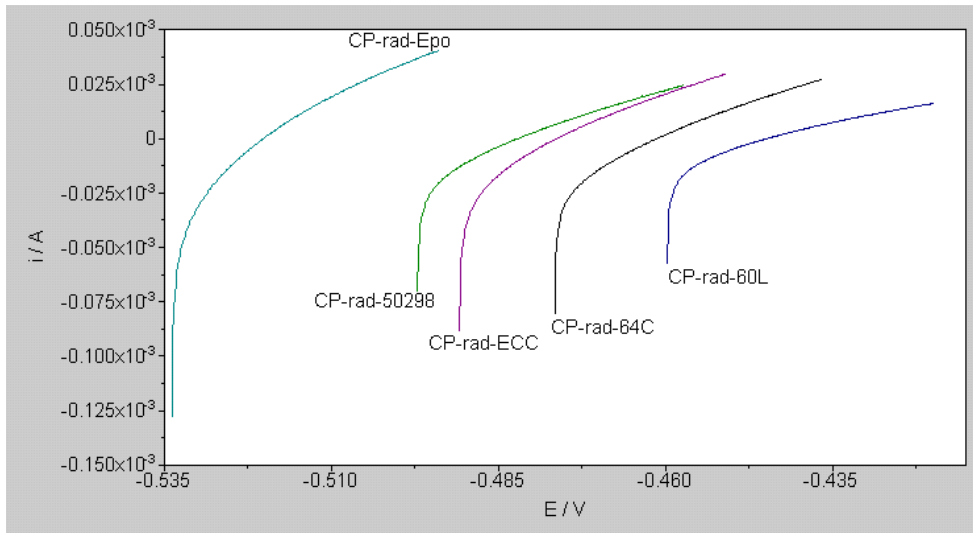
All axial b:



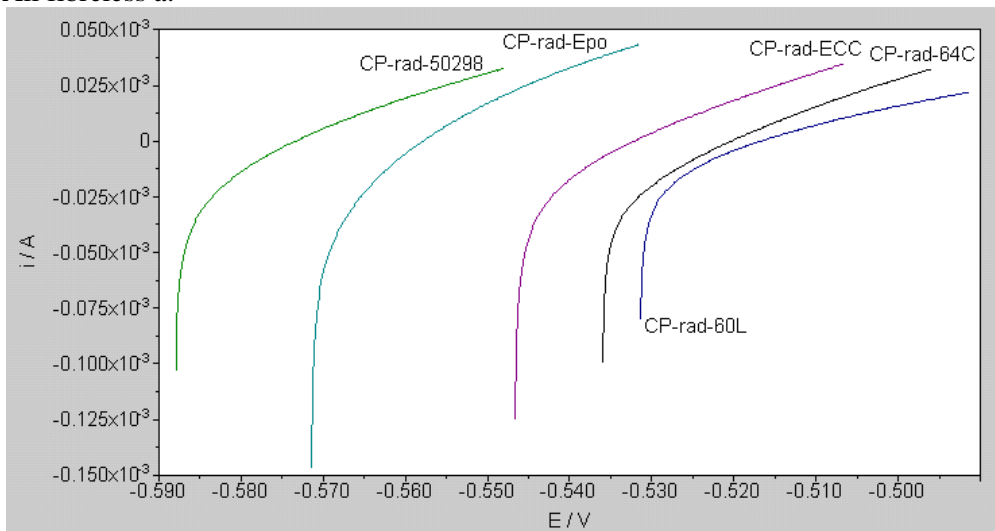
All radial a:



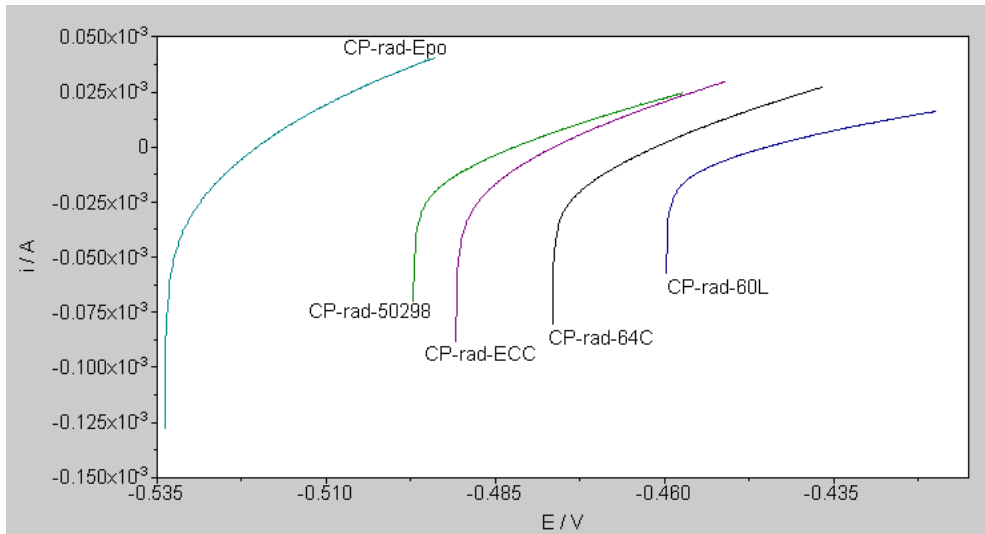
All radial b:



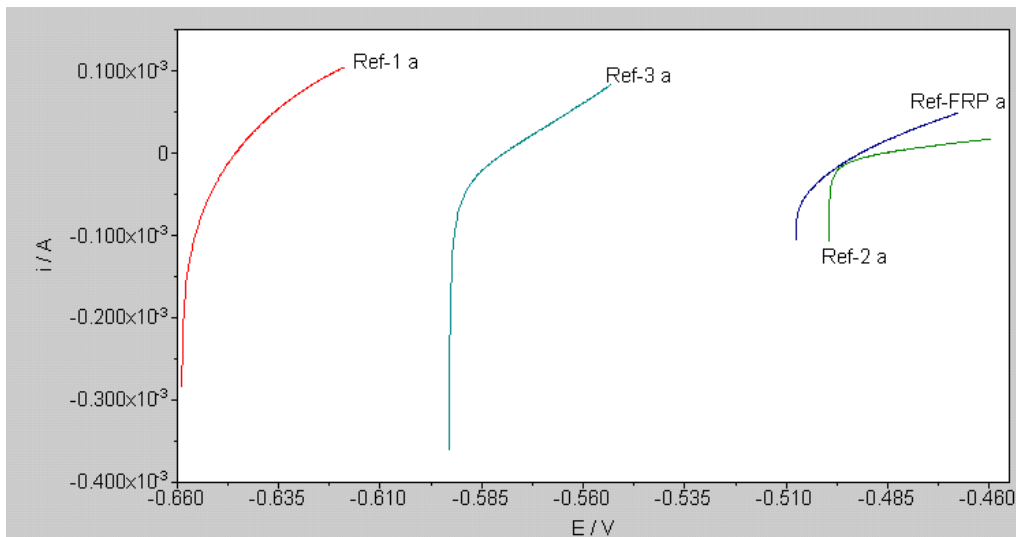
All fibreless a:



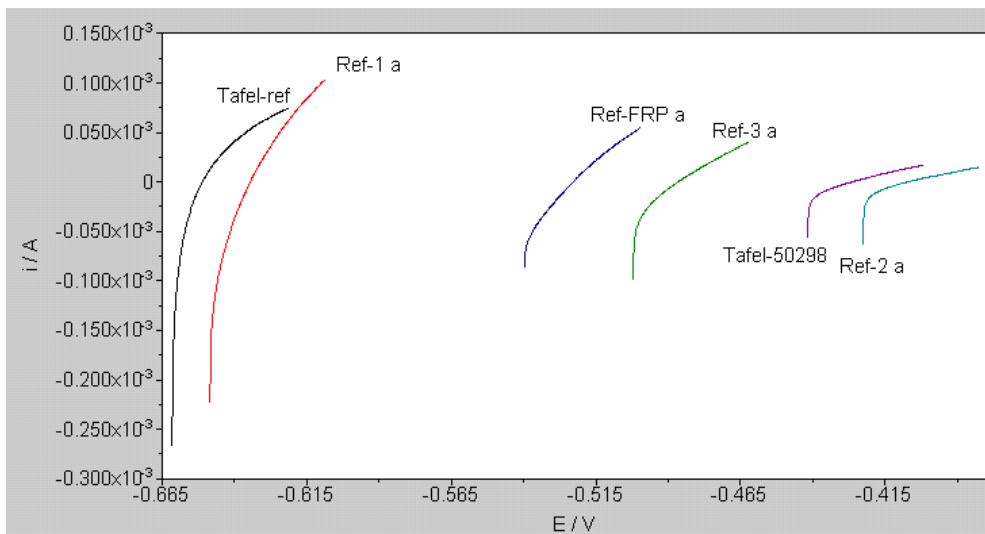
All fibreless b:



References a:



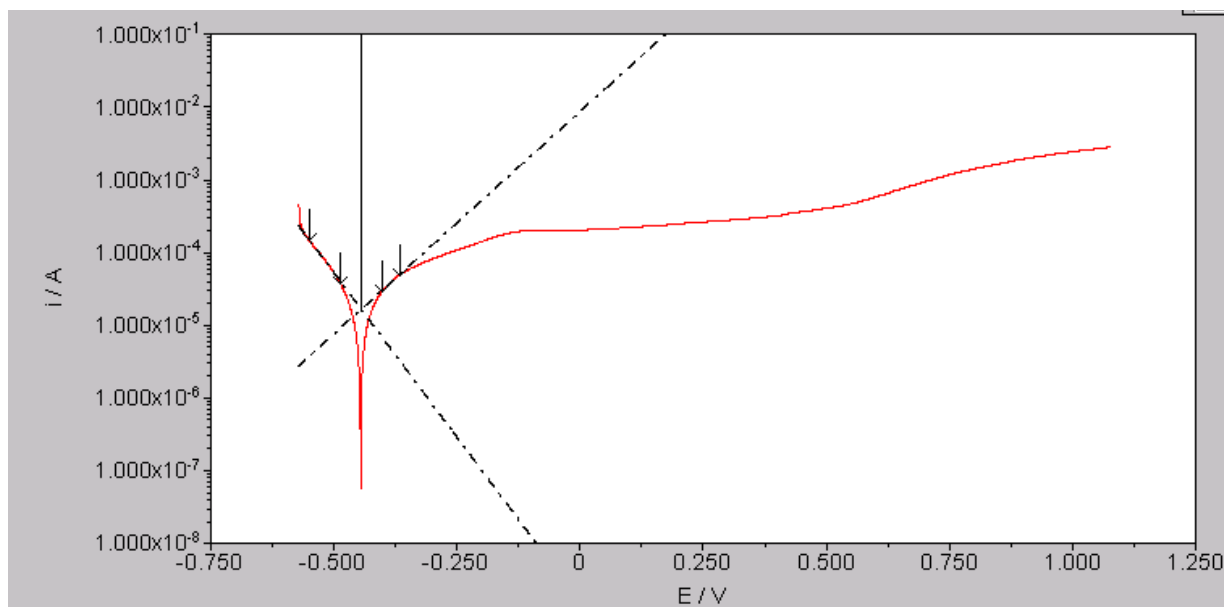
References b:



APPENDIX F

Tafel extrapolation plots. The linear regions (in $\log(i)$ vs. E) of the anode and cathode polarization curves are extrapolated. The intersection point points out the actual corrosion current and potential.

Tafel-ref:



Tafel-50298:

